universität wien

DIPLOMARBEIT

Titel der Diplomarbeit

„Validation of PP2A substrates Net1 and Kin4 via newly developed controls in M-Track“

Verfasserin

Sonja Kuderer, BSc.

angestrebter akademischer Grad

Magistra der Naturwissenschaften (Mag.rer.nat.)

Wien, 2012

Studienkennzahl:	A 490
Studienrichtung:	Diplomstudium Molekulare Biologie
Betreuer:	ao. Univ. Prof. Egon Ogris

Während meiner ganzen Arbeit bin ich von einigen Personen großartig unterstützt worden. Das einzige Wort, das passend wäre, um Ihnen zu zeigen wie wichtig sie für mich in dieser Zeit waren, habe ich aber viel zu selten verwendet.

Deswegen werde ich es an dieser Stelle für alle festhalten.

Ich danke euch!

Hypothesen sind wie Netze –

nur der wird fangen, der auswirft.

Novalis

Wenn ich die Folgen geahnt hätte,

wäre ich Uhrmacher geworden.

Albert Einstein

Summary

Protein Phosphatase 2A (PP2A), a heterotrimeric protein serine/threonine phosphatase (PSTP), conducts the dephosphorylation of many substrates. It is composed of a structural A, a catalytic C and a regulatory B subunit, which regulates different target proteins (Janssens et al, 2008). In *S.cerevisiae* the two regulatory subunits for substrate targeting are encoded by *CDC55* and *RTS1* (Shu et al 1997; Healy et al, 1991).

Identification of the PP2A substrates is difficult as their short-lived substrate contact can not be detected with today´s methods. The Ogris lab introduced M-Track, a Yeast-Two-Hybrid based method to detect and identify PP2A target proteins (Zuzuarregui et al, 2012). A histone lysine 9 (K9) methyltransferase (HKMT) is fused to the B subunit, whereas putative targets are fused to the N-terminus of histone 3 (H3), the HKMT target site. Upon a PP2A-substrate interaction the HKMT transfers stable methyl marks on K9 of the H3, which are detectable with monoclonal antibodies even after the interaction has taken place.

Using M-Track Zuzuarregui et al (2012) have identified two PP2A target proteins, Nucleolar silencing establishing factor and telophase regulator 1 (Net1) and kinase 4 (Kin4). Moreover, they have confirmed the specific subunit-substrate interaction by using HKMT only constructs. Experiments in this diploma thesis confirmed their findings and aimed to analyze parameters, which might negatively influence M-Track such as overexpression and sterical hindrance of fusion proteins as well as the effects of present endogenous substrates.

To analyze the sterical hindrance of fusion proteins, C- as well as N-terminally tagged bait and preys were compared. For N- and C-terminal variants of Rts1-Kin4 and Cdc55-Net1, the interaction was still detectable but showed a different mono- and trimethylation pattern.

A negative competition by endogenous bait and preys has been indicated as my colleagues have shown that the HKMT Cdc55 construct can not build trimeric complexes when endogenous Cdc55 and Net1 are present. In this diploma thesis, comparisons between strains harboring endogenous substrates and those lacking them revealed in three of four examined cases a stronger monomethylation level in the single knock-out strains.

As overexpressed M-Track fusion proteins might lead to false positive results, the Cdc55 construct was integrated into the *S.cerevisiae* genome. After an IP the bait at endogenous levels showed weak trimethylation signals with overexpressed Net1. Additionally, an alternative tetracycline regulated expression of the Rts1 bait was introduced to modulate expression levels of fusion proteins.

Results provided evidence that sterical parameters have an influence on the present methylation species whereas the presence of endogenous substrates has no or only little influence on M-Track. At endogenous levels an M-Track detection of PP2A substrates showed only weak signals and has to be further optimized.

Zusammenfassung

Protein Phosphatase 2A (PP2A), eine heterotrimere Protein Serin/Threonin Phosphatase (PSTP), dephosphoryliert viele Substrate und setzt sich aus einer strukturellen A, einer katalytischen C und einer regulatorischen B Untereinheit zusammen (Janssens et al, 2008). In *S.cerevisiae* werden die beiden regulatorischen Untereinheiten für Substrat-Ansteuerung von *CDC55* und *RTS1* codiert (Shu et al 1997; Healy et al, 1991).

Da die kurzlebigen PP2A-Substrat Kontakte nur sehr schwer detektierbar sind, hat das Ogris Labor M-Track eingeführt, eine Yeast-Two-Hybrid basierte Methode (Zuzuarregui et al, 2012). Die B Untereinheit wird dabei an eine Histon 3 Lysin 9 (K9) Methyltransferase (HKMT) fusioniert. Substrate werden an die Zielstelle der HKMT, den N-Terminus des Histon 3 (H3), gebunden. Die Methylierung durch HKMT am K9 des H3 ist durch monoklonale Antikörper auch noch nach einer PP2A-Substrat Interaktion detektierbar.

Mittels M-Track haben Zuzuarregui et al (2012) zwei PP2A-Zielproteine, Nucleolar silencing establishing factor and telophase regulator 1 (Net1) und Kinase 4 (Kin4) identifiziert. Zusätzlich belegen sie den spezifischen Untereinheit-Substrat Kontakt durch HKMT only Konstrukte. Experimente dieser Diplomarbeit bestätigten ihre Ergebnisse und analysierten Parameter, welche M-Track negativ beeinflussen könnten, wie Überexpression und sterische Probleme der Fusionsproteine sowie die Effekte von endogenen Substraten.

Durch Verwendung C- und N-terminaler Konstrukte sollten sterische Hindernisse für eine Interaktion ausgeschlossen werden. Rts1-Kin4 und Cdc55-Net1 zeigten in beiden Orientierungen einen Kontakt mit unterschiedlichen Mono- und Trimethylierungsmustern.

Der negative Einfluss von endogenen bait und preys wurde bereits von meinen Kollegen gezeigt, da das Cdc55 Fusionsprotein in Anwesenheit von endogenem Cdc55 und Net1 nicht in den trimeren PP2A-Komplex integrieren kann. Vergleichende Analysen der Stämme mit endogenen Substraten mit jenen ohne diese Substrate zeigten in drei der vier Fälle eine stärkere Monomethylierung im Einzel Knock-Out Stamm.

Da Überexpression der Fusionsproteine zu falsch positiven Ergebnissen führen kann, wurde der Cdc55 bait in das *S.cerevisiae* Genom integriert. Nach einer IP wurden auf endogenem Level mit überexprimiertem Net1 noch sehr schwache Methylierungssignale gefunden. Zusätzlich wurde eine alternative, Tetrazyklin regulierte Expression des Rts1 bait eingeführt, um die Expressionslevels der Fusionsproteine zu modulieren.

Ergebnisse dieser Diplomarbeit wiesen darauf hin, dass sterische Parameter die vorhandene Methylierungsspezies beeinflussen können und dass das Vorhandensein endogener Substrate M-Track nicht oder kaum beeinflusst. Die Substrat-Detektierung auf endogenen Levels zeigte sehr schwache Signale und muss noch optimiert werden.

Table of Contents

1 Introduction

1.1 Regulation of proteins by (de)phosphorylation processes

Protein phosphorylation is a common mechanism in cell signaling to control and regulate the activity of diverse substrates. An estimated third of all eukaryotic proteins is modified with a phosphate residue (Virshup & Shenolikar, 2009) thereby altering protein specific properties such as catalytic activity and subcellular localization as well as causing structural changes (Ptacek et al, 2005).

A posttranslational phosphor modification is an essential regulation tool for processes like signal transduction, cell cycle control and apoptosis. The fast, dynamic and reversible process of phosphorylation depends on the interplay of two groups of enzymes, protein kinases and protein phosphatases. The addition of a phosphor group is performed by protein kinases, while the counteracting process of dephosphorylation is catalyzed by protein phosphatases (Zolnierowicz, 2000).

The phospho-dependent regulation of proteins in eukaryotic cells primarily takes place on three different amino acid residues, namely serine (Ser), threonine (Thr) and tyrosine (Tyr). The Ser residue is identified as predominant target (86.4%), whereas Thr and Tyr are modified in 11.8% and 1.8% of examined cases, respectively (Shi, 2009; Olsen et al, 2006). The classification of protein kinases and phosphatases is based on the amino acid residues they target: Ser/Thr-specific and Tyr-specific enzymes (Figure 1). A third subgroup of protein phosphatases, the so-called dual specificity phosphatases (DSPs), is capable of targeting both, phospho-Tyr and phospho-Ser/Thr residues (reviewed by Patterson et al, 2009).

Until recently, 518 human protein kinases have been identified (Johnson & Hunter, 2005) in contrast to only 137 currently known protein phosphatases, which operate as antagonists (Alonso et al, 2004). Tyr-specific enzymes comprise approximately the same number of protein Tyr kinases (PTKs, 90) and phosphatases (PTPs, 107) of about 100 modifying enzymes. In contrast, the number of protein Ser/Thr phosphatases (PSTPs, 30) is about fourteen-fold less than the amount of antagonizing kinases (PSTKs; 428; reviewed by Shi, 2009).

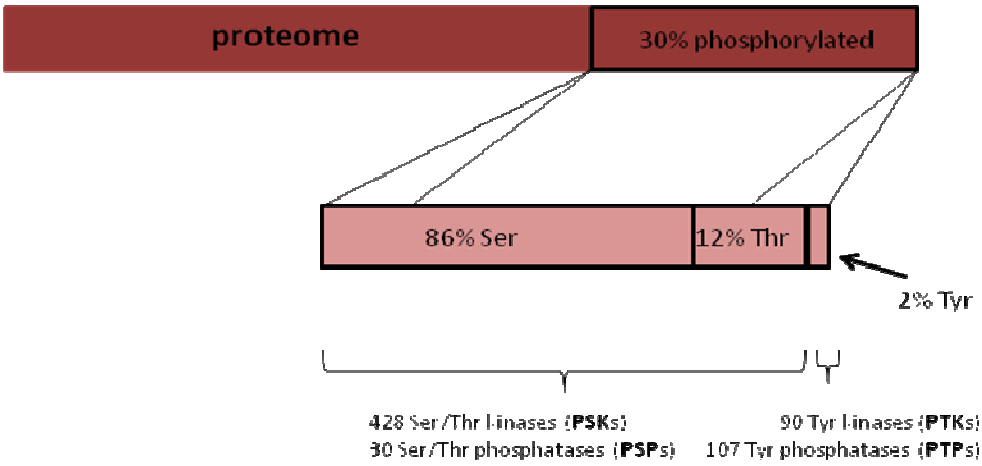

Figure 1. Phosphorylation processes within a cell. Approximately one third (30%) of the total proteome is posttranslationally modified by phosphorylation. The addition of phosphor groups can take place at three different amino acid residues: serine (Ser), threonine (Thr) and tyrosine (Tyr). As shown, with 86% Ser is targeted the most frequent. The brackets illustrate the subgrouping of kinases and phosphatases according the amino acid they target into Ser/Thr and Tyr modifying enzymes. Corresponding numbers of kinases (protein serine/threonine kinases (PSKs) and protein tyrosine kinases (PTKs)) and phosphatases (protein serine/threonine phosphatases (PSPs) and protein tyrosine phosphatases (PTPs)) are shown below (data from Olsen et al, 2006).

1.2 Mechanism of dephosphorylation by protein phosphatases

The process of dephosphorylation has been intensively studied in the last decades and differences in the mechanism of how these enzymes dephosphorylate the target proteins have been detected. PTPs and DSPs perform the dephosphorylation process via a transient intermediate cysteinyl phosphate group (Denu & Dixon, 1995). In contrast, it was revealed that PSTPs mediate the dephosphorylation reaction by hydrolysis of the phosphate group in a single step without an intermediate product (Barford, 1996). Hence, the process of dephosphorylation is short-lived and PSTPs only show transient interactions with their substrates without forming a covalent binding. As detection and identification of PSTP substrates is therefore hindered, this diploma thesis focuses on their specific transient substrate interactions and a recently developed method that tries to identify targeted substrates (Zuzuarregui et al, 2012).

1.3 Classification and structure of protein Ser/Thr phosphatases

As reviewed by Shi (2009), PSTPs are metallo-phosphoesterases and require metals in their active center for both, efficient catalysis as well as structural integrity. The PSTP family is currently subdivided according to the structure of the catalytic domain into three large families: phosphoprotein phosphatases (PPPs), metal dependent protein phosphatases (PPMs) and aspartate based transcription factor IIF (TFIIF) associating component of RNA polymerase II CTD phosphatases/small CTD phosphatases (FCPs/SCPs). PPPs include members like Protein Phosphatase 1 (PP1), Protein Phosphatase 2B (PP2B), Protein Phosphatase 4 (PP4) and Protein Phosphatase 2A (PP2A), which is the focus of this diploma thesis, as well as many others. PPMs need, as depicted by their designation, metal ions for their catalytic activity and comprise for example the Protein Phosphatase 2C (PP2C) enzyme. FCPs use a special mechanism for gaining phosphatase activity which is based on the amino acid aspartate and include amongst others the enzymes TFIIF associating component of RNA polymerase II CTD phosphatase 1 (FCP1) and small CTD phosphatase 1 (SCP1; reviewed by Shi, 2009).

The limited number of protein phosphatase catalytic subunit genes (30) has to counterbalance the activity and substrate specificity of a vast majority of protein kinases (428). The difference in number of counteracting enzymes consequently leads to the question how the seemingly lower number of PTSPs can be compensated. As revealed, the amount of PSTPs is not actually low as they build multisubunit complexes (reviewed in Shi, 2009). Usually, these complexes are represented by two or three different subunits, which can be assembled to different dimeric as well as trimeric holoenzymes. Their diversity derives from this combinatorial assembly of the single components, which provides a compensatory mechanism for the low numbers of PSTPs. This multisubunit architecture enables the enzymes to cope with a huge pool of substrates in different cellular compartments (Virshup & Shenolikar, 2009).

1.4 Protein Phosphatase 2A (PP2A): functions and subunits

One representative member of the PPP family of PSTPs is PP2A, which represents a key enzyme in many cellular activities and regulatory pathways. PP2A functions as a multimeric holoenzyme and is highly conserved between yeast and human. It is involved in processes like cell cycle regulation, programmed cell death, cell mobility and cytoskeleton dynamics (Xu et al, 2006) as well as in signal transduction like in the human mitogen activated protein (MAP) kinase pathway (Silverstein et al, 2002) and in the yeast target of rapamycin (TOR) pathway (Jiang & Broach, 1999).

Furthermore, PP2A regulates (viral) DNA replication and translation of e.g. simian virus 40 (SV40; Arroyo & Hahn, 2005; Janssens et al, 2005) and Cohesin cleavage during meiosis (Clift et al, 2009; DeWulf et al, 2009) and therefore seems to play an important role in cancer development and other pathological processes. Indeed, it could be shown that a deregulation of PP2A enzyme is linked with diverse pathological conditions like cancer (Junttila et al, 2007; Chen et al, 2004; Calin et al, 2000) and Alzheimer´s disease (Sontag et al, 2004; Price & Mumby, 1999). Mutational defects of PP2A subunits are linked to a variety of human tumors (Ruediger et al, 2001). Results of various gain- and loss-of function experiments indicate a role of PP2A as an important tumor suppressor (Sablina et al, 2010; Janssens et al, 2005).

Moreover, some data indicate that in yeast defects of PP2A catalytic subunit result in a cell cycle arrest at the G2-M transition (Evans & Stark, 1997). In mouse (Götz et al, 1998) a deletion of the catalytic subunit Cα encoding gene and in rat cells the absence of the Aα subunit (Strack et al, 2004) have been shown to be lethal, demonstrating that PP2A is essential in controlling cellular survival.

The prototypical form of PP2A is a multisubunit holoenzyme composed of three core subunits - catalytical, structural and regulatory - which enable the enzyme to target a broad variety of specific substrates in different cellular localizations. In a first step, a dimeric core enzyme is built of the structural A and the catalytic C subunit (Shi, 2009; Mumby, 2007). The attached regulatory B subunit coordinates the subcellular localization and substrate specificity of the differently built heterotrimeric holoenzymes (Virshup & Shenolikar, 2009). Structural analysis of the PP2A heterotrimer revealed that a horseshoe shaped A subunit ideally positions the regulatory B and catalytic C proteins (Shi, 2009; Xu et al, 2006). The association of a PP2A enzyme composed of a scaffold A, a catalytic C and a regulatory B subunit is schematically shown in Figure 2.

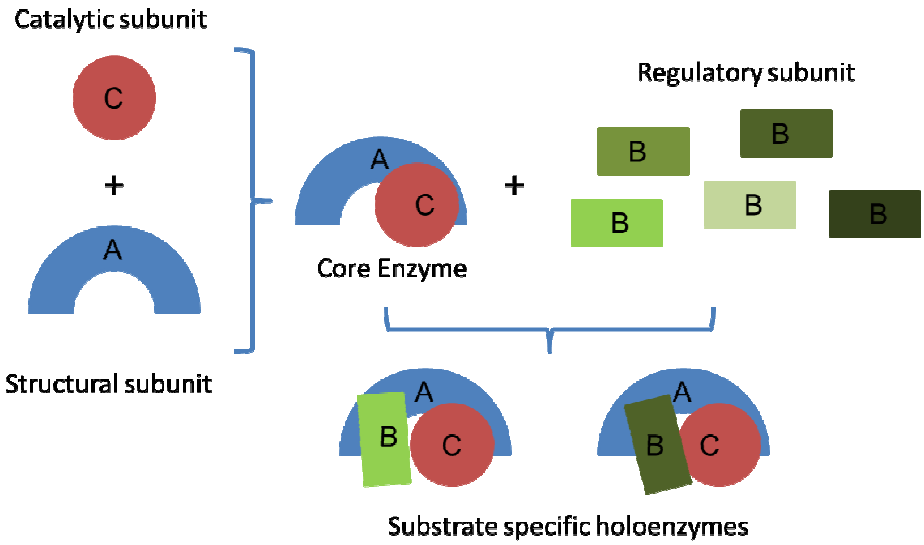

Figure 2. Schematic illustration of the PP2A holoenzyme assembly. The catalytic C subunit (red) interacts with the structural A subunit (blue) to build a dimeric PP2A core enzyme. Upon addition of one out of a large pool of regulatory B subunits (green) the substrate specificity of the PP2A enzyme is gained. The trimeric holoenzyme is capable of targeting different substrates depending on the incorporated regulatory subunit (data from Janssens & Goris, 2001)

Structural (A), catalytic (C) and regulatory (B) subunits of PP2A in mammals and budding yeast are summarized in Table 1.

Table 1. Summary of the three subunits of PP2A in mammals and yeast

	Mammal	**Yeast**
Structural A subunit	α/β	TPD3
Catalytic C subunit	α/β	PPH21/PPH22
Regulatory B subunit	B - PR55 (α, β, γ, δ) B' – PR61 (α, β, γ, δ, ε) B'' – PR48/59/72/130 B''' – Striatins (STRN, STRN3, STRN4)	CDC55 RTS1 RTS3 ?

1.4.1 Mammalian Protein Phosphatase 2A

The mammalian PP2A can be assembled out of two isoforms of the A and C subunit and out of a large pool of at least 16 members of B subunits (see Table 1). As some of the regulatory B subunits are alternatively spliced and translated, they give rise to at least 23 different subunits. Given the occurrence of a large pool of regulatory B subunits, more than 100 different trimeric mammalian PP2A holoenzymes can be assembled (reviewed Sents et al, 2012). Hence, generated PP2A holoenzymes can dephosphorylate numerous substrates at various cellular localizations. As PP2A comprises not only one single enzyme but rather many different enzyme subtypes the functions vary from dephosphorylation of microtubule binding protein Tau (Xu et al, 2008) to the interaction with Shugoshin (Kitajima et al, 2006; Riedel et al, 2006).

The catalytic subunit as well as type 2A related protein phosphatases like Protein Phosphatase 4 (PP4) and Protein Phosphatase 6 (PP6) seem to be in complex with alpha4 in mammalian cells. The contact of alpha 4 and the catalytic subunit has been suggested to inhibit the catalytic activity of PP2A in-vitro (reviewed by Yu et al, 2001). Moreover, PP2A targets methyltransferases and methylesterases as the catalytic subunit is specifically methylated by these enzymes e.g. in human leucine carboxyl methyl transferase 1 and 2 (LCMT 1 and 2) and PP2A methyl esterase 1 (PME1). This modification allows the association of the dimeric core enzyme with the third regulatory subunit (Wei et al, 2001; reviewed in Sents et al, 2012). Moreover, PP2A is regulated by phosphatase 2A phosphatase activator (PTPA), which was formerly known as phosphotyrosyl phosphatase activator. PTPA has been shown in-vitro in rabbit skeletal muscle cells to activate the phosphotyrosyl phosphatase activity of the PP2A core enzyme (Cayla et al, 1990). As summarized by Sents et al (2012) PTPA is part of a large number of molecules that is responsible for controlling the activity as well as the biogenesis of PP2A.

1.4.1.1 Three subunits of the mammalian PP2A holoenzyme

Structural studies revealed that the two isoforms α and β of the catalytic C subunit share 97% identity in their primary sequence (Arino et al, 1988). Furthermore, sequence analyzes confirmed large homology to catalytic subunits of other PSTPs and thereby proved the conservation of PP2A throughout evolution (Cohen et al, 1990). The interface of the catalytic C and regulatory B subunit is built of two major areas in which a change of one amino acid can lead to different enzymatic function. In one area the HEAT repeats interact with an α-helix of the C subunit via hydrogen bonds whereas in the other area the C-terminus of the catalytic subunit is placed in an acidic groove between the structural and the regulatory

subunit. A methylation modification of this C-terminus leads to a negative charge which enables a better interaction with the A and B subunit (Xu et al, 2006). Therefore, the regulation of the catalytic subunit by modification of the C-terminal tails seems to have a critical role in the regulation of the PP2A activity (Longin & Goris, 2006; Yu et al, 2001). The phosphorylation and methylation of Y307 and L309 might have an influence on the assembly of the regulatory subunit to the core enzyme (Longin et al, 2007). Interestingly, Xu et al (2006) describe, that the methylation of the C subunit seems to have almost no direct influence on the assembly of the PP2A-B' in-vitro. Furthermore in 2008 the Xu lab suggests that the methylation might serve as a signal for the start of PP2A assembly by supporting the correct localization to the target sites. Additionally, they propose that the modification can lead to the recruitment of additional factors for the assembly process (Xu et al, 2008).

In mammals the structural A subunit exists in two isoforms, α and β, which are constitutively expressed and share 86% sequence identity to each other. RNA-analysis of human cells showed that the α isoform was more abundant than the β (Hemmings et al, 1990). Each A type subunit consists of 15 imperfect 39 amino acid long Huntingtin/Elongation factor 3/Protein Phosphatase 2A/TOR1 (HEAT) tandem repeats, which are composed of two anti-parallel α-helices connected by an intrarepeat loop. A change of structural conformation of the A subunit due to interaction of HEAT repeats 11-15 allows the generation of the heterodimeric AC complex. This interaction with the C subunit is mediated by intrarepeat loops and the inner helices of the A subunit HEAT repeats 11-15. The association of the horseshoe shaped structural A subunit with the C subunit provides essential functionality for the whole PP2A enzyme (Cho & Xu, 2007; Xu et al, 2006).

The B subunits are derived from four different subunit families (B, B', B'' and B''') and show a large variety as some of the proteins are alternatively spliced and translated (reviewed in Sents et al, 2012; see Table 1). Shi (2009) suggests that the binding site for substrates is localized on the top face of the enzyme and can be found close to the active site of the catalytic C subunit. The conserved core region of the regulatory subunit interacts with the heterodimeric AC core enzyme. In contrast, the non-conserved N- and C-termini of the regulatory subunits are responsible for regulation of substrate specificity and subcellular targeting (McCright & Virshup, 1995; reviewed by Shi, 2009). McCright et al (1996) could reveal that members of the B' family are 71-88% identical in their conserved core region. Moreover, they revealed that the different members of the B' family target the PP2A to different cellular localizations.

To summarize, the mammalian PP2A complexes are localized on different specific cellular and subcellular compartments and target various substrates depending on the incorporated B subunit (Shi, 2009; Virshup & Shenolikar, 2009; Janssens et al, 2008).

1.4.1.2 Examples for substrates of mammalian PP2A

One of the neuronal functions of mammalian PP2A is the regulation of the phosphorylation state of microtubule-associated proteins like Tau. As the hyperphosphorylation of the protein Tau is one important feature of Alzheimer´s disease it is not surprising that PP2A seems to be linked to this human disease. Hyperphosphorylation of Tau leads to the formation of neurofibrillary tangles, one of the hallmarks of Alzheimer´s disease, which induce neuronal death (reviewed in Janssens & Goris, 2001). Via the Bα subunit the PP2A holoenzyme is localized at the microtubules where it can usually dephosphorylate Tau proteins. Xu et al (2008) describe a model of the binding of the phosphorylated Tau to the B subunit. The full length Tau molecule binds to an acidic groove on the top face of the B subunit, so that it can access the active site of the C subunit. Moreover, Tau seems to harbor at minimum two sites within the microtubule binding repeats to target the B subunits (residues 197-259 and 265-328 mainly consisting of positively charged amino acids) which facilitate the dephosphorylation process (Xu et al, 2008). A decreased Bα subunit expression seems to be linked to the phosphor-Tau pathology as present in Alzheimer´s disease (Sontag et al, 2004).

Vimentin is an intermediate filament protein, which is a phosphoprotein in mammalian cells. The dephosphorylation is important to control its dynamic rearrangement. As Turowski et al (1999) show, an inhibition of PP2A leads to hyperphosphorylation of Vimentin which causes a collapse of these filaments into bundles around the nucleus. These results indicate that Vimentin is directly targeted by PP2A. Moreover, they illustrate that the dephosphorylation seems to occur via the regulatory B55 subunit as a functional knock out of this subunit leads to an increased Vimentin phosphorylation.

The tyrosine hydroxylase (TH) is the rate-limiting enzyme in catecholamine synthesis. Saraf et al (2010) have shown that PP2A dephosphorylates the N-terminal phosphorylation sites of the TH. This dephosphorylation process occurs via an interaction of the TH and the B' β subunit of the PP2A enzyme. Saraf et al (2010) identified one Glutamic acid (Glu) residue within the regulatory subunit which seems to be important for this dephosphorylation and therefore the inactivation of the TH in-vitro.

Many inhibitor studies and knock-out analyzes of PP2A subunits revealed that various cellular processes are regulated by the PP2A holoenzyme (Gallego & Virshup, 2005; Kong et al, 2004; Götz et al, 1998). Due to the fact that PP2A and substrates only interact transiently in a single-step catalytic reaction the identification of substrates is hindered and allowed up to now only a detection via deletion studies. Therefore the Egon Ogris lab introduced a method, to detect and identify further targets of PP2A in-vivo and to analyze its role in cellular pathways (Zuzuarregui et al, 2012).

1.4.2 Yeast Protein Phosphatase 2A

The PP2A enzyme is highly conserved from yeast to human and thus research analysis is much simpler in the model organism *Saccharomyces cerevisiae*. The combinatorial assembly of the PP2A holoenzyme in yeast allows the building of no more than six different trimeric enzyme complexes, due to the fact that only three B, two C and one A subunit are present (see Table 1).

Alternative complexes can be formed from the PP2A catalytic subunit and the yeast type 2A phosphatase-associated protein 42 (Tap42). Tap42 competes with the A subunit to bind the catalytic subunit (Jiang & Broach, 1999). As Yang et al (2007) describe one conserved positively charged region seems to be important for the Tap42 interaction with the catalytic subunit. In *S.cerevisiae* Tap42 does not only bind the PP2A catalytic subunit but also Suppressor of Initiation of Transcripiton 4 (Sit4), a PP2A related protein phosphatase. Mutations of Tap42 can lead to rapamycin restistance as the Tap42 and PP2A interaction is regulated by the TOR signaling pathway components (DiComo & Arndt, 1996). Moreover, Queralt and Uhlmann (2008) show, that one the PP2A holoenzyme, incorporated with the Cdc55 regulatory subunit, seems to be downregulated by two proteins, Zillion Different Screens 1 and 2 (Zds1 and Zds2). Additionally, Calabria et al (2012) could reveal that the C-terminal domain of Zds1 interacts with the Cdc55 subunit and seems to regulate its localization.

1.4.2.1 Three subunits of yeast PP2A holoenzyme

The two isoforms of the yeast catalytic C subunit Protein Phosphatase 21 and 22 (Pph21 and Pph22) share 74% amino acid sequence similarity to the mammalian catalytic subunit. A double disruption of *PPH21* and *PPH22* genes in yeast leads to severe growth defects as well as abnormal morphology of cells and smaller buds (Sneddon et al, 1990). An overexpression of the catalytic subunit leads to multibudded and multinucleated strains (Shenolikar, 1994).

The tRNA processing deficient 3 (Tpd3) protein, the yeast homolog of the mammalian structural A subunit (44% identity, 19% similarity according to yeastgenome.org), was originally found to be involved in biosynthesis of tRNA. A lack of this component leads to viable cells, but they are multibudded and multinucleated at lower temperature (van Zyl et al, 1992).

Two main variants of regulatory B subunits could be identified in yeast: Cell division cycle mutant 55 (Cdc55) and Rox three suppressor 1 (Rts1), which share sequence homology to B and B' in mammalian cells. The Rts1 regulatory subunit shows 64% sequence

identity and 16% similarity to the human B56γ subunit. The same numbers are true for Cdc55 and the B55β subunit, thereby confirming homology of PP2A regulatory subunits. Based on studies of its interaction partners Rox three suppressor 3 (Rts3) was identified as a component of the PP2A enzyme (Samanta & Liang, 2008). It is a non-essential gene (Giaever et al, 2002) and a deletion of *RTS3* leads to a rapamycin hypersensitivity (Hood-DeGrenier, 2011; Xie et al, 2005). Moreover, it could be shown, that Rts3 interacts with several components of the PP2A holoenzyme (Pph21, Pph22, Cdc55 and Tpd3) as well as PP2A related enzymes like Sit4 (Hood-DeGrenier, 2011).

Gentry and Hallberg (2002) showed that B subunit variants in yeast seem to be far from being equimolar in the cell and Rts1 is up to 12-fold as abundant as Cdc55 (reviewed and questioned by Sents et al, 2012). In contrast, according to the yeast GFP fusion localization database there are 29 more Cdc55 than Rts1 molecules per cell (yeastgfp.yeastgenome.org).

An in-vivo PP2A subunit stochiometry in *S. cerevisiae* revealed that the A, B and C subunits are present at cellular levels in the ratio 1A:4B:8C (Gentry & Hallberg, 2002). This might indicate on the one hand that the structural A subunit is the limiting factor for the assembly of holoenzymes. On the other hand one can suppose that there are a lot more dimeric enzymes and enzymes with another third component present in the cell. In 2003 Ghaemmaghami et al published data of the subunit stochiometry in the ratio 17A:9B:10C. Although both used similar mechanisms to calculate the amounts, the results varied a lot and show that the exact PP2A subunit ratio remains still unanswered up to now.

1.4.2.2 Phenotypes of $PP2A^{Cdc55}$ and $PP2A^{Rts1}$ knock-out strains

Given the importance of the two yeast regulatory subunits for many cellular processes, it is not surprising that knock-out strains, although viable, show many defects.

The Cdc55 incorporated holoenzyme plays multiple roles in mitosis (Wang & Ng, 2006), is necessary for the spindle checkpoint in *S.cerevisiae* and controls late mitotic events (Yellman & Burke, 2006). Phenotype studies have provided insights into Cdc55 knock-out strains, which exhibit a cold sensitive phenotype and show an abnormal pattern of cell surface growth as well as a partially defective cytokinesis and/or cell separation (Healy et al, 1991). Moreover, mutants with defective Cdc55 subunits lack a functional spindle assembly checkpoint (Wang & Burke, 1997) and cannot prevent sister chromatid separation during yeast morphogenesis checkpoint (Chiroli et al, 2007). Studies of *cdc55*Δ strains suppose a promoting function of Cdc55 for the entry into mitosis and the absence of Cdc55 leads to mitotic arrest (Harvey et al, 2011). In meiosis a depletion of Cdc55 can lead to a delayed

meiotic division with randomly segregated chromosomes (Bizarri & Marston, 2011). Furthermore, Kerr et al (2011) could show that Cdc55 meiotic null alleles formed either short or no spindles and did not separate in their spindle pole bodies. These results indicated that Cdc55 is required in meiosis for bipolar spindle assembly.

The Rts1-PP2A complex is mainly involved in cellular stress response and required in cell cycle regulation. Rts1 deletion strains reveal a high temperature sensitive phenotype (Shu et al, 1997), show temperature and osmotic sensitivity (Evangelista et al, 1996) as well as a reduced Heat shock protein 60 (Hsp60) chaperonin level and, on this account, an abnormal heat shock response (Shu & Hallberg, 1995). An *rts1*Δ strain exhibits a phenotype with large buds harboring an undivided nucleus, thereby suggesting a premature stop in G2-M phase. As described by Artiles et al (2009) the absence of Rts1 leads to reduced polar growth as the kinases, that regulate the septins, are inactivated. Moreover, they showed that a loss of Rts1 results in a reduced and delayed expression of some G1 cyclins. Next to its role in cell division and cell growth control Rts1 is involved in many nutrient signaling pathways. As Eckert-Boulet et al (2006) show a deletion of Rts1 influences the SPS-mediated amino acid-sensing pathway negatively as the dephosphorylation process downregulates the signaling in the absence of extracellular amino acids.

Differences of $PP2A^{Cdc55}$ and $PP2A^{Rts1}$ knock-out phenotypes derive from the fact that both regulatory subunits are involved in different processes and thus most probably interact with various target proteins. It has already been demonstrated that Cdc55 and Rts1 are functionally not interchangeable (Shu et al, 1997; Zhao et al, 1997). Furthermore, it has been indicated that the loss of one regulatory subunit cannot be compensated by an overabundance of the other. A Cdc55 deletion phenotype cannot be suppressed by the overexpression of Rts1 and vice versa, an Rts1 null phenotype cannot be complemented by a higher Cdc55 level. Moreover, the Rts1-Cdc55 double knock-out strain shows the characteristic phenotypes of both single knock-out strains (Shu et al, 1997).

1.4.2.3 Putative interaction partners of yeast PP2A

The focus of current research lies on two proposed targets of the yeast PP2A holoenzymes. There exists strong genetic evidence that Nucleolar silencing establishing factor and telophase regulator 1 (Net1) and kinase 4 (Kin4) are targeted and dephosphorylated by the PP2A enzyme (Chan & Amon, 2009; Queralt et al, 2006). Although a lot of information of the two regulatory subunits is already present, no direct interaction to one of these substrates was shown. Therefore the Ogris lab has introduced a method, which is capable of catching the short-lasting PP2A interactions in-vivo and helps to identify and confirm the target proteins (Zuzuarregui et al, 2012).

1.4.2.3.1 Net1: a putative substrate of yeast PP2A^{Cdc55}

Recent publications indicate that PP2A^{Cdc55} seems to dephosphorylate Net 1 (Queralt et al, 2006; Wang and Ng, 2006) in mitotic cells. During meiosis it inhibits Cdc Fourteen early anaphase release (FEAR) network activation (Kerr et al, 2011).

As mitosis in budding yeast is controlled by the activity of cyclin dependent kinases (Cdks) in complex with mitotic cyclins, the mitotic exit requires an inhibition of these cyclin-Cdk complexes. Next to the main inhibition of Cdks via cyclin destruction a dual specificity protein phosphatase, Cell division cycle 14 (Cdc14) is important for the regulation (Mocciaro & Schiebel, 2010). During M phase phosphorylation of Cdks has to be maintained whereas a removal of these modifications leads to the exit of mitosis (Castilho et al, 2009).

Cdc14 is kept inactive from G1 until anaphase and sequestered in the nucleolus by its inhibitor Net1 (Traverso et al, 2001). Net1, as a component of the protein complex regulator of nucleolar silencing and telophase (RENT) together with Cdc14, Silent information regulator 2 (Sir2) and one yet uncharacterized component (Shou et al, 1999), is required for nucleolar integrity and for the localization of Cdc14 to the rRNA (Visintin et al, 1999). In early anaphase the FEAR network promotes a Cdk dependent phosphorylation of Net1 and thereby releases Cdc14 from the RENT complex partially into the nucleoplasm (Queralt et al, 2006). As Azzam et al (2004) found, a phosphorylated variant of Net1 shows less affinity for Cdc14 and therefore no longer inhibits it. The partial Cdc14 release is important for anaphase related tasks such as stabilization of the anaphase spindle (Khmelinskii et al, 2009). The full release of Cdc14 into the cytoplasm is controlled by the mitotic exit network (MEN), which is an important process for mitotic exit (Jaspersen et al, 1998). This network includes the GTPase Termination of M phase 1 (Tem1), which binds to the downstream kinase Cell division cycle 15 (Cdc15; Asakawa et al, 2001). As a result, Cdc15 can activate the DumbBell Forming 2 - Mps One Binder 1 (Dbf2-Mob1) kinase complex (Mah et al, 2001). The Dbf2-Mob1 complex phosphorylates Cdc14 and induces thereby the promotion of the mitotic exit (Mohl et al, 2009).

In a *CDC55* deletion strain Queralt et al (2006) could coprecipitate less Cdc14 from Net1 due to hyperphosphorylation of Net1. Thereby they could indirectly show that PP2A^{Cdc55} counteracts the Net1 phosphorylation. This supports the idea that at the onset of anaphase a separase-dependent downregulation of PP2A promotes the phosphorylation of Net1 leading to free Cdc14 (Queralt et al, 2006).

Furthermore, loss of PP2A^{Cdc55} activity leads to a premature FEAR activation in meiosis and therefore blocks bipolar spindle assembly and nuclear division (Kerr et al, 2011). Additionally, it was revealed that the first 600 amino acids of the Net1 protein are already sufficient for its regulatory control of Cdc14 in yeast (Azzam et al, 2004). These experiments

suggest that Cdc55 might interact with Net1 via its first 600 amino acids although it has not been confirmed experimentally.

1.4.2.3.2 Kin4: a putative substrate of yeast PP2A^{Rts1}

Kin4 is a Ser/Thr protein kinase and is localized asymmetrically to the mother cell cortex. In mitosis Rts1 regulates the spindle position checkpoint kinase Kin4 during the cell cycle entry by regulating its localization to spindle pole bodies via dephosphorylation (Chan & Amon, 2009). Kin4 seems to be not functionally involved in the meiotic divisions as described by Attner and Amon (2012).

Kin4 was identified in a genetic analysis where a deletion of *KIN4* decreased the number of surviving *kar9*Δ cells (Tong et al, 2004). Because the karyogamy 9 (Kar9) mutant strain showed misaligned spindles and relied on the spindle position checkpoint (SPOC) for survival, Kin4 was suggested to be an important part of the SPOC (D'Aquino et al, 2005; Pereira & Schiebel, 2005). Experiments revealed that *KIN4* knock-out strains cannot arrest in anaphase in response to spindle misalignment whereas high Kin4 levels are correlated with an anaphase arrest. Moreover, it was shown that Kin4 is not necessary for metaphase arrest which occurs upon microtubule depolymerization (D'Aquino et al, 2005; Pereira & Schiebel, 2005).

Kin4 is present in cell cortex throughout cell cycle but during anaphase Kin4 is found at the spindle pole body of the mother cells. In cells with misaligned spindles it is localized at both spindle pole bodies where it phosphorylates Byr four alike 1 (Bfa1) in response to a spindle mispositioning in anaphase. The phosphorylation inhibits further phosphorylation of Bfa1 by the Polo kinase Cell division cycle 5 (Cdc5) in-vivo (Pereira & Schiebel, 2005). The phosphorylation of Bfa1 by Kin4 promotes the Bfa1-Bub2 (budding uninhibited by benomyl 2) GAP activity. The Bfa1-Bub2 GAP complex in further consequence activates the GTP hydrolysis of Tem1, thus inhibiting Tem1 and mitotic exit (Geymonat et al, 2002; Lee et al, 2001).

The Kin4-dependent activation of the Bfa1-Bub2 GAP complex is counteracted by the kinase Cdc5. If the spindle is correctly aligned, Cdc5 catalyzes the phosphorylation of Bfa1 which inactivates the Bfa1-Bub2 complex. In further consequence Tem1 can activate Cdc15, which causes an activating phosphorylation of the Dbf2-Mob1 kinase complex (Mah et al, 2001). The Dbf2-Mob1 complex can then promote the dissociation of Cdc14 from Net1 and thereby initialize the mitotic exit (Mohl et al, 2009).

The role of Kin4 in SPOC depends on its localization and on its activity. The correct localization of Kin4 seems to be mediated via dephosphorylation by PP2A^{Rts1} (Chan & Amon,

2009). Data suggests that that $PP2A^{Rts1}$ controls Kin4 by localizing it to the spindle pole body as this is the site for the activation of Bfa1-Bub2. The association to the spindle pole body might be achieved via the dephosphorylation by Rts1. Rts1 keeps Kin4 in a hypophosphorylated state during S phase and mitosis and it is rephosphorylated by Low Temperature Essential 1 (Lte1) during the mitotic exit (Bertazzi et al, 2011). As findings of Chan & Amon (2009) indicate, an inhibition of the spindle pole body binding of Kin4 impairs its proper function in SPOC even when the spindle is misaligned.

When examining Kin4 proteins in deletion strains, hyperphosphorylated Kin4 proteins can be detected indicating a contact between Rts1 and Kin4 (Caydasi et al, 2010; Chan & Amon, 2009). As Pereira and Schiebel (2005) have already demonstrated a knock-out of Kin4 does not have any severe outcome and cells behave like wild type strains. Experiments of the phosphorylation state of Kin4 in *cdc55*Δ and *rts1*Δ have revealed that only the Rts1 regulatory PP2A subunit seems to dephosphorylate Kin4 as in *cdc55*Δ strains the phosphorylation level of Kin4 was comparable to that of wild type strains (Chan & Amon, 2009). In a recent publication Chan & Amon (2010) demonstrate the importance of the C-terminus of Kin4 for its localization as Kin4 lacking the C-terminal 146 amino acids cannot localize to the spindle pole body and therefore cannot engage the SPOC. Moreover, results show that Kin4 mediates the inhibition of mitotic exit via its N-terminal kinase domain.

The results of various knock-out experiments allow for the assumption that Net1 and Kin4 provide potential targets of the *S.cerevisiae* regulatory subunits Cdc55 and Rts1. Although many research groups have already attempted to identify Cdc55 and Rts1 interaction partners in-vivo the majority of interacting proteins could be identified via genetic screens (see Saccharomyces Genome Database).

A detection of PP2A substrates is difficult by the fact that PP2A targets its substrates only via short-lived and transient interactions. Despite the important role the B subunit plays for the PP2A holoenzyme, little is known about how they target the phosphatase to its substrates as they might not recognize specific sequences or motifs within their substrates (reviewed by Virshup & Shenolikar, 2009). Up to now the finding of such target sites within substrates is not that simple, but might be possible when some substrates are already identified. By using current methods it is impossible to identify these short-term enzyme-substrate interactions. As recent publications illustrate, mainly genetically defined interactions of PP2A and substrates could be detected up to date in Drosophila (Archambault et al, 2007; Chen et al, 2007; Silverstein et al, 2002). Therefore the Ogris lab has introduced a new method to detect transient and short-lived interactions such as these from PP2A and target substrates (Zuzuarregui et al, 2012).

1.5 M-Track: detection of transient protein - protein interactions

Identification of PP2A substrates is an essential determinant for gaining information about the role of the ubiquitous enzyme in controlling biological processes. To date, analysis of protein-protein interactions is relying on methods, which are based on a stable enough contact to survive lysis and purification procedures. Hence, an identification of transiently interacting PP2A substrates is almost impossible.

So far many approaches have been developed to investigate interactions in living cells for example Fluorescence Resonance Energy Transfer (FRET), Fluorescence Lifetime Imaging Microscopy (FLIM), Bimolecular Fluorescence Complementation (BiFC), Fluorescence Correlation Spectroscopy (FCS), but PP2A substrates have mainly been discovered in genetic screens (yeastgenome.org). The first step to the method applied for detection of PP2A substrates was the development of a Yeast-Two-Hybrid system by Fields and Song (1989). A newly developed method M-Track is based on this Yeast-Two-Hybrid system (tools provided by G. Ammerer). The concept of M-Track relies on a histone methyltransferase fused to a bait whereas its substrate, the N-terminal part of Histone 3 (H3) is fused to a prey protein. In the Ogris lab the bait protein is fused via a Glycine linker (GL) to a mutant SET domain (H320R, 20 fold increased activity) of a human Suv39H1 Histone Lysine 9 (K9) methyl transferase (HKMT), which catalyzes the mono-, di- and tri-methylation of K9 on the N-terminus of H3 (Cheung et al, 2000; Rea et al, 2000). The methyltransferase creates a permanent modification on K9 of the H3-tagged prey, which can be detected by specific monoclonal antibodies in a Western blot. Thereby the HKMT-H3 contact enables us to create a permanent label to detect short-lived PP2A interactions (Zuzuarregui et al, 2012).

In the N-terminal bait construct a myc-epitope tag is added next to the HKMT enzyme and the fusion construct is set under the control of the galactose inducible Gal1 promoter (myc HKMT GL bait). The prey protein is fused to three or four times tandemly repeated N-terminal H3 tags of 21 amino acids length (3H3 or 4H3), the target site of the HKMT. This construct is fused to a double hemagglutinine epitope tag (2HA) which is connected via a Glycine linker (GL) to the prey coding sequence. The whole prey construct is under the control of a constitutive TPI promoter (4H3 2HA GL prey). If there is a contact between the bait and its potential prey, also an interaction between the HKMT and the H3-tag is possible (Figure 3). This should enable an HKMT mediated methylation of the K9 on the H3-tag. The transferred methylation marks can be detected later on via specific monoclonal antibodies.

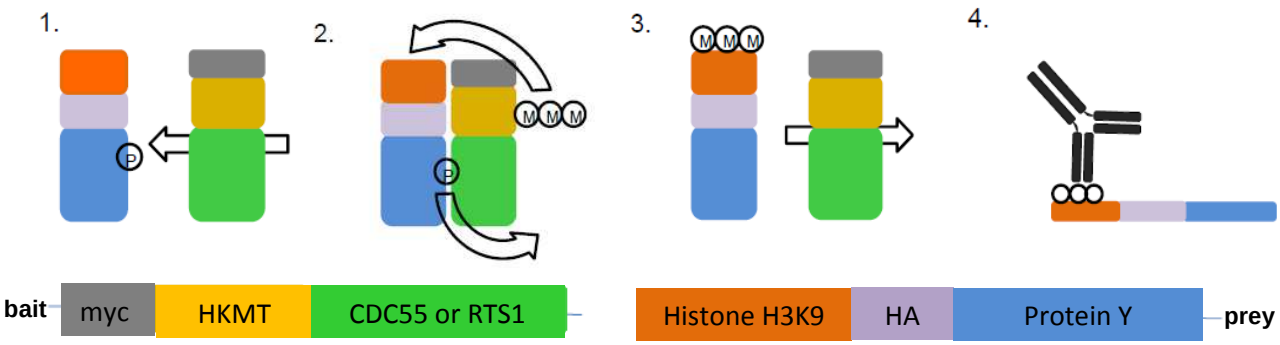

Figure 3. Schematic illustration of the M-Track method. (1.) The bait, the regulatory B subunit (green; Cdc55 or Rts1) recognizes its H3-tagged and phosphorylated substrate (blue; Protein Y). (2.) During the dephosphorylation process, the Histone Lysine (K) 9 methyl transferase (HKMT; yellow) transfers up to three methyl groups to the Histone 3 Lysine 9 (H3K9; orange) tag, which is fused to Protein Y. (3.) After detaching from the bait fusion protein, the methyl marks are still present on the prey protein and can be detected by monoclonal antibodies on a Western blot (4.).

The M-Track method is carried out in the model organism *S.cerevisiae* which lacks homologues of H3K9 specific HKMTs and thereby no unspecific methylation should occur. Moreover *S.cerevisiae* does not possess any H3K9 specific demethylases and thus the methylation mark on the PP2A substrates is present until the detection with monoclonal antibodies. In summary, in this method a persistent mark is generated as a read-out of the PP2A-substrate interaction process.

1.6 Aims of this diploma thesis

This diploma thesis aimed to further develop the novel method termed M-Track that the Ogris lab has pioneered for the detection of transient interaction between PP2A and its putative substrates (Zuzuarregui et al, 2012). New substrates remain to be discovered and analyzed in detail to understand more about the role of PP2A in intracellular pathways. Unfortunately, the transient and short-lived interaction between PP2A regulatory subunits and their substrates complicate analyzes and only allow a confirmation of PP2A interaction partners in deletion studies. As today´s methods are not capable of catching these short-lasting interactions a new assay, M-Track was adapted in the Ogris lab to discover putative substrates of the PP2A enzyme in-vitro (Zuzuarregui et al, 2012). The principle behind the M-Track method is to detect the interaction of two proteins via an enzyme catalyzed protein modification of the prey fusion proteins. Egon Ogris hypothesized that this enzyme based assay can overcome the problems of current methods to detect transient PP2A-substrate interactions. Indeed, research in his lab had already revealed that the Cdc55 substrate Net1 and the Rts1 substrate Kin4 could be detected by M-Track in-vivo (Zuzuarregui et al, 2012).

When using M-Track the influence of steric parameters and overexpression of fusion constructs as well as the presence of competing endogenous substrates might have an influence on the outcome of obtained results. Thus, the major goals of this study were to analyze the already identified substrates to prove the validity of results gained so far. To examine the influence of steric parameters on the interaction the fusion constructs were orientated differently. To analyze the interaction with fusion constructs under physiological conditions the bait constructs were integrated into the yeast genome. The competition of endogenous substrates was tested when comparing deletion strains with either bait only or with bait and prey double knock-out.

On the basis of the two interactions mentioned I further developed and characterized the M-Track method. Moreover, I focused on confirming previously gained results of my colleagues regarding the HKMT only constructs and on repeating experiments to illustrate Cdc55 and Rts1 complementarity.

With the results obtained by former lab members and the ones obtained in my diploma thesis we tried to establish M-Track guidelines, which should be applied for the characterization of putative transient interactions in M-Track assays. The usage of these guidelines should reduce the probability of obtaining false (positive) results and enable us to establish M-Track as the method of choice to detect transient interactions in-vivo.

2 Materials & Methods

2.1 Working with yeast

Solutions and media:

2xYP: dissolve 20g Yeast Extract, 40g Peptone in 800ml H_2O; autoclave

4% Agar: add 10g Agar (Applichem #A0949) to 250ml H_2O; autoclave

20% Glucose: dissolve 100g D(+)-glucose-monohydrat in 500ml H_2O; autoclave

10% Raffinose: dissolve 10g raffinose-pentahydrat in 100ml H_2O

20% Galactose: dissolve 100g D(+)-galactose in 500ml H_2O; filtersterilize

2x Complete Medium (CM): dissolve 3.4g Bacto YNB (w/o amino acids and $(NH_4)_2SO_4$), 2.86g Amino Acid Mix and 10g $(NH_4)_2SO_4$ in 740ml H_2O adjust to pH 5.5-6.0 with NH_3; autoclave

100xURA: dissolve 0.4g L-Uracil in 100ml H_2O; autoclave; store at room temperature

100xHIS: dissolve 0.6g L-Histidine in 100ml H_2O; autoclave; store at room temperature

100xLEU: dissolve 2.6g L-Leucine in 100ml H_2O; autoclave and store at -20℃

100xTRP: dissolve 0.8g L-Tryptophan in 100ml H_2O; store at 4℃ in the dark

YP-D: mix 200ml 2xYP, 50ml 20% glucose and 250ml H_2O; for plates use 250ml 4% Agar instead of H_2O

Complete minimal (CM) drop-out media: mix 50ml 20% glucose (or 50ml 20% galactose supplemented with 5ml 10% raffinose), 185ml 2x CM and 250ml sterile H_2O. Add 5 ml of 100xTRP. Depending on the selection medium prepared add 5ml 100xLEU and/or 5ml 100xURA and/or 5ml 100xHIS. Store at 4ºC. For selection plates use 250ml 4% Agar instead of H_2O.

1xGSD + Tris: mix 3ml 3xGSD, 4.65ml H_2O and 1.35ml of 1M Tris unbuffered

10xTE: dissolve 2.42g Tris, 0.74g Ethylenediaminetetraacetic acid (EDTA) in 200ml H_2O; adjust to pH 7.5

10xLiAc: dissolve 10.2g Lithium Acetate (LiAc) in 100ml H_2O; adjust to pH 7.5

LiAc TE: mix 10ml 10xTE, 10ml 10xLiAc and 80ml H_2O; store at room temperature

PEG/LiAc TE: mix 100g 40% PEG, 25ml 10xTE, 25ml 10xLiAc and fill up to 250ml with H_2O

STET buffer: mix 20g sucrose, 12.5ml TritonX-100, 25ml 0.5M EDTA and 12.5ml 1M Tris/HCl pH 8

Saccharomyces cerevisiae strains

S.cerevisiae strains used during this work are summarized in Table 2 below.

Table 2. Summary of *S. cerevisiae* strains used during this diploma thesis;

Name	**Relevant genotype**	**Source**
BY4741, wt	Mat a*; his3Δ1; leu2Δ0; met15Δ0; ura3Δ1*	Euroscarf
rts1Δ	BY4741 Mat a*; his3Δ1; leu2Δ0; met15Δ0; ura3Δ1; YOR014w::kanMX4*	Euroscarf
cdc55Δ	BY4741; Mat a*; his3Δ1; leu2Δ0; met15Δ0; ura3Δ1; YGL190c::HIS3MX6*	Ogris Lab
rts1Δ/kin4Δ	BY4741; Mat a*; his3Δ1; leu2Δ0; met15Δ0; ura3Δ1; YOR014w::kanMX4;YOR233W::natNT2*	Ogris Lab
cdc55Δ/net1Δ	BY4741; Mat a*; his3Δ1; leu2Δ; met15Δ0; ura3Δ1; YGL190c::HIS3MX6; YJL076W::natNT2* As a Net1 knock-out is not viable in the BY4741 context this strain is always supplied with a Net1 expressing plasmid.	Ogris Lab

LiAc transformation yeast

In the morning dilute an overnight culture 1/20 and grow it for 4h at 30℃. Centrifuge cells at 3500rpm and dissolve the pellet in 1ml LiAc TE. Shortly spin down the mixture and once again resuspend the pellet in less volume of LiAc TE. Finally incubate the cells on 30℃ for 15min at 1100rpm. In the meanwhile prepare a trafo mix: 3µl DNA (100ng - 1µg plasmid DNA), 36µl LiAc TE, 31µl H_2O, 20µl sheared Salmon Sperm and 240µl PEG/LiAc TE (amount for 1 transformation). For the transformation take 100µl of competent cells, spin down the cells and resuspend them in the transformation mix. First incubate the mixture at 30℃ for 30min at 1100rpm and afterwards incubate at 42℃ for 20min at 1100rpm. After shortly spinning down the transformed cells, wash pellet once with H_2O and plate the cells on the appropriate selection plate.

Transformation by electroporation of yeast cells

Harvest an overnight culture at 3000rpm in a 50ml Falcon tube and resuspend the pellet in 8ml H_2O, 1ml 10xTE and 1ml 1M LiAc. Incubate this mixture for 1h at 30℃, 150rpm and then add 250µl 1M DTT and incubate again for 30min at 30℃, 150rpm. Fill up the tube with sterile water and centrifuge cells and wash once with cold water and once with cold 1M Sorbitol. Finally resuspend pellet in 550µl 1M Sorbitol. For transformation use 43µl of competent cells, add 7µl of DNA (>3µg PCR knock-out cassette, for in-vivo cloning: 100ng vector backbone and 300ng insert) and transfer the mixture to an electroporation cuvette. After the electroshock (Bio Rad gene pulser 200Ω, 1.5kV, 25µF, time ~4.6) add 950µl YPD to the cell solution and shake for 1h at 30℃. Finally streak cells on the appropriate selection plate.

M-Track time course

Grow yeast strains in raffinose-CM drop out media at 30℃ overnight. The next day dilute the cultures to an OD_{600} of 0.5 and grow the cells for 2h at 30℃. Split cell culture and add glucose (uninduced) or galactose (induced) to a final concentration of 2%. Harvest at indicated time points the OD_{600} equivalents and prepare a yeast TCA crude extract from pelleted cells (see Working with proteins).

Check Flipping of Gal1 promoter

After transformation of a pYES Cre expression vector restreak the transformants and then set up an overnight culture in media with and without galactose. The next day dilute the cultures to 100 cells per plate and streak the cells on YPD plates. Patch the grown cells onto two plates, one YPD plate and one YPD plate containing Kanamycin. The cells grown can then be distinguished between those still harboring the Gal1 promoter (grow on YPD-Kan and YPD) and those which have floxed out the Gal1 promoter (grow only on YPD).

5’ FOA treatment

Inocculate an overnight culture of a strain with a genomically integrated Cdc55 fusion protein and an endogenous P_{Gal} regulated Cdc55 fusion protein as a negative control both harboring the pYES Cre plasmid (Ura3 marker) in glucose based media. Add 800µg/ml 5’ FOA and the next day measure the OD_{600} of the cultures. Calculate the number of cells per ml as 1 OD_{600} equals $1*10^7$ cells per ml. Dilute the samples with H_2O to 100 cells per plate and streak on YPD plates. Restreak the grown colonies on two different plates: one with Glu CM - Ura and one with YPD containing 800µg/ml 5’ FOA. The latter one is harboring the colonies where the pYES Cre expression plasmid (Ura3 marker) is removed.

Plasmid Rescue

Harvest 1.5ml of an overnight culture by centrifugation for 3min at 6000rpm and take off the supernatant. Add 200µl of STET buffer and 0.2g of glass beads to break the cells in a FastPrep (45sec, 5m/s). Add 100µl STET buffer and boil samples for 3min at 95°C. Then put samples on ice and pellet them for 10min at 14000rpm at 4°C. Mix 100µl of the supernatant with 60µl 7M CH_3COONH_4 and incubate at least 1h at -20°C. Then again spin down samples and add 100µl of the supernatant to 200µl ice cold 100% Ethanol. Place at -20°C to pellet DNA and then spin samples. In a next step wash DNA pellet with 200µl ice cold 70% Ethanol and spin again. After removing the Ethanol dissolve the pellet in 20µl H_2O.

2.2 Working with bacteria

Bacterial Solutions

Luria Bertani (LB)-medium: dissolve 5g Tryptone (AppliChem #A1553), 2.5g NaCl and 2.5g yeast extract (AppliChem #A1552)in 500ml H_2O, autoclave; store at room temperature

100x Amp stock (Gerbu #1046): dissolve 10mg Ampicillin/ml in H_2O; store at -20ºC

200x Kan stock (Sigma #K-4000): dissolve 10mg Kanamycin/ml in H_2O; store at -20°C

Bacterial strains

The bacterial strain XL1blue is nalidixic acid and tetracycline resistant (www.neb.com)

XL-1 blue: *endA1,gyrA96,hsdR17*(*rK-mK+*),*lac,recA1,relA1,supE44,thi-1,F´*[*proAB,lacI*^{q}*ZΔM15,Tn10(Tet*^{r}*)*

Growth of bacteria

Grow bacteria in LB-medium or on LB-agar plates with 100µg/ml Ampicillin or Kanamycin at 37°C.

Freezing of bacteria

Mix 800µl of a liquid bacterial overnight culture and 200µl glycerol and freeze at -80°C.

Thawing of bacteria

Scrape *E.coli* cells from frozen stocks and inoculate in LB Amp media for an overnight incubation at 37°C.

Transformation into TSS competent bacteria

Thaw already prepared TSS competent *E.coli* cells and incubate 100µl cell suspension with plasmid DNA (10µl of ligation or 50ng of DNA) for 20min on ice. Streak cells on LB plates and incubate overnight at 37℃.

2.3 Working with DNA

Solutions and Media

50x TAE: mix 484g Tris, 114ml acetic acid and 200ml 0.5M EDTA pH 8.0 and fill up to 2l with H_2O; store at room temperature. Use a 1x TAE working solution.

6x DNA loading dye (Fermentas #R0611)

Gene RulerTM 1kb DNA Ladder (Fermentas #SM0311)

Mini Preparations

Three preparation variants are used during this diploma thesis as described below.

-) Plasmid MINI preparation using QIAprep® Spin Miniprep Kit (Qiagen #27106)

Follow the guidelines provided by the supplier´s protocol.

-) "Dirty" MINI preparation adapted from Maniatis

Resuspend the pellet of a bacterial overnight culture in 250µl of Solution I (50mM glucose; 25mM Tris pH 8.0; 10mM EDTA pH 8.0). Subsequently add 250µl of Solution II (0.2M NaOH; 1% (w/v) SDS) and 350µl of Solution III (3M Potassium acetate; 2M Acetic acid) and mix by inverting. After centrifugation use the supernatant to precipitate DNA with isopropanol for 30min at -20℃. After another centr ifugation step wash the DNA pellet with 70% ethanol at 4℃. Resuspend the pellet in appropr iate amount of water.

-) Plasmid MINI preparation using thermic lysis protocol (Holmes & Quigley, 1981)

Resuspend the pellet of a bacterial overnight culture in STET buffer (8g saccharose, 0.5ml TritonX-100, 10ml 0.5M EDTA, 5ml 1M Tris/HCl pH 8.0) and keep on ice. Lyse the sample by addition of lysozyme for 70sec on 95℃. After a centrifugation step, remove the pellet with a toothpick, add isopropanol to the supernatant to precipitate DNA, centrifugate the sample and wash the pellet with 70% ethanol. Resuspend the pellet in appropriate amount of water.

Plasmid Midi preparation using PureYieldTM Plasmid Midiprep System (Promega #252219):

For large amounts of plasmid DNA preparation use the Pure YieldTM Plasmid Midiprep System kit and follow the guidelines provided by the supplier´s protocol.

DNA Elution

Elute DNA fragments using the Wizard ® SV Gel and PCR Clean Up System (Promega) #TB308. Dissolve agarose gel fragments with DNA of interest in Membrane Binding Solution at a ratio of 10µl per 10mg of gel slice. For further steps use supplied guidelines.

Restriction digest

Digest 1µg plasmid DNA with 1U of the restriction enzyme and prepare a digestion mix as suggested by supplier. Incubate the mixture for at least 1h until up to an overnight incubation at 37℃. Stop the restriction digest by addition of 1/10 of volume of loading dye.

Ligation of DNA fragments

Mix 50-100ng plasmid DNA with insert DNA in a molar ratio of 1:1, 1:3 or 1:6, in a final volume of 20µl containing T4 Ligase buffer and 1U T4 DNA ligase (NEB). Incubate samples for 30min at room temperature and use 10µl for a transformation into competent *E.coli* cells.

Annealing of oligos

For annealing of oligos, dilute 100µM of corresponding forward and reverse oligo in a 1:1 ratio. Incubate the mixture for 5min at 95℃ in a P CR machine and cool to room temperature.

Phosphorylation of annealed oligos

Treat 1-2µg (0.051pmol) of oligonucleotides with 10U of T4 PNK (Polynucleotidekinase, NEB #M0201L) in a reaction mix containing 1mM ATP and 10xT4 PNK buffer for 30min at 37℃. Stop the reaction by incubating the mix 20min on 65℃.

CIP treatment of digested plasmids

After a digestion treat the vectors (1µg of 1000bp equals 1.52pmol) with 20U of calf intestinal alkaline phosphatase (CIP, NEB #M0290S or CIAP, Fermentas #EF0341) and incubate for 1h at 37℃. Inactivate the enzyme by addition of 3µ l 0.5M EDTA.

Purification of DNA by Ethanol precipitation

Add 1/10 volume of 3M $C_2H_3NaO_2$ pH 5.2 and 2.5x volume of cold 96% ethanol to the DNA. Mix and keep sample for on -20℃ to precipitate DNA . Centrifuge 10min at 14.000rpm at 4℃, discard supernatant and wash pellet once with 70% ethanol. Finally resuspend the pellet in appropriate amount of H_2O.

PCR

All Phusion polymerase PCR reaction mixtures used are finally composed of the following: 1x Phusion Polymerase HF buffer (Fermentas), 200µM of each dNTP, 0.5µM of each primer, 0.02U Phusion polymerase (Fermentas) and 10-100µg DNA.

Standard PCR Program:

98℃ - 30sec

98℃ - 10sec
55℃ - 15sec
72℃ - 15-30sec/1 kb
} 35 cycles

72℃ - 10min

4℃ - hold

Colony PCR

For use of Promega GoTaq Polymerase two sets of Master Mixes (M1, M2) are prepared and added at different time points during the PCR Program as indicated by the arrows:

M1: 0.2mM of each dNTP, 0.5µM of each primer, template yeast colony, H_2O

M2: H_2O, 5xGreen GoTaq Reaction Buffer (Promega), 1.25U GoTaq DNA Polymerase

Standard PCR Program:

→ M1

95℃ - 5min

→ M2

95℃ - 5min
95℃ - 30sec
50℃ - 10sec
72℃ - 1min/kb
} 30 cycles

72℃ - 10min

4℃ - hold

Primers for PCR and Colony PCR experiments are listed in Table 3 below.

Table 3. Summary of forward (fwd) and reverse (rvs) primers of this diploma thesis

#	Name	Description	Sequence 5'→ 3'
1329	Cdc55 Prom fwd	Check via colony PCR genomic insertion of KanMX4 Gal1P LoxP myc HKMT GL CDC55 and myc HKMT GL CDC55 (5' end)	CCTATCAGAGGGTGAATAAGGC binds in promoter region 148bp before *CDC55* coding region
1204	HKMT rvs		CGTCCAGGTCCACCTCATTC binds within *HKMT* coding sequence 206bp after start codon
1063	HKMT fwd	Check via colony PCR genomic insertion of KanMX4 Gal1P LoxP myc HKMT GL CDC55 and myc HKMT GL CDC55 (3'end)	ACCTCTTTGACCTGGACTAC binds within *HKMT* coding sequence 652bp after start codon
1271	Cdc55 rvs		TTTGGGGTGGCAGCAATGA binds within *CDC55* coding sequence 505bp after start codon
1269	pBS1761 fwd	PCR amplification of KanMX4 Gal1P LoxP myc HKMT GL CDC55 construct from pBS1761 vector	TTTGTTCCCTTTAGTGAGGGTTCGAGGTCAAACTGGAGAGATCTTACGCATAAAGAAATATAATATAGCGC Underlined sequence binds to pBS1761 vector backbone, next to KanMX4 (52bp) and to LoxP site (11bp); the rest binds next to genomic *CDC55* sequence within the promoter region
1271	Cdc55 rvs		TTTGGGGTGGCAGCAATGA binds within *CDC55* coding sequence 505bp after start codon
1104	Kin4 *Asc*I fwd	Insert C-terminally KIN4 coding sequence into backbone vectors	AACCCGGCGCGCCATGGCTTCTGTACCTAAACG binds to first 20bp of *KIN4* coding sequence, has *Asc*I restriction site (underlined) and 6 additional bases
1105	Kin4 *BamH*I rvs		CAACCGGGATCCAACCCTCATGCTCCTTCTTTTG binds to last 22bp of *KIN4* coding sequence without stop codon, has *BamH*I restriction site (underlined) and 6 additional bases
1115	Net1 *Hind*III fwd	Insert C-terminally NET1 coding sequence into backbone vectors	GAATAGAAGCTTATGTACAAGCTACAAGTGGTC binds to first 21bp of *NET1* coding sequence, has *Hind*III restriction site (underlined) and 6 additional bases
1116	Net1 *Xho*I rvs		GCATAGCTCGAGAACTTCATCATTATCATTGCC binds to 2780 – 2800bp after the start codon of *NET1* coding sequence, has *Xho*I restriction site (underlined) and 6 additional bases

Plasmids

All plasmids used in this diploma thesis are listed in Table 4 and corresponding maps are illustrated in the Appendix.

Table 4. Summary of plasmids used during this diploma thesis

Construct	Marker	Source
pYX213 P_{Gal} myc HKMT GL Rts1 (2µ)	Ura3, AmpR	Ogris Lab
pYX213 P_{Gal} myc HKMT GL Cdc55 (2µ)	Ura3, AmpR	Ogris Lab
pYX142 P_{TPI} 4H3 2HA GL Kin4 (CEN)	Leu2, AmpR	Ogris Lab
pYX242 P_{TPI} 4H3 2HA GL Net1 (2µ)	Leu2, AmpR	Ogris Lab
pYX242 P_{TPI} 3H3 2HA GL Net1 (2µ)	Leu2, AmpR	Ogris Lab
pYX213 P_{Gal} Cdc55 GL HKMT myc (2µ)	Ura3, AmpR	Ogris Lab
pYX213 P_{Gal} Rts1 GL HKMT myc (2µ)	Ura3, AmpR	Ogris Lab
pYX242 P_{TPI} Kin4 GL 2HA 4H3 (2µ)	Leu2, AmpR	this study
pYX242 P_{TPI} Net1 GL 2HA 4H3 (2µ)	Leu2, AmpR	this study
pYX213 P_{Gal} myc HKMT (2µ)	Ura3, AmpR	Ogris Lab
pBS1761 P_{Gal} LoxP	KanMX4, AmpR	Ogris Lab
pBS1761 P_{Gal} LoxP myc HKMT GL Cdc55	KanMX4, AmpR	this study
tTA P_{CMV} P_{ADH} tetO myc (CEN)	Ura3, AmpR	Ogris Lab
pYX142 P_{TPI} myc HKMT GL Rts1 (CEN)	Leu2, AmpR	Ogris Lab

DNA constructs and plasmids have been generated using restriction and ligation methods and PCR.

- Cloning of pYX242 P_{TPI}Kin4 GL 2HA 4H3 and pYX242 P_{TPI}Net1$_{1-600}$ GL 2HA 4H3 (2µ)

For creating the vectors which express the fusion proteins KIN4 GL 2HA 4H3 or NET1 GL 2HA 4H3 under control of a TPI promoter, the coding sequence of Net1 and Kin4 was amplified from the yeast genome via PCR. Primers used for KIN4 and NET1 gene amplification are listed in Table 3 in Materials & Methods. The forward primers bind to the first 20bp of each coding sequence, NET1 and KIN4, respectively. The Kin4 reverse primer binds to the last 22bp of the coding sequence without the stop codon whereas the reverse primer of Net1 binds to the base pairs 2780-2800 within the NET1 coding sequence. As Net1 protein is a large protein and experiments of Azzam et al (2004) have revealed that the first 600 amino acids of Net1 enable the regulatory control of Cdc14, we used only the first 600 amino acids. Nevertheless, other lab members have also tested a full length variant for Net1

in some experiments and they have shown similar results as the 1-600 amino acids protein (unpublished data). The PCR primers revealed overhangs with different restriction sites to introduce the coding sequence in the same cut GL 2HA 4H3 vector (created by I. Frohner). The PCR amplified KIN4 sequence was digested with *Asc*I and *BamH*I and introduced into an *Asc*I/*BamH*I cut vector, which contained the GL 2HA 4H3 tag. Similarly to Kin4, the 600 amino acid encoding NET1 sequence was cleaved with *Hind*III and *Xho*I and ligated into a *Hind*III/*Xho*I GL 2HA 4H3 backbone vector. The correct insertion of the coding sequence was checked by an *Nco*I (Kin4) and a *Puv*II (Net1) digest. The corresponding maps of the resulting pYX242 GL 2HA 4H3 KIN4 and NET1 vectors are shown in the Appendix. The vectors encoding C-terminal CDC55 and RTS1 have already been cloned by I. Frohner (vector maps see Appendix).

- Cloning of LoxP KanMX4 P_{Gal} LoxP myc HKMT GL Cdc55 vector

To express the fusion protein under the control of the endogenous promoter the bait construct “myc HKMT GL CDC55” was genomically integrated by using a LoxP system. This enabled us to flox out the Gal1 promoter and a resistance marker with help of the pYES Cre-expressing plasmid after the genomic integration.

To integrate the bait fusion genes into *S.cerevisiae* genome the bait construct “myc HKMT GL CDC55” was cloned into the backbone of the vector pBS1761. The original vector pBS1761 (Seraphin et al, 2002) harbors a Kanamycin resistance marker (KanMX4), LoxP sites and an inserted TEV CBP protein, which is under the control of a Gal1 promoter (P_{Gal}, vector map see Appendix). The originally inserted TEV CBP gene was removed by partial digestion with *Xho*I and *Nco*I and replaced by the *Xho*I-*Nco*I cut “myc HKMT GL CDC55” tag from pYX213 P_{Gal} myc HKMT GL CDC55 (Ogris lab) in a ligation process resulting in the pBS1761 KanMX4 P_{Gal} LoxP myc HKMT GL CDC55 plasmid (vector map see Appendix). In a next step the cassette, the promoters and the resistance marker sequence were PCR amplified (Figure 4) and integrated via homologous flanks into to the *S.cerevisiae* target region. PCR amplification of the “integration cassette” occurred with primers binding upstream of the LoxP site and within the CDC55 coding sequence (primers listed in Table 3 Materials & Methods).

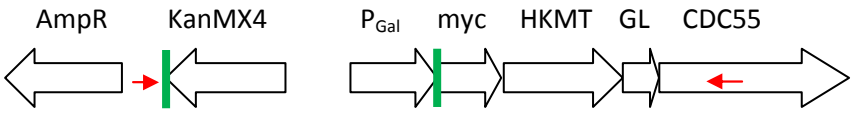

Figure 4. PCR amplification of the “GL HKMT myc LoxP P_{Gal} KanMX4 LoxP” cassette. The cassette was amplified from the pBS1761 KanMX4 P_{Gal} LoxP myc HKMT GL CDC55 plasmid with two primers indicated with red arrows (Table 3, #1269 and #1271). The 5’ primer binds within the CDC55 coding sequence (505bp after start) whereas the 3’ primer binds in the vector backbone (close to KanMX4 and the LoxP site). The amplified cassette should reveal a size of 3849bp. LoxP sites in this figure are indicated by green bars.

The PCR amplified cassette with a size of 3849bp was transformed into a wild type *S.cerevisiae* strain via electroporation (described in Materials and Methods) and tested for Kanamycin resistance. Moreover, integration into the genome was checked via colony PCR (primers #1329, #1204 and #1063, #1271 listed in Table 3). Figure 5 shortly illustrates how to obtain the 907bp (3' end) and the 2637bp (5'end) fragment, which should confirm the correct integration at the 3`end in the colony PCR.

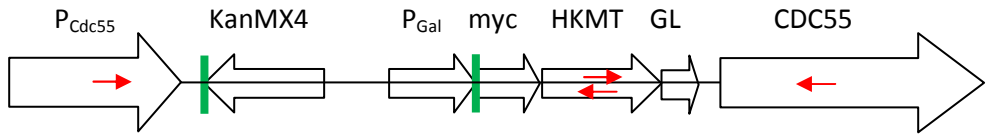

Figure 5. Check genomic insertion of the cassette at the 3' and 5' end. After integrating the "LoxP KanMX4 P_{Gal} LoxP myc GL HKMT" cassette via homologous flanks into the *S.cerevisiae* genome, the integration was checked in a colony PCR. Primers are indicated by red arrows and bind within HKMT (652bp after start) and within the *CDC55* coding sequence (505 bp after start) to check the 3` integration. To check the 5` integration the forward primer binds within the Cdc55 promoter (148bp upstream the *CDC55* coding sequence) and the reverse primer within the HKMT (206bp after start codon) coding sequence. Thereby two fragments at a size of 907bp and 2637bp should be obtained. LoxP sites in this figure are indicated by green bars.

The pYES Cre plasmid was transformed via electroporation into positive recombination clones and streaked on YPD plates. Finally, if the P_{Gal} promoter and the KanMX4 resistance marker were floxed out (see Check Flipping in Materials and Methods), the pYES Cre plasmid was removed from cells again via 5' FOA treatment (see Materials and Methods) and the flipping of the promoter and the resistance marker was again checked via colony PCR (primers see Table 3, same as for Figure 5). If the flipping worked correctly, the colony PCR should lead to a fragment of 402bp at the 5`end and a 907bp fragment at the 3`end (Figure 6).

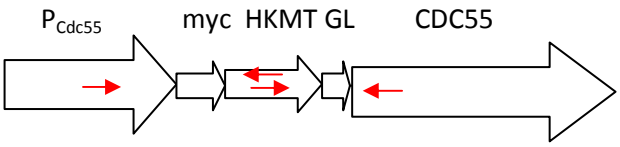

Figure 6. Check the flipping of P_{Gal} promoter via the LoxP system in a colony PCR. After floxing out the LoxP flanked P_{Gal} and the KanMX4 resistance marker the strains were tested for the missing construct. In a colony PCR two different fragments (402 and 907bp) were obtained with primers indicated by red arrows. The amplification was done with same primers as used for Figure 5, but led to a smaller fragment at the 5`end as no Gal1 promoter and the resistance marker should be present any more.

- Cloning of tTA P_{CMV} PADH tetO myc HKMT GL Rts1 (CEN) vector

To establish an alternatively regulated expression of bait proteins, the N-terminally tagged Rts1 fusion proteins were placed under control of a tetracycline (tet) regulated promoter. The generation of a tet-controlled Rts1 expression vector required a stepwise cloning procedure. First I cut out the bait construct “myc HKMT GL Rts1” from the original vector pYX142 myc HKMT GL Rts1 (vector map see appendix) and ligated it into a cut backbone vector harboring a reverse tet-controlled promoter region (Ogris lab, unpublished).

The tet backbone vector (prevTET-A Ura Cen myc) harbors next to the resistance (Ampicillin) and auxotrophic marker (Uracil) genes the reverse tetracycline transactivator (tTA) coding sequence under the control of a Cytomegalovirus (CMV) promoter. The expression of target genes is controlled via the reverse tTAs which bind to tetracycline response elements (TRE) within an inducible tetracycline operator (tetO). The vector therefore further contains seven copies of the tetO sequences (7xtetO) to which the reverse tTA will bind controlling the activity of a Cyctochrome C1 (CYC1) minimal promoter. The reverse tTA is only capable to bind the operator DNA sequence and start the transcription of target genes if it is bound by doxycyline (Bujard & Gossen, 1992). Moreover, the vector contains an Alcohol Dehydrogenase 1 (ADH1) terminator site and a CYC1 terminator sequence. Former lab members inserted a myc tag followed and a multiple cloning site into this vector. Figure 7B gives a schematic illustration of this tet backbone vector and highlights the *Nco*I and *Xho*I restriction sites used for the further cloning steps (another map is in the Appendix).

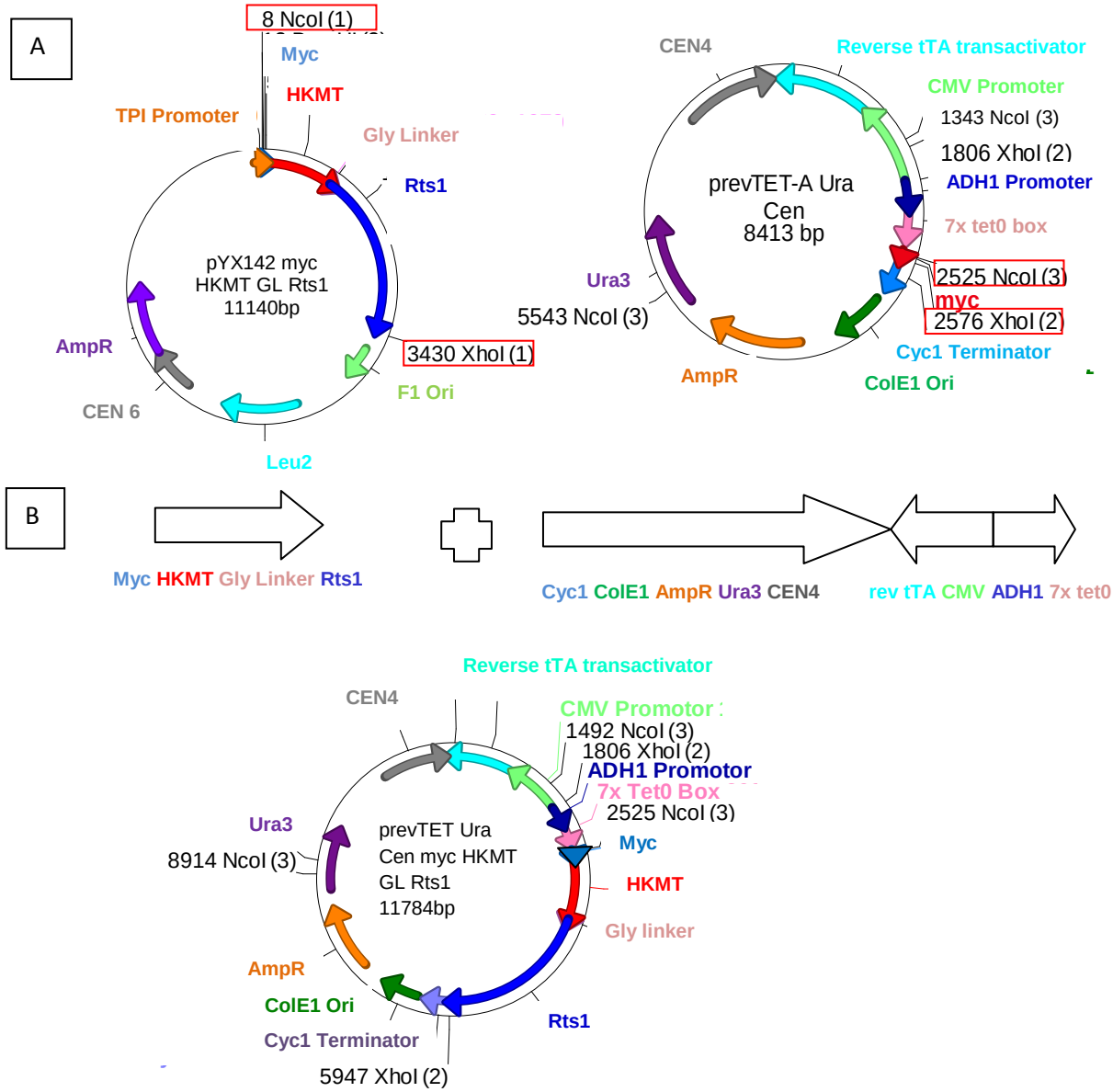

Figure 7. Schematic illustration of the stepwise cloning procedure of the tetracycline regulated Rts1 bait expression vector. (A) First, the vector pYX142 myc HKMT GL Rts1 was cut with *Xho*I and *Nco*I to obtain the fragment consisting of myc (blue), Histone 3 lysine 9 (K9) methyl transferase (HKMT, red) a Glycine linker (GL, pink) and Rts1 (dark blue). In a next step the tet backbone vector (prevTET-A Ura Cen) was partially digested with *Xho*I and *Nco*I to remove the originally inserted myc tag (red) and to obtain the vector backbone for further cloning. (B) The two obtained fragments (illustrated as linearized arrows) were ligated and then checked via restriction digest for correct integration of the insert.

To create the final Rts1 containing tet vector, I had to introduce a fragment from the pYX142 myc HKMT GL Rts1 vector (Zuzuarregui et al, 2012). To obtain this sequence the vector was digested with *Nco*I and *Xho*I, which led to two fragments, one containing the coding sequence of myc HKMT GL Rts1 (3422bp) and the other with vector backbone (7718bp). Simultaneously, the tet backbone vector had to be digested with *Xho*I and *Nco*I but as there are three *Nco*I and two *Xho*I sites present within the vector (see map in Figure 7) a partial digest was done. I firstly cut the tet backbone vector backbone with *Xho*I overnight and then

digested it partially for 1, 5 and 10min with *Nco*I (Figure 8). Thereby only a 51bp small fragment, the present myc tag, should be removed from the tet backbone vector and leave a remaining 8362bp sized vector.

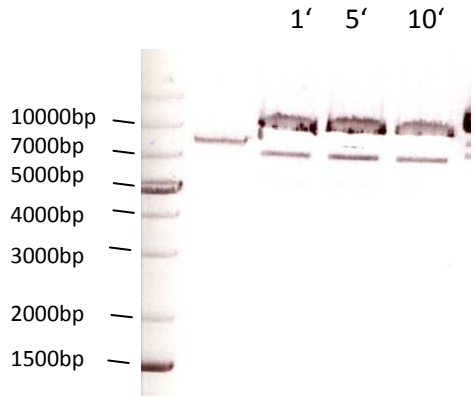

Figure 8. Agarose gel after partial digest with *Nco*I for 1, 5 and 10 minutes. The bands at the size of approximately 8362bp were cut out to further use for integration.

After the elution of the correct fragments of 8362bp size, the backbone vector was treated with Calf Intestine Phosphatase (CIP) enzyme. In a next step a ligation was set up with 60ng of the myc HKMT GL Rts1 fragment and 200ng of the eluted tet backbone vector. After transformation of the ligation mixes into *E.coli* the plasmid DNA of the transformants was digested with *Sca*I to see if the integration worked correctly (Figure 9). *Sca*I cuts once within the Rts1 and three times within the tet backbone vector, which should lead to a band pattern as summarized in the table in Figure 9C.

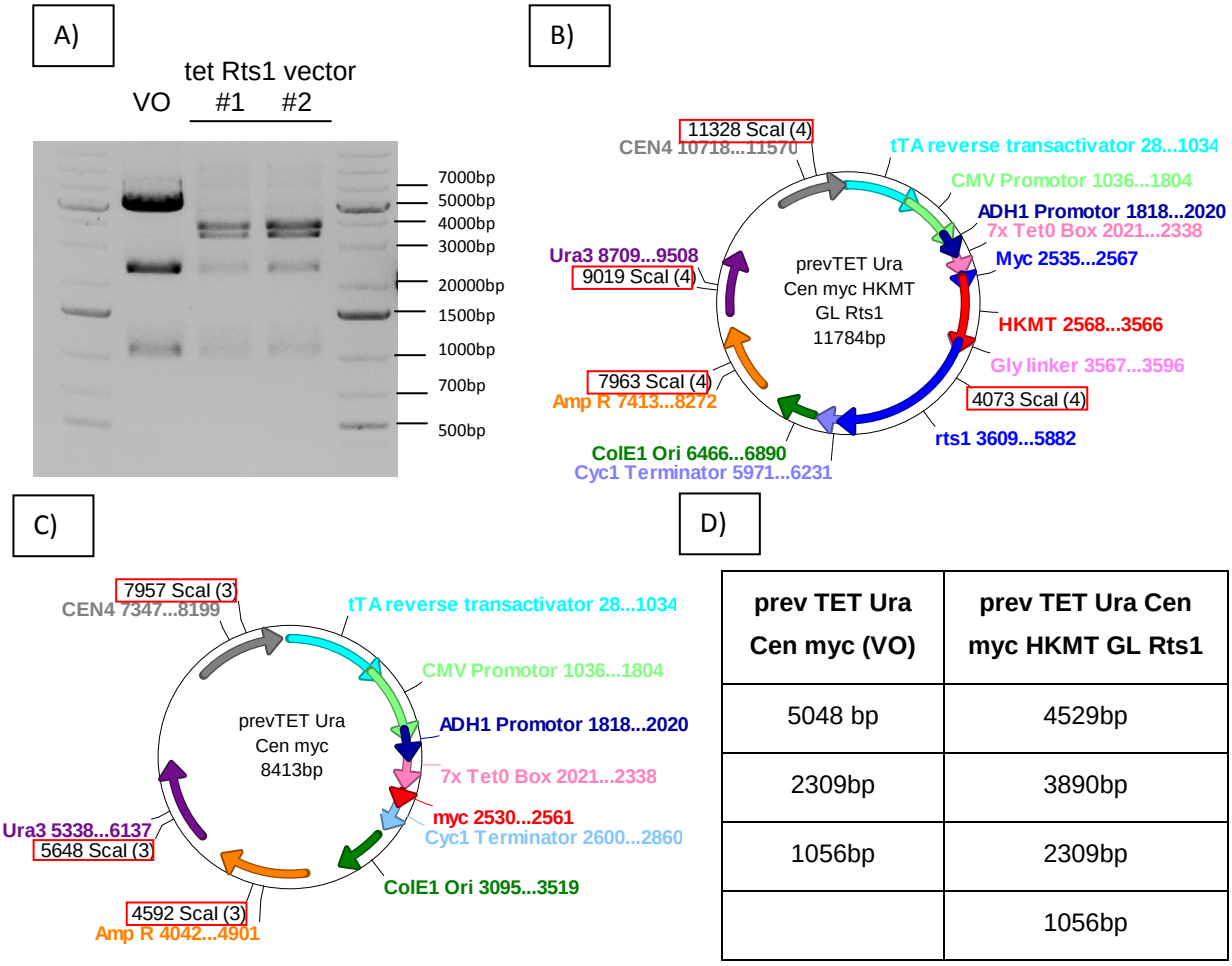

prev TET Ura Cen myc (VO)	prev TET Ura Cen myc HKMT GL Rts1
5048 bp	4529bp
2309bp	3890bp
1056bp	2309bp
	1056bp

Figure 9. *Sca*I control digest of ligation samples of "myc HKMT GL Rts1" into tet backbone vector. After isolation from *E.coli* transformants the vector tet-Rts1 was digested with *Sca*I enzyme. (A) Samples were loaded on a 1% agarose gel to check the insertion of the "myc HKMT GL Rts1" fragment into the tet backbone vector. Two clones of the transformants were analyzed and compared to the band pattern of a tet backbone vector only (VO) negative control. The two schematic figures illustrate the vector tet backbone vector with an Rts1 insert (B) and the tet backbone vector VO (C). In both, the *Sca*I restriction sites are highlighted in red squares. (D) The table summarizes the expected band pattern of a *Sca*I digest of correctly ligated and tet backbone vectors.

As the band pattern of clones #1 and #2 (Figure 9A) seemed to be similar to the expected band pattern the sequence was checked. Unfortunately, the analysis revealed a ligation of the myc HKMT GL Rts1 cassette with a smaller tet backbone vector. Contrary to our expectations the vector was not missing the 51bp myc coding sequence but instead lacked a sequence of 719bp containing the ADH1 promoter region and the 7xtetO box (see Figure 7, between 1806 *Xho*I and 2525bp *Nco*I restriction site).

To repair the obtained tet Rts1 vector, it was cut with *Nco*I, which cuts the vector in two fragments, by cutting within the uracil marker and close to the myc HKMT tag (see Figure 7B). The missing fragment of 7x tetO box was PCR amplified from the original tet backbone vector (Figure 9). The forward primer binds within the CMV promoter whereas the

reverse primer binds to a sequence within the myc - HKMT tag (see Figure 9 below; primers CMV fwd and Myc rvs as listed in Table 3).

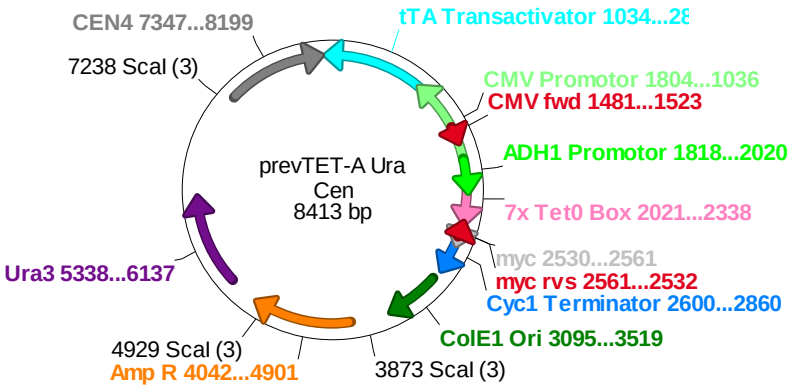

Figure 9. Cartoon to show binding of primers for PCR amplification of 7xtetO box. The sequence of the missing tetO box was amplified in a PCR. With use of the CMW forward (fwd) and myc reverse (rvs) primers (indicated by red arrows) a 1008bp long sequence coding for the ADH1 promotor and the 7x tetO box was obtained. As primers bind within sequences, which were present on the tet Rts1 vector, these sequences could be used for the integration of the tetO box fragment into the tet Rts1 vector.

The PCR amplified fragment harbors two overlapping sequences to the tet Rts1 vector. One can be found in the CMV promoter and the other in the myc tag, which allow an integration of the 7xtetO box fragment into the tet Rts1 vector via homologous recombination (Figure 10). Furthermore an Uracil oligonucleotide GCGGCTTAACTGTGCCCTCAATGGAAAAATCAGTCAAGATATC was introduced at the same time to create a point mutation (C--> A) within the *Nco*I restriction site (underlined) of the Uracil marker. Thereby the restriction site in the backbone vector is made uncleaveable (Figure 10).

As a first step the *Nco*I cut tet Rts1 vector, the PCR amplified 7xtetO box fragment and a 1:10 dilution of an annealed Uracil oligonucleotide (1.5µg/µl) were transformed into yeast via electroporation. The obtained yeast transformants were checked in a colony PCR with same primers as used for the PCR amplification of the 7xtetO box fragment (CMV fwd and Myc rvs). In a next step the plasmid was rescued from PCR positive yeast transformants (see Materials and Methods) and transformed into *E.coli*.

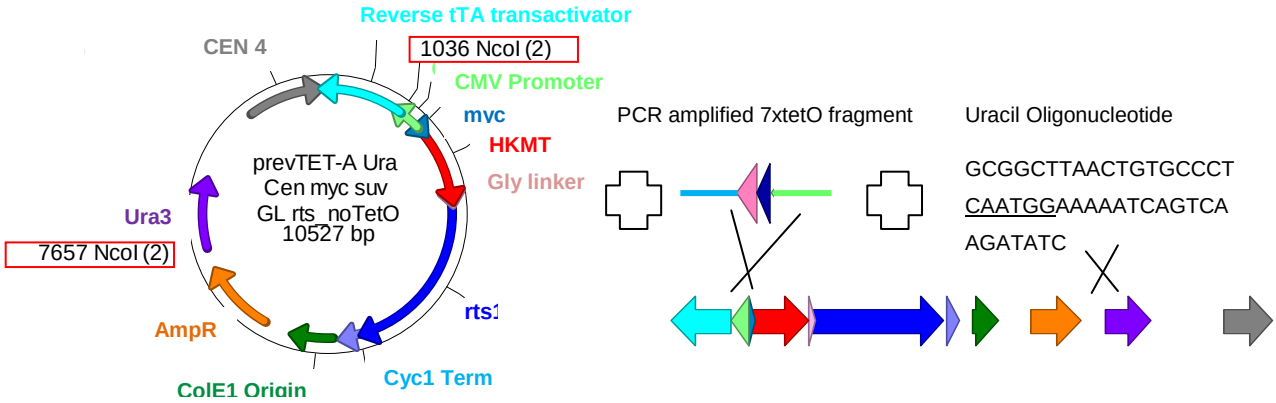

Figure 10. Reparing the tet – Rts1 vector via homologous recombination. To repair the obtained tet Rts1 vector the *Nco*I (highlighted with red squares) cut vector was transformed with the missing 7xtetO box fragment (amplified in a PCR, see Figure 9) and an Uracil oligonucleotide into yeast to integrate these fragments via homologous recombination. Colors of arrows on the right match with the labeling of arrows in the vector map.

Unfortunately, during the research time of my diploma thesis it was not possible to complete these cloning steps. To finish the procedure, the plasmid DNA of transformants has to be digested to check the sequence of the rescued plasmid. Finally, these clones can be used to transform them into yeast cells and use them for further research.

2.4 Working with proteins

Solutions and media:

50% (w/v) Trichloracetic acid (TCA): dissolve 50g TCA (Applichem #A1431) in 100ml H_2O

YEX Lysis Buffer: dissolve 7.4g NaOH in 100ml H_2O (1.95M) and mix with 7.5g 7.5% ß-Mercaptoethanol in 100ml H_2O

30% Acrylamide: mix 292g acrylamide and 8g bisacrylamide and fill up to 1l with H_2O and add mixedbed, ion-exchange resin (BioRad AG 501-X6); store in dark at 4℃

1M Tris pH 8.8: dissolve 242.3g Tris in 1l H_2O; adjust to pH 8.8; add H_2O to 2l, store at 4℃

1M Tris pH 6.8: dissolve 60.5g Tris in H_2O; adjust to pH 6.8; add H_2O to 500ml; store at 4℃

20% Sodiumdodecylsulfat (SDS): dissolve 40g SDS in 100ml H_2O; slightly heat, fill up to 200ml with H_2O and store at room temperature

10% APS: dissolve 1g ammoniumperoxodisulfate (Merck #1201) in 10ml H_2O; store at 4℃

TEMED (N,N,N',N'-Tetramethylenediamine, Fluka #87689)

10x Running buffer: dissolve 250mM Tris, 2M Glycine and 35mM SDS in 5l H_2O and store at room temperature

Transfer buffer with methanol: dissolve 25mM Tris and 190mM Glycine in 8l H_2O; add 20% (v/v) methanol; store at 4℃

Ponceau S stock solution (10x): mix 2g Ponceau S (Serva #33429), 30g Trichloroacetic acid (AppliChem #A1431) and 30g Sulfosalicylic acid (Merck #1.00691) and fill up to 100ml with H_2O; store at room temperature

Ponceau S working solution: Dilute Ponceau S stock solution 1:10 with H_2O

20% Sodiumazide (Merck #67188): dissolve 2g sodiumazide in 10ml H_2O; store at 4℃.

3x GSD stock: mix 335mM DTT (Gerbu #1008), 230mM SDS, 4.5M Glycerol (Merck #1.04092) and 20ml H_2O. Add a bromphenolblue (Amresco #0312) and a few drops 1M Tris pH 6.8 until solution appears blue; store at -20℃; to obtain 1x GSD, dilute the stock with H_2O

Prestained Protein Molecular Weight Standards (Biorad #161-0373) store at -20℃

1% Thimerosal (Sigma #T-5125): dissolve 0.5g Thimerosal in 50ml H_2O; store at 4℃

10xPBS: dissolve 400g NaCl, 10g KCl, 72g Na_2HPO_4 and 10g KH_2PO_4 in 5l H_2O; autoclave and use a 1xPBS working solution

100x Phenylmethylsulfonylfluoride (PMSF) stock: dissolve 0.697g PMSF (Roche #837091) in 20ml isopropanol; store at room temperature in the dark

200x Aprotinin-stock: store aliquots of 1ml Aprotinin (Sigma #A-6012) at 4℃

25x Complete TM: dissolve CompleteTM Protease Inhibitor cocktail tablet (Boehringer Mannheim #1836145) in 2ml IP-Lyse buffer; store at 4℃ for a maximum of 2 weeks

IP Wash: mix 10% Glycerol, 20mM Tris pH 8.0 and 135mM NaCl; filter sterilize; store at 4℃

IP lysis buffer: mix 20mM Tris/HCl pH 8.0, 135mM NaCl, 10% Glycerol and 1% NP-40 in H_2O; store at 4℃

3% Non Fat Dry Milk (NFDM, blocking solution): dissolve 30g NFDM in 1l PBS-T, add 50µl 20% sodium azide; store at 4ºC

0.5% NFDM (incubation solution): dissolve 5g non fat dry milk (NFDM) in 1l PBS-T, add 1ml 1% Thiomersal; store at 4ºC

Yeast TCA crude extracts

Spin down a yeast culture at 3500 rpm for 10min at 4℃. Add 50µl of YEX lysis buffer per OD_{600} x ml = 1 and incubate for 10min on ice. Similar to this volume add 50% TCA and once again incubate for 10min on ice. After a centrifugation step for 10min at 14.000rpm at 4℃ resuspend pellet in 36µl 1xGSD and Tris per OD_{600} x ml = 1. Finally boil samples for 5min before loading on an SDS-PAGE.

SDS-PAGE (SDS-Polyacrylamide gel electrophoresis)

Assemble the gel unit, mix the components of the separating gel solution as listed in Table 5 below (without APS and TEMED) and degas the mixture by applying vacuum. Add 10% APS and TEMED, pour the gel and cover with ethanol until polymerization is finished. In a next step prepare and pour the stacking gel and insert an appropriate gel comb. After polymerization remove the comb and wash slots. Insert the gel into the running unit and add 1x running buffer. Finally load boiled samples and run the gel overnight at 8mA per gel.

Table 5. Components of separating and stacking Gel

	10% separating Gel	**7.5% separating Gel**	**5% stacking Gel**
30% Acrylamide (ml)	13.4	10.1	1.7
Tris pH 6.5 or 8.8 (ml)	15	15	1.25
20% SDS (µl)	200	200	50
H_2O (ml)	11.7	15	7.1
10% APS (µl)	134	134	50
TEMED (µl)	26	26	10

Western blotting

Assemble a Western sandwich in the following order:

support pad - 2 sheets of 3MM Whatman paper - Gel - nitrocellulose membrane (Whatman #10402096) - 2 sheets of 3MM Whatman paper - support pad

Insert the Western sandwich into the transfer unit and start protein transfer at 4℃ for 3.5h at 500mA. After the blotting process stain proteins on membranes with Ponceau staining solution to check if the protein transfer worked. Afterwards add blocking solution (3% NFDM and sodium azide) for 1h at room temperature. Incubate the membrane with the primary antibody (in 0.5% NFDM and 1ml 1% Thiomersal) overnight at 4℃. Wash three times for

5min with PBS-T and add the appropriate secondary antibody for 1h at room temperature. Finally wash membranes three times for 10min with PBS-T and develop blots via enhanced chemoluminescence (ECL, mix beforehand ECL oxidizing reagent and enhanced luminal reagent in equal amounts and incubate on the membrane) on X - ray films.

Antibodies used for western blotting

Dilute primary and secondary antibodies in 0.5% NFDM in PBS-T with 1ml 1% Thiomersal. All primary antibodies used during the diploma thesis are listed in Table 6 below.

Table 6. Summary of primary antibodies of this diploma thesis

Primary Antibody	Clone	Dilution	Species
α-myc	4A6	1:1000	Mouse, monoclonal; Ogris Lab, Millipore
α-HA	16B12	1:10.000	Mouse, monoclonal; Covance research product
α-me1K9H3	7E7H12	1:50	Mouse, monoclonal; Ogris Lab
α-me2K9H3	5E5G5	1:20	Mouse, monoclonal; Ogris Lab, hybridoma sup
α-me3K9H3	6F12H4	1:100	Mouse, monoclonal; Ogris Lab, Fiber Cell sup

Use secondary antibodies, coupled to horse radish peroxidase (HRP), in a 1:5000 dilution in 0.5% NFDM in PBS-T and 1ml 1% Thiomersal. The antibodies are directed against mouse or rabbit primary antibodies (goat anti mouse Jackson ImmunoResearch, #115-035-008, goat anti rabbit Jackson ImmunoResearch #111-035-008).

Immunoprecipitation with non - crosslinked beads

Dilute an overnight culture of yeast of OD_{600} x ml = 100 into 100ml of media and grow it for 4h. Afterwards lyse cells and wash them once with cold water. Determine the protein concentration with BioRad detergens and equilibrate lysates to similar protein concentrations with IP - buffer. Keep 1/20 of the sample, resuspend it in 1xGSD and Tris and boil it ("Lysate"). In a next step incubate the samples with 40µl of the α-me3K9H3 antibody for 30min at 4℃. Subsequently shake the cells with 50µl suspension of a BSA-coated protein A/G Sepharose beads mix for further 30min at 4℃. Centrifuge the suspension for 1min at 1000rpm, take 1/20 of the supernatant, resuspend and boil it in 1xGSD and Tris. Wash beads once with IP-buffer ("Wash") and three times with TBS. Finally remove the supernatant, boil immunoprecipitates in 3xGSD ("IP") and load the samples on an SDS-PAGE.

3 Results

3.1 Demonstrating M-Track by showing already identified interaction partners of PP2A regulatory subunits

Experimental research during this diploma work aimed to track already confirmed interaction partners of PP2A regulatory subunits Rts1 and Cdc55 via M-Track in *S.cerevisiae* (Zuzuarregui et al, 2012).

3.1.1 M-Tracking of the short-lived protein-protein interaction between $PP2A^{Cdc55}$ and its substrate Net1 in a *cdc55*Δ strain

The realization of these experiments was based on two fusion constructs that have already been cloned by my colleagues I. Mudrak and T. Kupka. To get to know how the M-Track method works, I tried to repeat the results of the previously published interaction of Cdc55 and Net1 (Zuzuarregui et al, 2012) in this diploma thesis (Figure 11). The bait and prey fusion proteins were expressed under heterologous promoters (TPI and Gal1) on 2µ plasmids in a *cdc55*Δ strain. During a time course of 8h after the addition of galactose, samples were taken at indicated time points and TCA lysates were prepared. One uninduced sample was taken before galactose induction and was further grown with additional glucose for 6h. These samples are labeled with (-) in each figure and no methylation signal was expected as no bait should be expressed.

For best illustration of the band patterns the expression levels of bait and prey as well as methylation signals are shown exemplary from one experiment at one time point of exposure (Figure 11A). Longer exposure times did not reveal any differences in band pattern or upcoming bands, but showed for all samples an increase of signal intensity. Moreover, levels of bait, prey and methylation signals are shown in a line diagram after calculating data of three different experiments (n=3, Figure 11B).

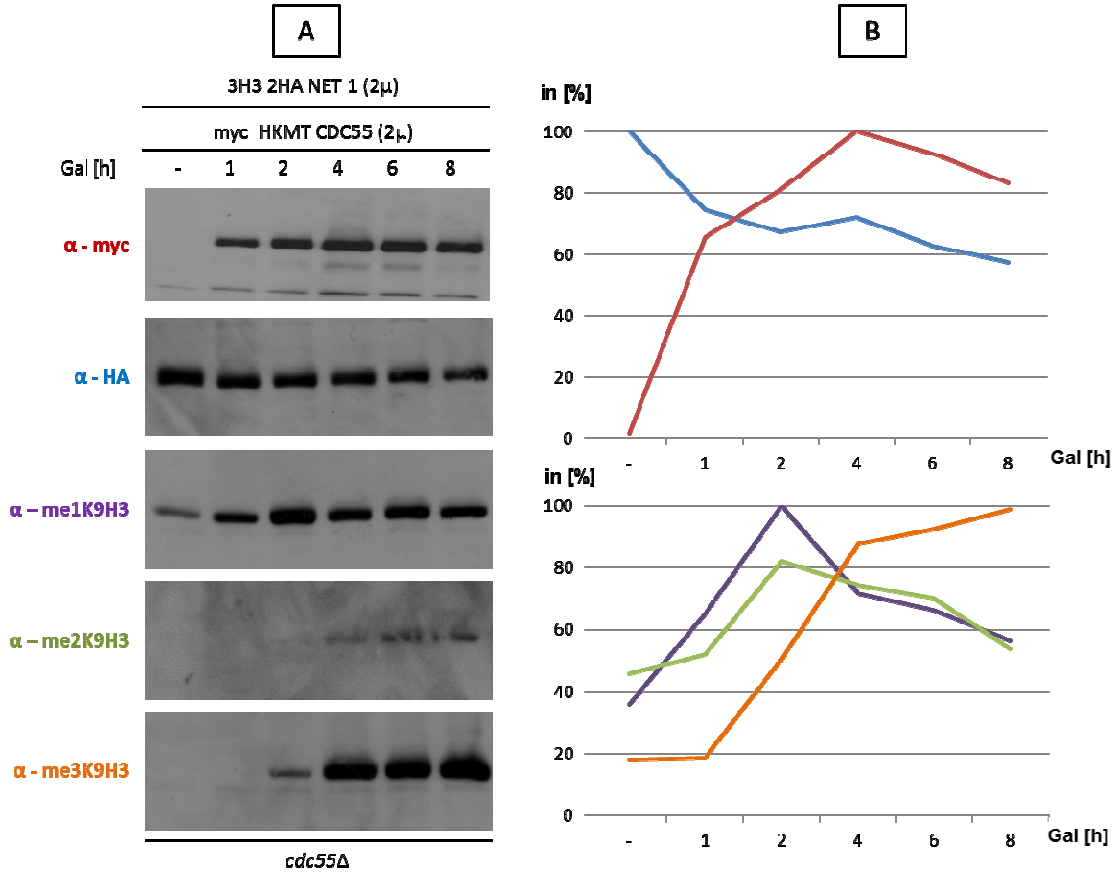

Figure 11. M-Track detects the interaction of PP2A^{Cdc55} holoenzyme with its substrate Net1. (A) At indicated time points after galactose induction TCA lysates were prepared from a *cdc55*Δ strain expressing constitutively the prey protein P_{TPI} 3H3 2HA GL Net1 (2µ) and inducibly the bait P_{Gal} myc HKMT GL Cdc55 (2µ). Samples were analyzed by a 10% SDS-PAGE on 5 separate gels, immunoblotted and incubated with specific monoclonal antibodies against HA and myc tagged proteins as well as mono- (α-me1K9H3), di- (α-me2K9H3) and tri-methylated K9H3 (α-me3K9H3). Blots are exemplarily shown at one exposure time: myc and HA after 90sec, mono-and tri methylation signals after 3min and dimethylation after 1h. (B) For the evaluation, the signal intensity of HA, myc, mono- and trimethylated preys of three similarly conducted experiments (n=3) was quantified with Image Quant Analysis program at different exposure time points: HA (90sec, 3min, 1h), myc (1min, 90sec, 3min, 1h), me1K9H3 (90sec, 3min, 1h), me2K9H3 (1h), me3K9H3 (90sec, 3min, 1h). Data was normalized to the HA levels and the highest value was set to 100%.

As the bait protein was expressed under the control of a galactose inducible promoter the expression of myc HKMT Cdc55 increased up to 4h after the addition of galactose. After this peaking it decreased towards the 8h time point. The constitutively present prey signals showed the highest level in the uninduced, glucose based sample. In all conducted experiments a decrease towards the 8h time point could be observed.

For monomethylation (α-me1K9H3), a probably unspecific signal was observed in the uninduced sample. This unspecific signal has already been observed by T. Kupka and might be a result of the monomethyl antibody, because it is not detectable in every experiment. The

signal increased until it reached its peak after 2h and then further decreases. Dimethylation (α-me2K9H3) levels were very weak during the whole time course as maybe the antibody was not working that well. Signals of all conducted experiments varied in a range between 40 and 80% of the maximal level. Whilst the blots in Figure 11A showed the peak at the 6h time point the mean peak of all data was detected after 2h (see line diagram). Trimethylation (α-me3K9H3) increased constantly during the time course and reached its maximal level at the 8h time point (Figure 11).

These data are in accordance with already shown interaction profiles of other lab members. The repeated experiments confirmed their results and once again show that M-Track method is able to track the transient $PP2A^{Cdc55}$-Net1 interaction. As obvious from Figure 11A monomethylation could be seen peaking at early time points after bait expression whereas dimethylation and trimethylation signals peaked delayed. These findings support the hypothesis raised by Zuzuarregui et al (2012) that the PP2A enzyme works in a non-processive manner to dephosphorylate its substrates and therefore Cdc55 seems to target Net1 several times.

3.1.2 M-Tracking of the short-lived protein-protein interaction between $PP2A^{Rts1}$ and its substrate Kin4 in a *rts1*Δ strain

The interaction of Rts1 and Kin4 has already been investigated by I. Mudrak and B. Bhatt before, who could show the specific PP2A-substrate contact via M-Track. To familiarize myself with the M-Track method, their experiments were repeated to verify Kin4 as an interaction partner of $PP2A^{Rts1}$ (Figure 12). Both bait and prey fusion proteins were expressed under control of heterologous promoters (TPI and Gal1) on 2µ plasmids in an *rts1*Δ strain. Preparation of samples for the time course and presentation of results were carried out as described for Figure 11. Mean values of data of two similarly conducted experiments are shown in line diagrams (n=2; Figure 12B) whereas the blots illustrate the expression level and methylation signals at one exemplary exposure time point of a single experiment (Figure 12A).

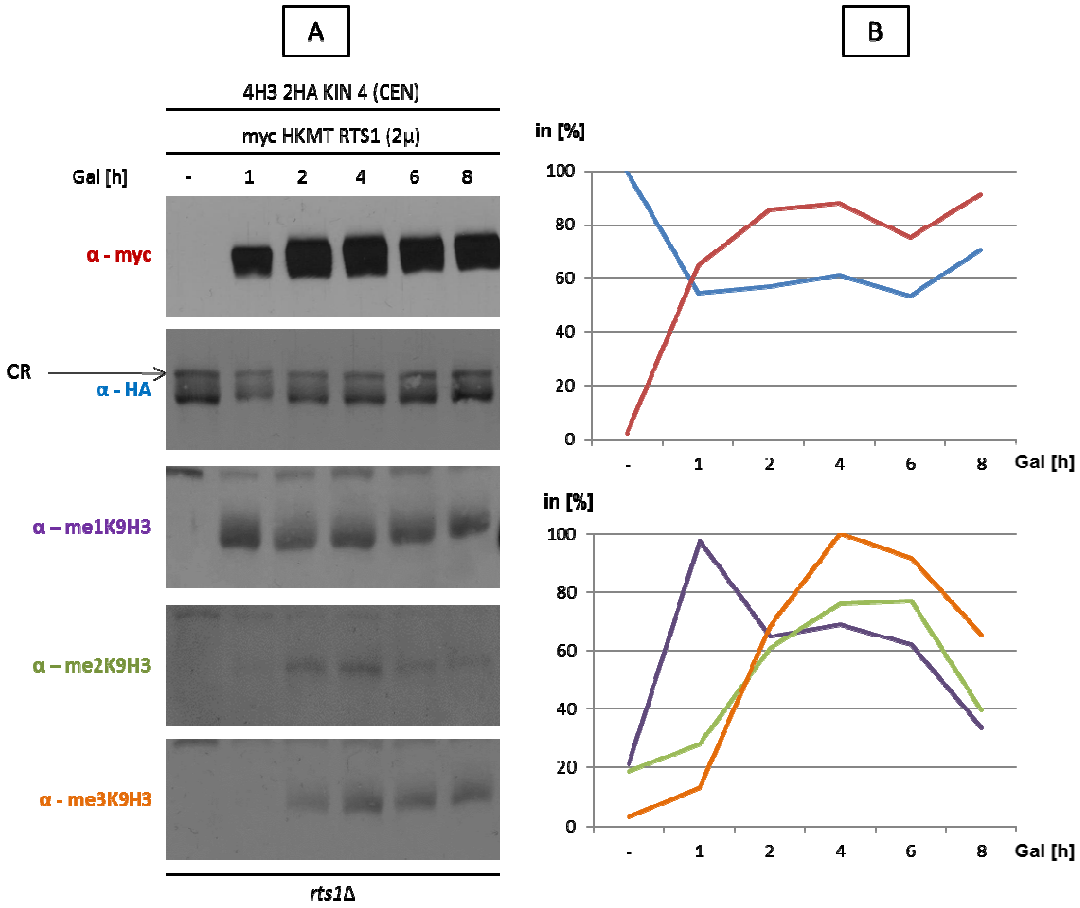

Figure 12. M-Track detects the interaction of PP2A^{Rts1} holoenzyme with its substrate Kin4. (A) At indicated time points after galactose induction TCA lysates were prepared from a *rts1*Δ strain expressing constitutively the prey protein P_{TPI} 4H3 2HA GL Kin4 (CEN) and inducibly the P_{Gal} myc HKMT GL Rts1 (2µ) bait. Samples were analyzed by a 10% SDS-PAGE on 5 separate gels, immunoblotted and incubated with specific monoclonal antibodies against HA and myc tagged proteins as well as mono- (α-me1K9H3), di- (α-me2K9H3) and tri-methylated K9H3 (α-me3K9H3). The HA-antibody specific cross reaction is indicated by an arrow above the Kin4 protein band. Blots are exemplarily shown at one exposure time: myc, HA, mono- and tri methylation signals after 3min and dimethylation after 1h. (B) For the evaluation, the signal intensity of HA, myc, mono- and trimethylated prey of two similarly conducted experiments (n=2) was quantified with Image Quant Analysis program at different exposure time points: HA (1min, 3min, 1h), myc (10sec, 1min, 1h), me1K9H3 (1min, 3min, 1h), me2K9H3 (1h), me3K9H3 (1min, 3min, 1h). Data was normalized to the HA levels and the highest value was set to 100%.

The galactose inducible expression of the bait protein revealed a high level starting from the 2h time point. The prey exhibited the highest expression of 4H3 2HA KIN4 in the uninduced sample, then decreased and showed a faint increase in the last sample. The results of the shown single experiment (Figure 12A) were in accordance with results gained from other experiments (Figure 12B), as a similar expression pattern was observed.

Monomethylation signals (α-me1K9H3) peaked 1h after galactose induction and then decreased. Expression stayed almost at similar levels until the 6h time point, where a sudden decrease could be observed. Averaged values of the very weak dimethylation signal (α-me2K9H3) showed a maximum expression level after 6h. In the last two hours of measurement the signal intensity decreased to about 40% of its maximal level. The onset of trimetylation signals (α-me3K9H3) could be observed at the 2h sample in the blots and showed its maximal level in the 4h sample (Figure 12A). The line diagram shows the same results for the data of two conducted experiments and moreover revealed a decrease to 60% of the maximal level at the 8h time point (Figure 12B).

These data are in line with findings from other lab members indicating that Kin4 is a substrate of PP2A subunit Rts1 (Zuzuarregui et al, 2012). Moreover, data indicates a time-shifted presence of the three methylated species. The blots clearly show the presence of monomethylation at first, followed by dimethylation and trimethylation which was detectable in later time points of the measurement.

3.2 Testing additional controls for M-Track to verify the detected PP2A interactions

To substantiate the obtained results concerning the interaction of $PP2A^{Cdc55}$-Net1 and $PP2A^{Rts1}$-Kin4 different controls were introduced for further M-Track experiments (Figure 13 and 14).

With one control we aimed to test, whether the localization of the tag on the prey and bait (N- or C-terminus) has an influence on the M-Track ability of detecting proteins of interest. So far, it is only known that the core region of the regulatory subunit interacts with the AC heterodimer. Moreover, Shi (2009) reveals that the B` subunit interacts strongly with the AC dimer whereas B subunits only interact poorly. The N- and C-termini of each subunit might to be involved in targeting substrates (Li & Virshup, 2002; Zhao et al, 1997). As Shi (2009) describes the site for substrate binding seems to be localized on the top site of the regulatory subunits. Therefore one can assume that the position of the tag might have an influence on the ability of the bait to target its prey. To examine the effects of differently positioned bait and preys on the detectability, C-terminal tags for our bait and preys were cloned.

The second control which has already been established in the lab (I. Mudrak, T. Kupka, B. Bhatt) includes a bait construct which does neither harbor Cdc55 nor Rts1. This experimental condition shall prove if the reaction is driven predominantly by the regulatory subunit and to determine to what extent the HKMT and its intrinsic affinity to the H3-tag take

part in substrate detection. This additional control in M-Track shall ensure the validity of the gained results.

The third control has been established by I. Mudrak, T. Kupka and B. Bhatt on the assumption that PP2A regulatory subunits do not have overlapping target substrates (Mui et al, 2010; Shu et al, 1997). They have shown that Net1 is not trimethylated by Rts1 and neither is Kin4 modified when tested with Cdc55. Nevertheless, these experiments have only been done with the N-terminal bait and prey fusion constructs. To investigate this hypothesis of non-overlapping substrates of PP2A regulatory subunits, Cdc55 and Rts1 were tested for interaction with the corresponding substrate of the other subunit in M-Track.

To verify obtained results these three controls were included in my diploma thesis in the following experiments.

3.2.1 M-Tracking with C-and N-terminal constructs to prove the Net1-Cdc55 interaction

To gain further information about the Net1-Cdc55 interaction an M-Track assay with Net1 as prey protein was performed. The used constructs have either been cloned by my colleagues T. Kupka and I. Mudrak (C- and N-terminal bait, N-terminal prey) or were cloned during this diploma thesis (C-terminal prey). Hence, I could check N-terminal tagged Net1 for interaction with the bait Cdc55, tagged either at the C- (“CDC55 GL HKMT myc”) or at the N-terminus (“myc HKMT GL CDC55”). Furthermore, a possible interaction of Net1 and Rts1 was analyzed using C- (“NET1 GL 2HA 4H3”) and N-terminal (“4H3 2HA GL NET1”) tagged Net1 as prey (Figure 13). Expression of bait and preys was induced as already described for Figure 11, but only at two time points (4h, 8h) and compared to uninduced samples. The shown gel blots illustrate the M-Track components and methylation signals at one exemplary exposure time point of one experiment (Figure 13). Additionally, the absolute mono- and trimethylation values normalized to the HA levels of three different experiments (n=3) are shown in a bar diagram (Figure 13).

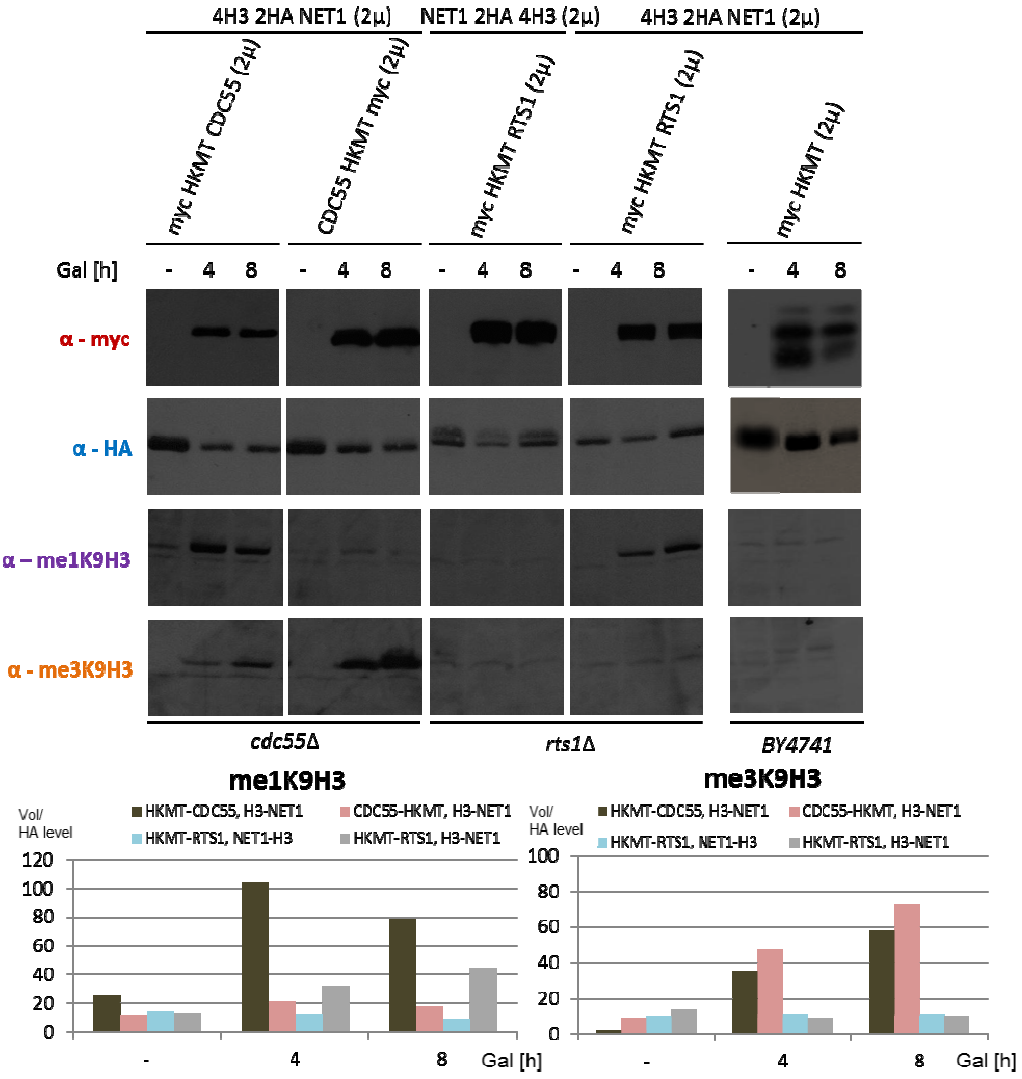

Figure 13. M-Track controls to confirm the interaction of PP2A^{Cdc55} holoenzyme with its substrate Net1. At indicated time points (4h, 8h) after galactose induction TCA lysates were prepared from a *cdc55*Δ strain expressing constitutively the prey protein P_{TPI} 4H3 2HA GL Net1 (2µ) and inducibly either the C- or N-terminal tagged CDC55 (panel 1: P_{Gal} myc HKMT GL Cdc55 (2µ) and 2: P_{Gal} Cdc55 GL HKMT myc (2µ)) as well as from an *rts1*Δ strain, which expressed either C- or N-terminal tagged NET1 prey (panel 3: P_{TPI} Net1 GL 2HA 4H3 (2µ) and 4: P_{TPI} 4H3 2HA GL Net1 (2µ)) with a P_{Gal} myc HKMT GL Rts1 (2µ) bait. As a negative control the HKMT-only samples prepared from a BY4741 wild-type strain expressing the prey protein P_{TPI} 4H3 2HA GL Net1 (2µ) and the HKMT only control (P_{Gal} myc HKMT (2µ); panel 5) are shown from a similarly conducted experiment. Samples were analyzed by a 10% SDS-PAGE on 4 separate gels (exclusive HKMT only control), immunoblotted and incubated with specific monoclonal antibodies against HA and myc tagged proteins as well as mono- (α-me1K9H3) and tri-methylated K9H3 (α-me3K9H3). Blots are shown at one exposure time: myc and HA after 3min, mono- and tri-methylation signals after 1h. Different amounts of sample were loaded: panel 1 - 20µl per $1OD_{600}$ x ml = 1, panel 2 and 3 - 60µl per $1OD_{600}$ x ml = 1, panel 4 - 30µl per $1OD_{600}$ x ml = 1 and panel 5 - 15µl per $1OD_{600}$ x ml = 1. For the evaluation, the mono- and trimethylation signal intensity of three similarly conducted experiments (n=3) was quantified with Image Quant Analysis program at different exposure time points: me1K9H3 (1min, 1h) and me3K9H3 (3min, 1h). Data was normalized to the HA levels and is shown in a bar diagram respectively of the loading amount.

Expression of bait proteins was detectable in all samples at the 4h and 8h time points. It was obvious that the expression level of C-terminal Cdc55 was higher than that of the N-terminal one (α-myc) even when considering the different loading amounts. The HA signals indicated the presence of the prey construct during all time points of measurement (α-HA). By loading the double of the amount of C-terminal Net1, it showed a similar expression level as the N-terminal prey. The methylation pattern and time course of N-terminal Net1 with N-terminal Cdc55 was very similar to the results obtained before (see Figure 11). Monomethylation of the two N-terminal constructs (panel 1) led to a stronger signal compared to the N- and C-terminal one (panel 2) whereas the latter revealed a stronger trimethylation signal (Figure 13). These results are supported by the bar diagram, showing additionally the data of two similarly conducted experiments. The bars show clearly the highest monomethylation level with the N-terminal constructs (brown), whereas trimethylation levels are stronger with the C-terminal CDC55 (pink).

The *rts1*Δ strains expressing the C-terminal construct of Net1 and N-terminal bait Rts1 did neither show any mono- (α-me1H3K9) nor any tri-methylation signal (α-me3H3K9) although both, bait and prey were present in sufficient amounts (panel 3). When bait and prey were tagged C-terminally (panel 4) a monomethylation signal was present, that in contrast to Cdc55-Net1 peaked at the 8h time point. Trimethylation of Net1 however could not be detected. When considering the higher loading amount of these samples, the obtained signal might be a background band.

The data of Figure 13 provided strong evidence that PP2A subunits Rts1 and Cdc55 have non-overlapping targets. As already shown by Zuzuarregui et al (2012) Rts1 does not trimethylate N-terminal tagged Net1, which could be confirmed in this M-Track assay. Moreover, the influence of differently tagged subunits revealed a variation in the methylation pattern of the prey. Whilst two N-terminally tagged constructs led to more monomethylation signal, the C-terminal bait and an N-terminal prey led to a higher trimethylation level.

3.2.2 M-Tracking with C- and N-terminal constructs to prove the Kin4-Rts1 interaction

The Kin4-Rts1 interaction has been analyzed by my colleagues I. Mudrak and B. Bhatt who could clearly demonstrate a contact between Rts1 and Kin4. In these experiments only N-terminally tagged Rts1 and Kin4 have been used and therefore the repeated experiments tested the interaction of both bait and prey when tagged either at the C- or N-terminus. Furthermore the theory of non-overlapping targets of the two regulatory PP2A subunits (Shu et al, 1997) was tested. In order to distinguish the Kin4-Rts1 contact from false positive results, the obtained signals were compared to a negative control already established in the lab. This control uses no bait protein but only the HKMT enzyme and shall therefore exclude that the interaction is driven by the HKMT (Figure 14). Samples were induced with galactose and compared to one uninduced sample at three time points (2h, 4h and 8h) as described for Figure 11.

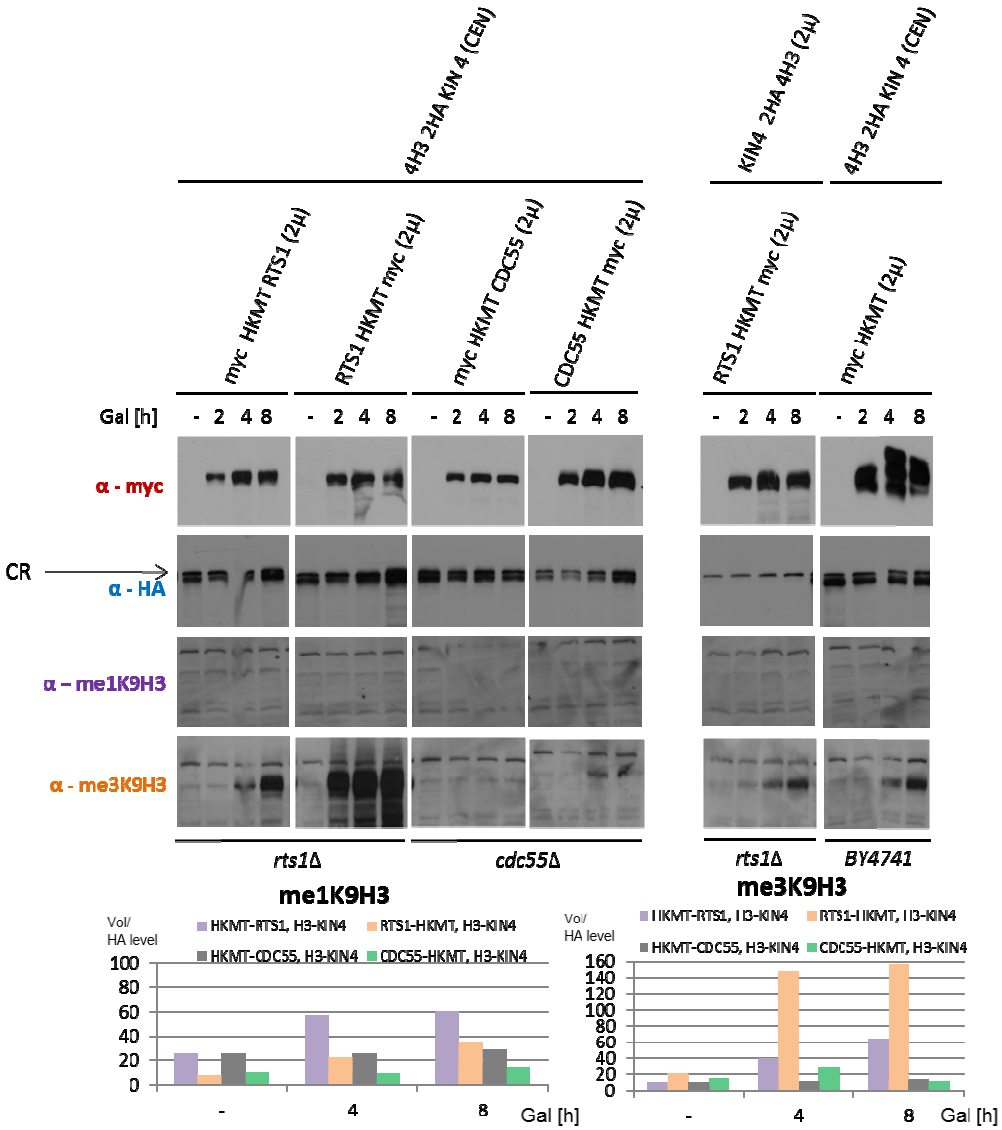

Figure 14. M-Track controls to confirm the interaction of PP2A^{Rts1} holoenzyme with its substrate Kin4. At indicated time points (2h, 4h, 8h) after galactose induction TCA lysates were prepared from a *rts1*Δ strain expressing constitutively the P_{TPI} 4H3 2HA GL Kin4 (CEN) prey with either the P_{Gal} myc HKMT GL Rts1 (2µ) constructs (panel 1) or the P_{Gal} Rts1 GL HKMT myc (2µ) bait (panel 2), from a *cdc55*Δ strain, which expressed constitutively P_{TPI} 4H3 2HA GL Kin4 (CEN) with either C- or N-terminal tagged CDC55 (panel 3: P_{Gal} myc HKMT GL Cdc55 (2µ) and 4: P_{Gal} Cdc55 GL HKMT myc (2µ)), from a *rts1*Δ strain expressing a C-terminal prey protein P_{TPI} Kin4 GL 2HA 4H3 (2µ) and inducibly expressed P_{Gal} Rts1 GL HKMT myc (2µ) (panel 5) and from a BY4741 wild type strain expressing the P_{TPI} 4H3 2HA GL Kin4 (CEN) and the HKMT only (P_{Gal} myc HKMT (2µ); panel 6). Samples were analyzed by a 10% SDS-PAGE on 4 separate gels, immunoblotted and incubated with monoclonal antibodies against HA and myc tagged proteins as well as mono- (α-me1K9H3) and tri-methylated K9H3 (α-me3K9H3). The HA-antibody specific cross reaction is indicated by an arrow above the Kin4 protein. Blots are exemplarily shown at one exposure time: myc and HA after 30sec, mono- and tri-methylation signals after 1h. Different amounts of sample were loaded: panel 1 - 50µl per $1OD_{600}$ x ml = 1, all other panels - 25µl per $1OD_{600}$ x ml = 1. For the evaluation, the mono- and trimethylation signal intensity of two similarly conducted experiments (n=2) was quantified with Image Quant Analysis program at different exposure time points: me1K9H3 (1h) and me3K9H3 (3min, 1h). Data was normalized to the HA levels and is shown in a bar diagram respectively of the loading amount.

Expression of galactose inducible Rts1 and Cdc55 bait protein was detectable in all strains from the 2h time point showing slight increases towards the later time points of measurement. The expression levels of the C-terminal Cdc55 were much higher than the N-terminal variants (Figure 14, panel 3 and 4), whereas the C-terminal Rts1 was only slightly higher then N-terminal Rts1 (Figure 14, panel 1 and 2). The highest expression of myc tagged HKMT could be found in the HKMT only negative control (α-myc).

In all strains a constitutive 4H3 2HA KIN4 expression appeared at all time points of measurement at almost equal levels. When using the C-terminal variant of Kin4 (Figure 14, panel 5) only the antibody specific cross reaction band could be discovered (see arrow in Figure 10, α-HA).

Monomethylation signals could not be detected in all samples as there was a high level of background signals. Interestingly, the second experiment done for this comparison revealed a monomethylation pattern similar to that observed for Cdc55 and Net1 (see bar diagrams). The C-terminal Rts1 bait construct revealed a lower monomethylation level than the N-terminal bait. In contrast trimethylation levels of C-terminal Rts1 and N-terminal Kin4 showed the highest level of trimethylation compared to all other variants (panel 2). The observed pattern of higher monomethylation with N-terminal bait and higher trimethylation with C-terminal bait seems to be true for both, Cdc55-Net1 as well as Rts1-Kin4.

Although the C-terminal tagged Kin4 could not be detected with the HA antibody, there was a pretty strong trimethylation signal detectable in the *rts1*Δ strain harboring C-terminally tagged KIN4 and RTS1 (Figure 14, panel 5). Moreover, trimethylation signals were even detectable in the highly expressed HKMT negative control when expressed together with N-terminal Kin4 (panel 6). Both strains harboring Cdc55 (panel 3: N-terminal, panel 4: C-terminal) and Kin4 did not show any methylation signal at all, neither mono- nor tri-methylation could be observed.

In summary, data provided strong evidence for an Rts1-Kin4 interaction and could also be detected with C-terminally tagged fusion construct. As Kin4 did not show any methylation signal with the Cdc55 regulatory subunit, the non-complementarity of the two yeast regulatory subunits was confirmed and extended to C-terminally expressed baits and preys. Similarly to the results observed for Cdc55 and Net1 (Figure 13) the C-terminal Rts1 showed much higher trimethylation levels than the N-terminal variant whereas the latter showed a higher monomethylation signal.

3.3 Continuative analyses of influences of endogenous substrate expression on M-Track

As experiments of T. Kupka and B.Bhatt have revealed differences in the time course of methylation when comparing single and double knock-out strains, the experiments were repeated to determine the effects of endogenous substrate expression. A single knock-out strain of each regulatory PP2A subunit (*rts1*Δ, *cdc55*Δ) was compared to a double deletion strain lacking the Cdc55 or Rts1 subunit and the substrate Net1 or Kin4, respectively.

The comparison of these knock-out strains shall reveal the effect of the endogenous PP2A substrate on the detection of the interaction between the PP2A bait and substrate prey fusion proteins. The endogenous substrate might for example compete with inserted prey constructs or prevent the correct localization of the prey. Strong competition of the endogenous substrate and M-Track fusion proteins can lead to a reduced number of methylated species. In further consequence, lower methylation signal might lead to the wrong assumption that a weaker or no interaction occurs between the PP2A subunits and analyzed substrates.

3.3.1 M-Tracking of Cdc55 and Net1 interaction in *cdc55Δ* and *cdc55Δ/net1Δ* deletion strains

Already created *CDC55* single as well as *CDC55* and *NET1* double knock-out strains from I. Mudrak and T. Kupka were used in these experiments. As previous data regarding the double knock-out strain shows, there might be an influence of endogenously present substrates on the M-Track method. Therefore their experiments were repeated and the two knock-out strains *cdc55*Δ and *cdc55*Δ/*net1*Δ were compared side by side to examine the influence of endogenously expressed Net1. Moreover, these effects were tested when using C- and N-terminal tagged bait constructs to see if the differently placed tags could overcome a competition of endogenous substrates.

At first the single and double knock-out strain were compared when expressing constitutively the N-terminal Net1 prey proteins together with the galactose inducible C-terminal variant of Cdc55 (Figure 15). The time course was prepared similarly as described for Figure 11. To illustrate the levels of bait and (methylated) prey the best, gel blots are shown exemplary at one exposure time point. Mean values of different exposure times were calculated for each blot and shown in line diagrams. Moreover, the average absolute values of mono- and tri-methylation signals of the single and double knock-out strains are compared in bar diagrams (Figure 15).

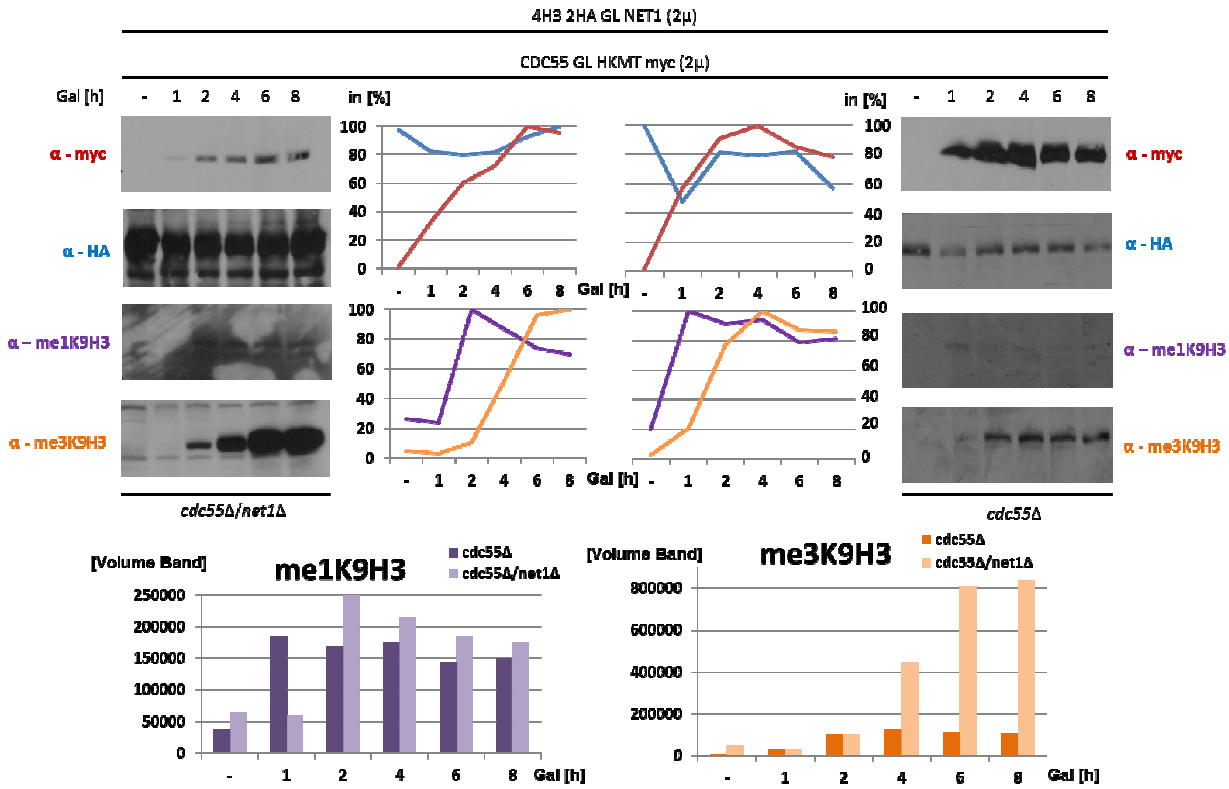

Figure 15. M-Track to compare the interaction of C-terminal Cdc55 with N-terminal Net1 in single (*cdc55*Δ) and double (*cdc55*Δ/*net1*Δ) knock-out strains. At indicated time points after galactose induction TCA lysates were prepared from a *cdc55*Δ (right) and a *cdc55*Δ/*net1*Δ strain (left) both expressing constitutively P_{TPI} 4H3 2HA GL Net1 (2µ) prey protein and inducibly the P_{Gal} Cdc55 GL HKMT myc (2µ) bait protein. Samples were analyzed by a 10% SDS-PAGE on 8 separate gels, immunoblotted and incubated with specific monoclonal antibodies against HA and myc tagged proteins as well as mono- (α-me1K9H3) and tri-methylated K9H3 (α-me3K9H3). All experiments were conducted under the same conditions but the samples of the compared strains were loaded on different gels. Blots of both strains are exemplarily shown at one exposure time: HA, mono- and tri-methylation after 1h and myc after 90sec. For the evaluation, the signals of one experiment (n=1) were quantified with Image Quant Analysis program at different exposure time points: HA (*cdc55*Δ:1h, *cdc55*Δ/*net1*Δ: 30sec, 90sec, 1h), myc (*cdc55*Δ: 10sec, 1min, 1h, *cdc55*Δ/*net1*Δ: 90sec, 3min, 1h), me1K9H3 (*cdc55*Δ and *cdc55*Δ/*net1*Δ: 1h), me3K9H3 (*cdc55*Δ: 3min, 1h, *cdc55*Δ/*net1*Δ: 90sec, 3min, 1h). Data was normalized to the HA levels and the highest value of normalized data was set to 100%. The bar diagrams illustrate the average absolute values of mono- (purple) and tri- (orange) methylation in a *cdc55*Δ and a *cdc55*Δ/*net1*Δ strain after quantification of blots at different exposure time points.

Both strains exhibited an inducible expression of the Cdc55 fusion protein upon galactose addition. While the bait in the single knock-out strain reached already after 2h 90% of its maximal expression level and peaked after 4h, the bait expression in the *cdc55*Δ/*net1*Δ strain revealed after 2h only 60% of its maximum and showed a later peaking at the 6h time point. Band signals of constitutively present Net1 were much higher in the double knock-out strain than in the single knock-out strain (Figure 15).

Both strains showed only faint monomethylation signals. In the *cdc55*Δ/*net1*Δ strain the signals peaked at the 2h time point and then decreased again whereas in the *cdc55*Δ strain a faint signal of monomethylated substrates could be detected in the 1h sample. Trimethylation signals of the double deletion strain (*cdc55*Δ/*net1*Δ) showed at first a faint band in the 2h sample and then further increased to its maximal levels till the 8h time point. Similarly, the single knock-out strain (*cdc55*Δ) revealed an increasing trimethylation signal, but only at weak levels and it peaked earlier (4h). Nevertheless, the level of trimethylated prey was higher in the double knock-out strain than in the single knock-out strain. The obtained lower amount of methylated species in the single knock-out strain might be attributed to the lower level of prey protein Net1 present than in the double knock-out strain (see absolute values).

Results clearly indicated that already proven interactions take place in both, single and double knock-out strains. Both strains showed at first a peaking in monomethylation signal, followed by a later peak of trimethylation. Nevertheless, the double knock-out strain revealed later peaking of mono- and tri-methylation compared to the single knock-out strain. Besides this delayed peaking in the *cdc55*Δ/*net1*Δ strain, data indicated no strong influence of the endogenous substrate when comparing the two strains.

In a second experiment the effects of endogenously present Net1 were analyzed using single (*cdc55*Δ) and double knock-out (*cdc55*Δ/*net1*Δ) strains that express constitutively the N-terminal Net1 prey and the galactose inducible N-terminal variant of Cdc55 (Figure 16). Samples for the time courses were prepared as described for Figure 11. Similarly to Figure 15 one exemplary blot of each fusion construct expression as well as mono-and tri-methylation levels is imaged. Furthermore, line diagrams show the mean values of HA-standardized signal intensity at different exposure times and bar diagrams visualize the averaged absolute values of methylation levels (Figure 16).

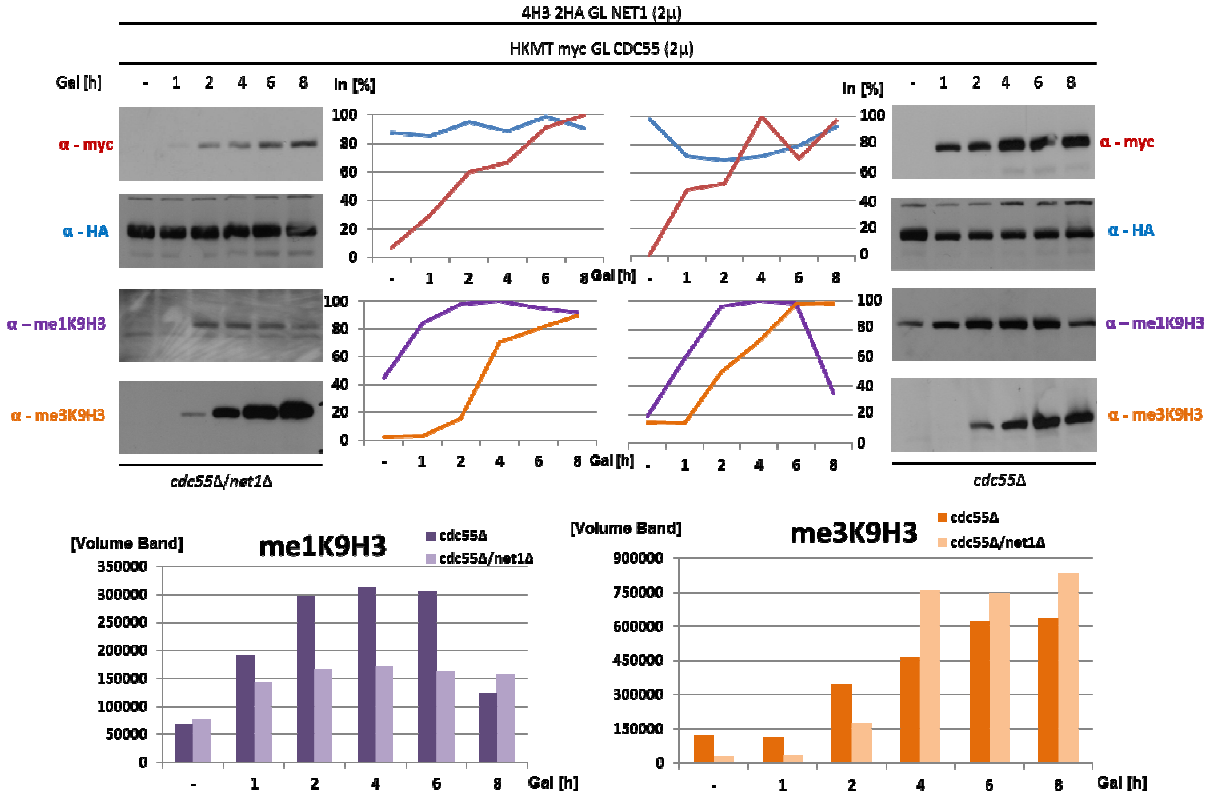

Figure 16. M-Track to compare the interaction of N-terminal Cdc55 with N-terminal Net1 in single (*cdc55*Δ) and double (*cdc55*Δ/*net1*Δ) knock-out strains. At indicated time points after galactose induction TCA lysates were prepared from a *cdc55*Δ (right) and a *cdc55*Δ/*net1*Δ strain (left) both expressing constitutively the P_{TPI} 4H3 2HA GL Net1 (2µ) prey protein and inducibly expressed P_{Gal} myc HKMT GL Cdc55 (2µ) protein. Samples were analyzed by a 10% SDS-PAGE on 8 separate gels, immunoblotted and incubated with monoclonal antibodies against HA and myc tagged proteins as well as mono- (α-me1K9H) and tri-methylated K9H3 (α-me3K9H3). All experiments were conducted under the same conditions but the samples of the compared strains were loaded on different gels. Blots of both strains are exemplarily shown at one exposure time: HA and myc after 30sec and mono- and tri-methylation after 3min. For the evaluation, the signals of one experiment (n=1) were quantified with Image Quant Analysis program at different exposure time points: HA (*cdc55*Δ:30sec, 90sec, *cdc55*Δ/*net1*Δ: 30sec, 90sec, 1h), myc (*cdc55*Δ: 30sec, 90sec, *cdc55*Δ/*net1*Δ: 30sec, 90sec, 1h), me1K9H3 (*cdc55*Δ: 90sec, 3min, *cdc55*Δ/*net1*Δ: 3min, 1h), me3K9H3 (*cdc55*Δ: 3min, 1h, *cdc55*Δ/*net1*Δ: 90sec, 3min, 1h). Data was normalized to the HA levels and the highest value of normalized data was set to 100%. The bar diagrams illustrate the average absolute values of mono- (purple) and tri- (orange) methylation in a *cdc55*Δ and a *cdc55*Δ/*net1*Δ strain after quantification of blots at different exposure time points.

Both strains showed an inducible bait expression with both increasing towards the later time points. The prey was constitutively present and showed a slightly higher level in the double knock-out strain.

Monomethylation levels in the *cdc55*Δ/*net1*Δ strain showed an early peaking (2h time point) followed by a slight decrease towards the end of the time course. Signals were much lower compared to the *cdc55*Δ strain, which showed a reduction in the last 2h down to a level of 35% of the maximal intensity. Interestingly, the monomethylation signals in the single knock-out strain seemed to be present already in the uninduced sample. In both strains trimethylation levels increased during the time course whilst the *cdc55*Δ/*net1*Δ strain showed a later peaking of signals compared to the *cdc55*Δ strain. Whilst the single knock-out strain revealed a higher monomethyl signal the same was true for the trimethylation levels in the double knock-out strain (Figure 16). Moreover, a later peaking of trimethylated prey could be observed similarly to the described pattern for Figure 15.

In summary, as both deletion strains (*cdc55*Δ/*net1*Δ and *cdc55*Δ) revealed mono- and tri-methylation signals, the results indicate an interaction between Cdc55 and Net1. When comparing the data of the double knock-out strain with C- and N-terminal Cdc55 (Figure 15 and 16), no obvious difference in methylation pattern was detectable depending on the localization of the bait protein. Nevertheless, when comparing these two experiments both double knock-out strains showed a much stronger increase of trimethylation in the later time points than the single knock-out strains. If this effect can be explained due to the missing endogenous substrate, has to be further experimentally tested.

3.3.2 M-Tracking of Rts1 and Kin4 interaction in *rts1*Δ and *rts1*Δ/*kin4*Δ deletion strains

I. Mudrak and B. Bhatt have tested the interaction of N-terminal constructs of Rts1 and Kin4 in single (*rts1*Δ) and double knock-out (*rts1*Δ/*kin4*Δ) strains and have thereby revealed that there might be an influence of endogenous Kin4 on the M-Track assay. The repetition of these experiments included a comparison of the interaction of C-terminal Rts1 with Kin4 in both strains (Figure 17). The bait and prey constructs were prepared as described for Figure 11 during the time courses to compare the interaction of N-terminal Kin4 prey with the C-terminal Rts1 in an *rts1*Δ/*kin4*Δ and an *rts1*Δ strain (Figure 17).

Gel blots are shown exemplary at one exposure time while the line diagrams show data of the average values of different exposure times. Additionally mean absolute values of mono- and tri-methylation signals of single and double knock-out strains are compared in bar diagrams (Figure 17).

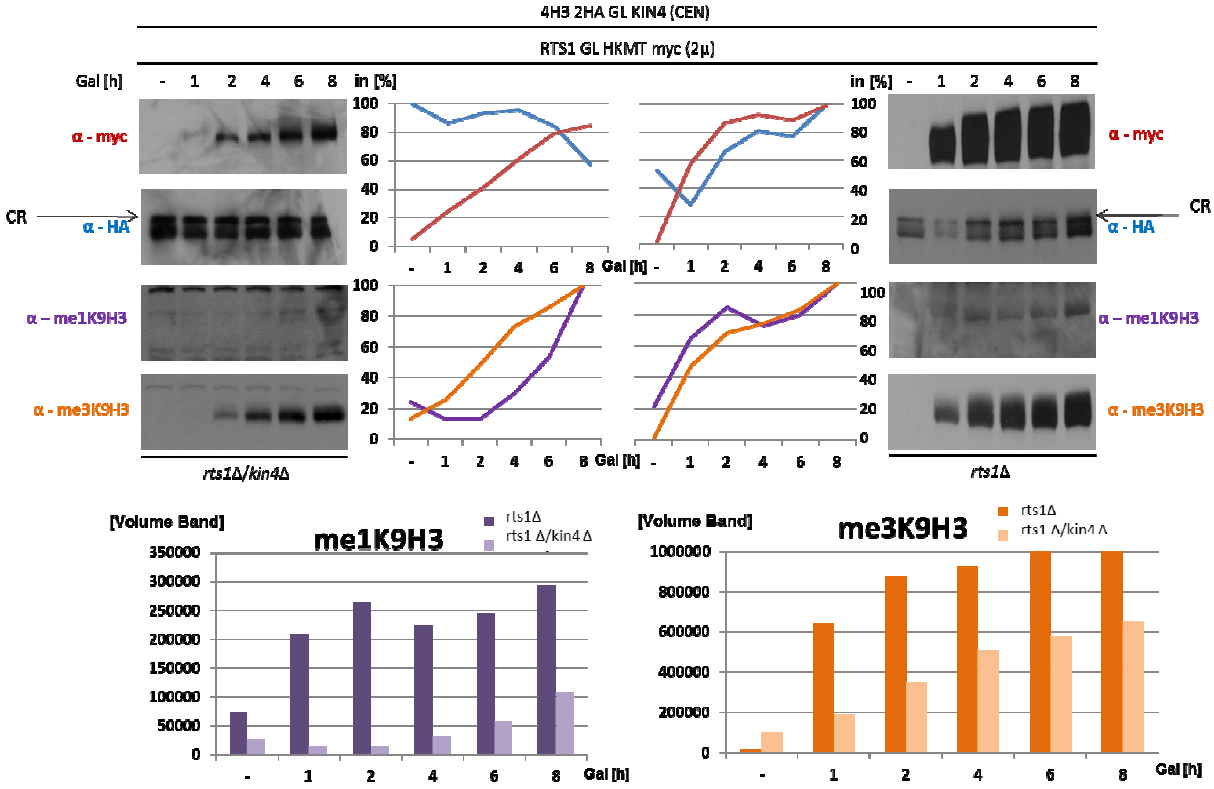

Figure 17. M-Track to compare the interaction of C-terminal Rts1 with N-terminal Kin4 in single (*rts1*Δ) and double (*rts1*Δ/*kin4*Δ) knock-out strains. At indicated time points after galactose induction TCA lysates were prepared from a *rts1*Δ (right) and a *rts1*Δ/*kin4*Δ strain (left) both expressing constitutively the P_{TPI} 4H3 2HA GL Kin4 (CEN) prey protein and inducibly expressed P_{Gal} Rts1 GL HKMT myc (2µ) bait protein. Samples of the two strains were analyzed by a 10% SDS-PAGE on 8 separate gels, immunoblotted and incubated with monoclonal antibodies against HA and myc tagged proteins as well as mono- (α-me1K9H3) and tri-methylated K9H3 (α-me3K9H3). The HA-antibody specific cross reaction is indicated by an arrow above the Kin4 protein. All experiments were conducted under the same conditions but the samples of the compared strains were loaded on different gels. Blots of both strains are exemplarily shown at one exposure time: HA and myc after 3min, monomethylation after 1h and trimethylation after 1min. For the evaluation, the signals of one experiment (n=1) were quantified with Image Quant Analysis program at different exposure time points: HA (*rts1*Δ:10sec, 1min, 1h, *rts1*Δ/*kin4*Δ: 90sec, 3min, 1h), myc (*rts1*Δ: 1min, 3min, 1h, *rts1*Δ/*kin4*Δ: 90sec, 3min, 1h), me1K9H3 (*rts1*Δ and *rts1*Δ/*kin4*Δ: 1h), me3K9H3 (*rts1*Δ: 10sec, 1min, 1h, *rts1*Δ/*kin4*Δ: 1min, 1h). Data was normalized to the HA levels and the highest value of normalized data was set to 100%. The bar diagrams illustrate the average absolute values of mono- (purple) and tri- (orange) methylation in an *rts1*Δ and an *rts1*Δ/*kin4*Δ strain after quantification of blots at different exposure time points.

Increasing expression levels of bait in both strains were inducible upon galactose induction and led to a much higher level in the single knock-out strain. Both knock-out strains revealed a constantly expressed prey Kin4, which exhibited different patterns. While in the *rts1*Δ/*kin4*Δ strain the Kin4 level decreased during the time course to 60% of its maximal value, the prey signals in the *rts1*Δ strain increased from 40% to the maximal level after 8h.

As indicated by the bar diagrams, monomethylation signals in the double knock-out strain were barely above the background. The faint monomethylation levels in the single knock-out strain seemed to peak at the end of the time course. Trimethylation signals showed for both knock-out strains (*rts1*Δ/*kin4*Δ and *rts1*Δ) a peaking towards the late time points as expected and revealed a higher methylation level in the single knock-out strain. Moreover, the *rts1*Δ strain seemed to have an earlier onset of trimethylation (1h time point) in contrast to the *rts1*Δ/*kin4*Δ strain, which revealed a first faint band at the 2h sample.

Interestingly results show the opposite behavior of methylation patterns as for the comparison done with C-terminal Cdc55 and N-terminal Net1 (Figure 15). Whilst Cdc55 and Net1 showed a lower mono- and tri-methylation in the single knock-out strain, Rts1 and Kin4 revealed a higher mono- and tri-methylation signal in the single knock-out strain. From the gained results it seems that endogenously present Kin4 was no barrier in this M-Track assay but rather might have served as an adjuvant for the method.

As already compared by my colleagues, the influence of endogenous Kin4 on the M-Track assay was repeatedly tested with N-terminal Rts1 and N-terminal Kin4 in a double (*rts1*Δ/*kin4*Δ) and a single (*rts1*Δ) knock-out strain. Samples were prepared in a time course as described for Figure 11. Gel blots are shown at one exemplary exposure time next to the line diagrams, illustrating the mean values of data from different exposure times. Additionally averaged means of absolute mono- and tri-methylation levels are presented in bar diagrams (Figure 18).

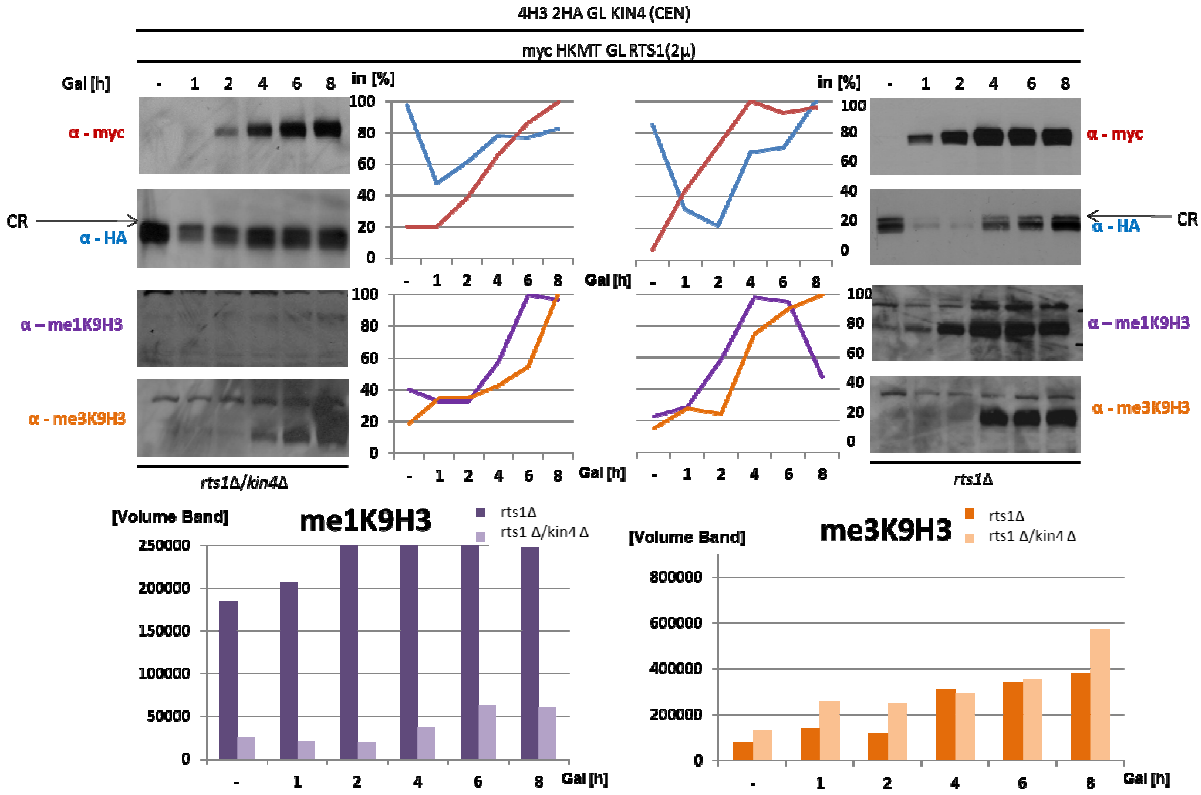

Figure 18. M-Track to compare the interaction of N-terminal Rts1 with N-terminal Kin4 in single (*rts1*Δ) and double (*rts1*Δ/*kin4*Δ) knock-out strains. At indicated time points after galactose induction TCA lysates were prepared from a *rts1*Δ (right) and a *rts1*Δ/*kin4*Δ strain (left) both expressing constitutively the P_{TPI} 4H3 2HA GL Kin4 (CEN) prey protein and inducibly the P_{Gal} myc HKMT GL Rts1 (2µ) protein. Samples were analyzed by a 10% SDS-PAGE on 8 separate gels, immunoblotted and incubated with monoclonal antibodies against HA and myc tagged proteins as well as mono- (α-me1K9H3) and tri-methylated K9H3 (α-me3K9H3). The HA-antibody specific cross reaction is indicated by an arrow above the Kin4 protein. All experiments were conducted under the same conditions but the samples of the compared strains were loaded on different gels. Blots of both strains are exemplarily shown at one exposure time: HA after 3min, myc after 90sec and mono-and tri-methylation after 1h. For the evaluation, the signals of one experiment (n=1) were quantified with Image Quant Analysis program at different exposure time points: HA (*rts1*Δ:90sec, 3min, 1h, *rts1*Δ/*kin4*Δ: 30sec, 3min, 1h), myc (*rts1*Δ: 30sec, 90sec, 1h, *rts1*Δ/*kin4*Δ: 30sec, 3min, 1h), me1K9H3 (*rts1*Δ:90sec, 1h and *rts1*Δ/*kin4*Δ: 1h), me3K9H3 (*rts1*Δ: 90sec, 3min, 1h, *rts1*Δ/*kin4*Δ: 1min, 1h). Data was normalized to the HA levels and the highest value of normalized data was set to 100%. The bar diagrams illustrate the average absolute values of mono- (purple) and tri- (orange) methylation in an *rts1*Δ and an *rts1*Δ/*kin4*Δ strain after quantification of blots at different exposure time points.

Whilst the bait expression of the double knock-out strain was constantly increasing the expression in the single knock-out strain did stay at a similar level from the 4h time point. Preys were constitutively expressed in both, single and double knock-out strains.

Monomethylation signals in the double knock-out strain *rts1*Δ/*kin4*Δ were barely above the background. The monomethylation signals in the single knock-out strain revealed an increase of monomethylation to the 4h time point which was followed by a decrease down to 40% of the maximal expression levels. The different monomethylation levels were clearly visible in the bar diagrams as they revealed different absolute values. Both strains showed an increasing trimethylation signal at a pretty similar level as shown by the bar diagram.

Results gave strong evidence that the interaction of Kin4 and Rts1 can be detected independently of the presence of endogenous substrate. Similarly to the analogue Cdc55 Net1 experiment (Figure 16) the monomethylation levels were much higher in the single knock-out strain than in the double knock-out strain. Moreover, both showed for the single knock-out strain trimethylation signals at a similar level in the last two time points while the level in the double knock-out strain increased about the 1.5-fold.

Despite proving the M-Track method by showing the two analyzed interactions, almost no influence of the presence of endogenous substrates could be detected. The experiments revealed for the trimethylation signals a strong increase towards the later time points in the double knock-out strain whereas in the single knock-out strains the trimethylation levels stayed almost the same. Moreover, an interesting fact observed in three of the experiments were the increased monomethylation levels of the single knock-out compared to the double knock-out stains. How the extent of these different levels is related to the presence of endogenous substrate has to be further analyzed.

3.4 Influences of the amount of bait fusion protein on M-Track

Up to date all our M-Track assays have been done under overexpression of the bait and prey fusion constructs. As overexpression raises the possibility to obtain false positive interactions, the number of fusion proteins within the cell was reduced by a genomic insertion of bait construct.

3.4.1 Introducing bait proteins into the *S.cerevisiae* genome via homologous recombination

To achieve a decreased number of bait fusion proteins, an endogenous integration of the construct into the *S.cerevisiae* genome was necessary. A PCR amplified cassette was designed for the expression of an HKMT tagged Cdc55 fusion protein, which should integrate into the genome of an *S.cerevisiae* wild type strain. The cloning steps are described in detail in Materials and Methods. On the one hand, this method enabled the expression of the construct of interest under the control of the corresponding endogenous promoter. On the other hand, a moderate up-regulation of the expression level of bait fusion protein could be provided using the construct (before floxing), which still contains the inserted P_{Gal} promoter. This enables us to control the expression on two different levels and further tests the sensitivity of the M-Track method.

3.4.1.1 Detection of the interaction between Cdc55 and Net1 at endogenous expression levels of HKMT-Cdc55

The generation of the fusion vector for genomic integration and the subsequent genomic integration into the *S.cerevisiae* genome (see Materials and Methods) were only successful for the Cdc55 subunit as the cloning of the Rts1 construct did not work well. Two different variants of bait protein expression were used for testing the $PP2A^{Cdc55}$ interaction with Net1 (Figure 19). One under control of a P_{Gal} (“LoxP P_{Gal} myc HKMT GL CDC55 endo”) promoter and the other under control of the native endogenous promoter (“myc HKMT GL CDC55 endo”). Both strains expressed constitutively either the prey protein Net1 or Kin4. Kin4 served as a negative control because it did not show trimethylation signals when tested with Cdc55 in M-Track (Zuzuarregui et al, 2012; this diploma thesis, Figure 14). Furthermore, the signal strength under low bait expression levels was compared to the one under high expression levels (high copy number plasmid).

Samples were taken at two time points (uninduced and 6h after galactose induction) and TCA lysates were prepared and analyzed for expression levels of the bait (α-myc) and prey (α-HA) proteins as well as for prey trimethylation (α-me3K9H3, Figure 19A).

All samples containing the genomically integrated P_{Gal} myc HKMT GL tagged Cdc55 constructs were expressed upon galactose induction (α-myc, lane 1+2 and 5+6). Removing the P_{Gal} promoter via floxing led to the constitutive expression of the bait fusion protein (lane 3+4 and 7+8). In both cases, when expressed with Kin4 prey the bait levels were much higher than in the strain with Net1 prey. The expression of the myc HKMT CDC55 sample expressed on a plasmid was at a higher level (lane 9) than the endogenous variants. The constitutively present prey protein Net1 was expressed at a lower level compared to Kin4. At first sight a trimethylation signal of the overexpression system (both constructs expressed on plasmids, lane 9) was visible confirming once again the enzyme-substrate interaction. In comparison, the signal intensity of endogenous Cdc55 constructs could hardly be distinguished from background bands (lanes 1 - 8) and was not detectable by eye.

Because the Cdc55 bait protein was expressed significantly lower than the exogenous version a plain TCA lysis-Western blot might not be sensitive enough to catch the weak methylation signal on the prey. To increase its amount for the Western blot analysis the trimethylated prey Net1 was specifically immunoprecipitated from strains expressing the bait on a plasmid (myc HKMT GL CDC55 (2µ)), or as an endogenous insert with (LoxP P_{Gal} myc HKMT GL CDC55) and without (myc HKMT GL CDC55) an inducible promoter (protocol see Materials and Methods). Thereby the trimethylation of the plasmid expressed prey Net1 was examined in more detail.

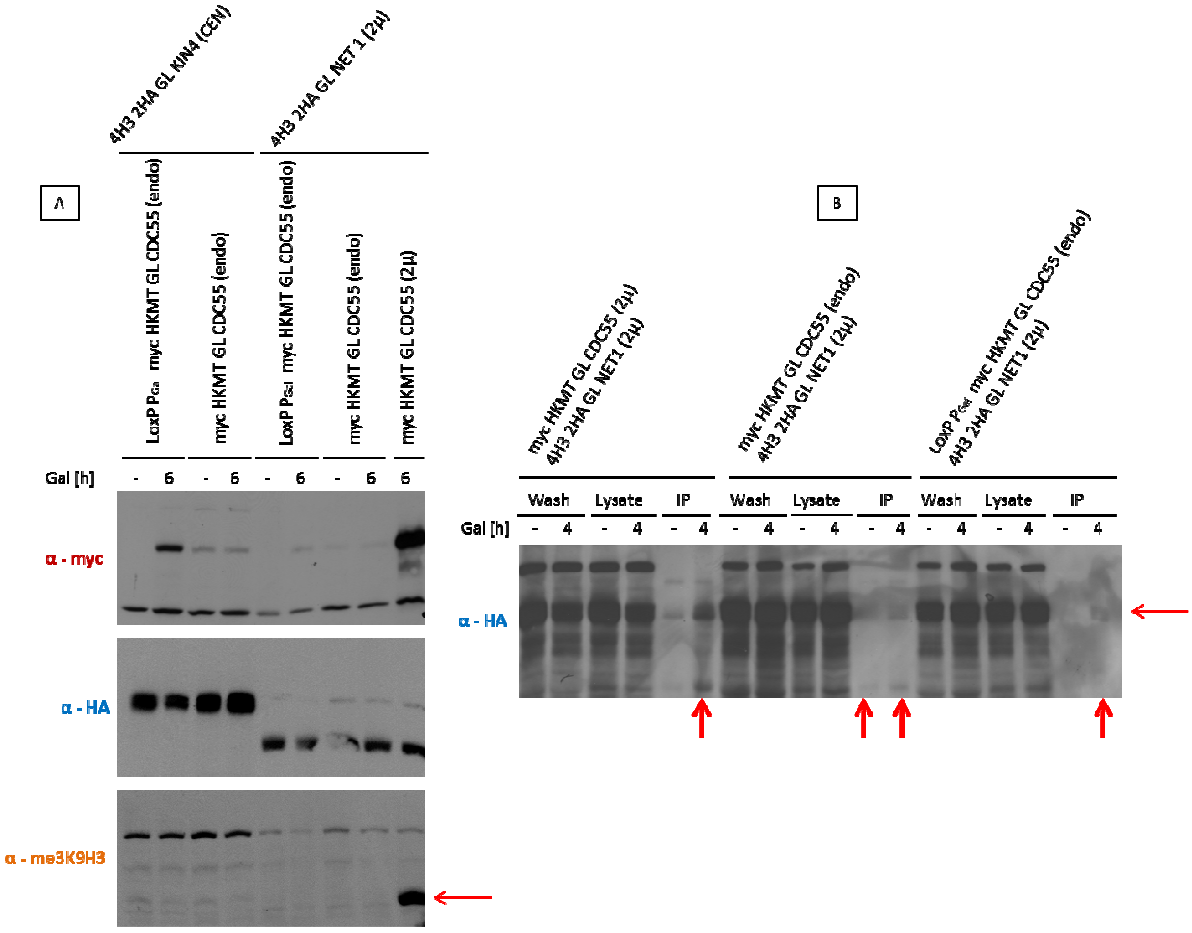

Figure 19. M-Track detection of the Cdc55-Net1 interaction at a low expression level of bait. (A) At indicated time points after galactose induction TCA lysates were prepared from strains expressing either P_{TPI} Net1 GL 2HA 4H3 (2µ) or P_{TPI} Kin4 GL 2HA 4H3 (2µ) preys with constitutively present myc HKMT GL Cdc55 under the control of the endogenous Cdc55 promoter, inducibly present P_{Gal} LoxP myc HKMT GL Cdc55 under control of the Gal promoter or with a P_{Gal} myc HKMT GL Cdc55 (2µ) encoding vector. Samples were analyzed by a 10% SDS-PAGE on separate gels, immunoblotted and incubated with monoclonal antibodies against HA and myc tagged proteins and tri-methylated K9H3 (α-me3K9H3). The faint red arrow next to the m3K9H3 blot indicates the tri-methylated prey Net1. (B) With the same strains an IP was performed according to Materials & Methods with a trimethyl specific antibody and protein A sepharose beads. One aliquot of the lysate was taken before the IP ("Lysate"), one was taken after the IP after spinning down the beads from the supernatant ("Wash") and one from the boiled proteins after the IP ("IP"). Samples were analyzed by 10% SDS-PAGE, immunoblotted and incubated with a monoclonal HA antibody (α-HA). Precipitates are labeled with red arrows below the gel blot, while the faint arrow next to the me3K9H3 blot shall indicate the height of detectable methylated prey.

The trimethylated Net1 species were isolated in an IP from the lysates via a monoclonal antibody against trimethylated Lysine 9 on Histone 3 (α-me3K9H3; Figure 15B). From the strain overexpressing the bait and prey proteins substantial amounts of trimethylated prey could be IPed after galactose induction (left arrow). The faint signal in the uninduced sample was due to spill over of samples. For the endogenous Cdc55 expression trimethylated Net1 could be detected in the induced as well as the uninduced sample (parallel arrows in the middle). These faint bands were present due to constitutive Cdc55 expression and showed a lower level under glucose conditions. For the endogenous P_{Gal} controlled Cdc55 expression trimethylated Net1 could be detected only in the induced sample as no bait protein was present without galactose addition (right arrow).

The present trimethylated substrate indicated that the interaction of Cdc55 and Net1 can be detected in an M-Track assay even at endogenous expression levels of the bait. Nevertheless, the endogenous expression has to be further optimized and extended to the Rts1 prey proteins.

3.4.2 Controlling the expression of the bait protein by using a tetracycline inducible promoter

To establish an alternative to the galactose induced expression of the bait, the N-terminally tagged bait was placed under control of a tetracycline (tet) regulated promoter. Therefore I inserted the bait fusion construct from the original vector pYX142 myc HKMT GL Rts1 into a backbone vector harboring a reverse tet-controlled promoter region as described in Material & Methods. As the research time during my diploma thesis did not leave enough time for all cloning steps, the last controls have to be done by other lab members. This vector could be used in future experiments to analyze the interactions of the PP2A regulatory subunit Rts1. Both M-Track systems, the original galactose regulated and the tet-controlled bait system can further be compared, adapted and optimized.

4 Discussion

So far methods to detect enzyme-substrate interactions have not been able to catch PP2A substrates in-vivo. Hence a recently developed method called M-Track (Zuzuarregui et al, 2012), which is based on a Yeast-Two-Hybrid system, was used in this diploma thesis to detect these short-lived PP2A substrate interactions. As substrate specificity of PP2A is gained upon addition of the regulatory B subunit, the two yeast B subunits Cdc55 and Rts1 were analyzed to prove two already investigated interaction partners. Furthermore, this diploma thesis focused on the analysis of different parameters that might influence M-Track results as for example sterical hindrance and overexpression of fusion proteins and the presence of endogenous substrates. Additionally, the cloning of a tetracycline regulated Rts1 expression vector was initiated for an alternative regulation of the bait protein expression.

Using the M-Track method, the work of my colleagues, who have revealed Net1 as a substrate of $PP2A^{Cdc55}$ holoenzyme (Zuzuarregui et al, 2012), could be confirmed by repeated experiments. Additionally data of this diploma thesis were in accordance with the findings of my lab colleagues, who have identified Kin4 in an M-Track assay as an in-vivo substrate of the Rts1 regulatory PP2A subunit (Zuzuarregui et al, 2012). Results indicated that there is an interaction between Cdc55-Net1 and Rts1-Kin4, as three different forms of methylation signals (mono-, di- and tri-methylation) could be detected. Zuzuarregui et al (2012) describe a time-shifted progression of the methylated species for Cdc55 and Net1 indicating a non-processive mechanism of the HKMT enzyme. In contrast to their findings my data showed the peaks of methylation at similar time points for mono- and di methylation (Cdc55-Net1) or di-and trimethylation (Rts1-Kin4) suggesting maybe rather a processive manner of the HKMT. The single experiments partly exhibited a similar time-shift of methylation peaks as described by Zuzuarregui et al (2012). Mean values of all conducted experiments did not show this time-dependent shift as clearly. Nevertheless, a pattern was recognizable in which the monomethylation peaked the latest at the 2h time point whereas the trimethylation peak occurred at the earliest after 4h.

Results of Zuzuarregui et al (2012) have revealed faint bands of trimethylation with an HKMT only construct, which suggests that the interaction of $PP2A^{Cdc55}$ and Net1 is mainly depending on these two interaction partners. In the experiments of this diploma thesis Cdc55 revealed only weak bands, which could not clearly be distinguished from background bands. In contrast Kin4 led to a quite strong trimethylation signal when co-expressed with a HKMT only construct. Nevertheless, the expression levels of the bait have to be considered as the HKMT only protein was highly overexpressed compared to the HKMT Rts1 constructs.

Although more bait was present the trimethylation level was even less than for the Rts1 baits. Due to the expectations of E. Ogris a background signal can be present with overexpressed constructs, as the HKMT and the H3 possess a strong affinity for each other resulting in a background methylation level. By fusing the PP2A regulatory subunit and a putative substrate, the level of methylation shall be increased as the single affinities of both HKMT to H3 and PP2A to substrate accumulate.

The results raise the question, how the different methylation states correlate with the type of interaction. Collins et al (2005) describe that a few key residues in the active site of HKMTs determine how many methyl groups they add. As analyzes of methyltransferases have revealed the enzymes are restricted in their modification due to structural hindrances (Zhang et al, 2003). Hence, a monomethylase does not transfer more than one methyl residue as there is no space for other residues left. As E. Ogris assumes, the methylation levels might indicate the status of the interaction as short-lived interactions can be described by monomethylation whereas longer lasting contact results in trimethylation (E. Ogris, research grant). Hence, a monomethylation signal which occurs quickly after the start of the interaction in high amounts might be present only due to the spatial proximity of the two constructs. In further consequence, monomethylated species might even occur upon overexpression of the two interaction partners. The results gained in this diploma thesis gave strong evidence that during the progression of the reaction the proportion of trimethylated species increases. Thus, the present (di- or) tri-methylation signal could indicate a more stable interaction of the enzyme and its interaction partner.

A putative interactor of Protein Phosphatase 2B (PP2B), the protein yeast AP1 (YAP1), has led to similar results with just showing monomethylation signals at high overexpression levels (unpublished data of T. Kupka, B. Bhatt and myself). Recently Yap1 has been identified to interact with the PP2A catalytic subunit in cells with a reduced α-Catenin level (Schlegelmilch et al, 2011). These findings suggest that the increased Yap1 activity in α-Catenin depleted cells is dependent on the PP2A catalytic subunit activity. This might be an indicator that if just a monomethylation signal is detectable in M-Track, the signal does not exclusively depend on specific contact with regulatory subunit only but rather show the approximation to the B subunit or a contact to another component of the PP2A holoenzyme.

As data obtained by my colleagues (Zuzuarregui et al, 2012) mainly relies on the N-terminal expression of bait and prey fusion construct one major goal in this diploma thesis was to test, if steric parameters can influence the interaction process. To further analyze the interaction of $PP2A^{Cdc55}$ and Net1 as well as $PP2A^{Rts1}$ and Kin4, C- and N-terminal fusion proteins were used for M-Track assays.

Data indicated a contact of both, N- as well as C-terminal constructs with Cdc55-Net1 and Rts1-Kin4 as mono- and trimethylation signals were detectable. Results of N-terminal bait and preys were in accordance with previously described data (Zuzuarregui et al, 2012). One finding was surprising as it showed for both interaction-pairs different patterns of methylation. While the N-terminal construct led mainly to high monomethylation and low trimethylation the C-terminal variant showed high trimethylation levels and only faint bands of monomethylation. These findings could be either a result of the higher C-terminal bait expression levels or indeed because of steric reasons.

In the vice versa testing of substrates no methylated prey could be observed when analyzing the interaction of Rts1 with C-terminal Net1 confirming the theory of non-overlapping PP2A substrates. In contrast, N-terminal Net1 showed a quite strong level of monomethylation with an Rts1 bait. The observed monomethylation peak might be an overexpression artifact due to the following observations. Firstly, although high amount of bait proteins was present the monomethylation level was even less than for a Cdc55-Net1 experiment. Secondly, the peak of the Rts1-Net1 monomethylation signal could be observed in the last time point in contrast to other M-Track data, where monomethylation peaks usually occurred at earlier time points. Finally, no further methylation took place as no trimethylation signals could be observed. Taken together these results most probably indicate that the observed Net1 monomethylation was a result of overexpressed fusion proteins. Besides, as described for Yap1, the monomethylation signal could be an indicator of an interaction with other components of the PP2A holoenzyme or an approximation of Net1 to the PP2A holoenzyme.

To examine influence of endogenously expressed PP2A substrates a comparison of single and double knock-out strains has been done by my colleagues. When they have compared these strains with N-terminal bait and prey construct differences in the peaks of mono-, di- and tri-methylation have been observed. The repeated experiments in this diploma thesis showed methylation signals and thereby confirmed the interaction of Cdc55-Net1 as well as Rts1-Kin4 in both, single and double knock-out strains. Due to the fact that all conducted experiments for the single vs. double knock-out comparison were only done once, the data did not really display a certain pattern of methylation signals. Moreover, obtained single results are only valid in a certain extent and should not be generalized. Future research should include further comparisons of single and double knock-out strains to analyze the influence of the presence of endogenous substrates. Nevertheless, data could provide a starting basis for further research. An interesting fact observed was that trimethyl levels in all double knock-out strains showed a strong increase in the last time points while the single knock-out strains revealed an almost constant level. Moreover, in three of four experiments higher monomethylation levels were detectable in the single knock-out strains. These results raised the question why monomethylation is less in strains with endogenous

substrates. One assumption could be, that in the case of monomethylation the present endogenous substrates might serve as a positive factor whereas for trimethylation it functions as a competitive target. Nevertheless, the experiments have only been done once and did not clearly show an influence of endogenous substrates on the M-Track assay.

As overexpression can lead to non specific interactions and background signals, the level of inserted fusion proteins was reduced down to physiological levels in order to create a less artificial system within the cells. A major goal was the reduction in number of bait proteins from a high copy vector to endogenous expression levels via genomically tagging Cdc55 with myc HKMT under the control of a P_{Gal} promoter. The integration succeeded only in the case of the Cdc55 fusion protein. The two constructs, one with the galactose inducible promoter and another with the galactose promoter already floxed out did not definitely reveal in a TCA lysis-Western blot whether an interaction between endogenously expressed Cdc55 and overexpressed Net1 occurs. Only when the trimethylated prey was enriched by using an Immunoprecipitation (IP) protocol, a large amount of protein was supplied to prove the enzyme-substrate interaction at endogenous level. Signals of methylation were reduced compared to the overexpression system used in previous experiments, but the interaction of Cdc55 and Net1 could be confirmed. In the future integration of the prey fusion constructs of Kin4 and Net1 into the *S.cerevisiae* genome can be performed to provide physiological conditions.

M-Track provides a tool for analyzing and validating transient interactions. The results of this diploma thesis confirm the already identified substrates of the two yeast PP2A regulatory substrates. Moreover, these data shall provide additional information about barricades and drawbacks of the M-Track method to overcome false positive results with appropriate controls. Given the fact that many control experiments have to be carried out, M-Track should be used rather for validation of substrates than an identification screen.

5 References

Alonso, A., Sasin, J., Bottini, N., Friedberg, I., Friedberg, I., Osterman, A., Godzik, A., Hunter, T., Dixon, J. And Mustelin, T. (2004). Protein Tyrosine Phosphatases in the Human Genome. Cell. **117**(6). 699-711.

Archambault, V., Zhao, X., White-Cooper, H., Carpenter, A.T. and Glover, D.M. (2007). Mutations in Drosophila Greatwall/Scant reveal its roles in mitosis and meiosis and interdependence with Polo kinase. PLoS Genet **3** (11): e200.doi:10.1371/journal.pgen.0030200

Arino, J., Woon, C.W., Brautigan, D.L. and Miller Jr, T.B. (1988). Human liver phosphatase 2A: cDNA and amino acid sequence of two catalytic subunit isotypes. Proc NatI Acad Sci USA. **85**: 4252 - 5256.

Arroyo, J.D. and Hahn, H. (2005). Involvement of PP2A in viral and cellular transformation. Oncogene. **24**: 7746-7755.

Artiles, K., Anastasia, S., McCusker, D. and Kellog, D.R. (2009). The Rts1 Regulatory Subunit of Protein Phosphatase 2A Is Required for Control of G1 Cyclin Transcription and Nutrient Modulation of Cell Size. PLOS Genetics, Nov 2009.

Asakawa, K., Yoshida, S., Otake, F. and Toh-e, A. (2001). A novel functional domain of Cdc15 kinase is required for its interaction with Tem1 GTPase in Saccharomyces cerevisiae. Genetics. **157**:1437-1450.

Attner, M.A and Amon, A. (2012). Control of the mitotic exit network during meiosis. Mol. Biol. Cell. 23 (16): 3122-3132.

Azzam, R., Chen, S.L., Shou, W., Mah, A.S., Alexandru, G., Nasmyth, K., Annan, R.S., Carr, S.A. and Deshaies, R.J. (2004). Phosphorylation by cyclin B Cdk underlies release of mitotic exit activator Cdc14 from the nucleolus. Science. **305**: 516-519.

Barford, D. (1996). Molecular mechanisms of the protein serine/threonine phosphatases. Trends Biochem Sci. **21**: 407-412.

Bertazzi, D.T., Kurtulmus, B. and Pereira, G. (2011). The cortical protein Lte1 promotes mitotic exit by inhibiting the spindle position checkpoint kinase Kin4. JCB. 193(6):1033-1048.

Bizarri, F. and Marston, A.L. (2011). Cdc55 coordinates spindle assembly and chromosome disjunction during meiosis. JCB 193(7):1213-1228.

Calabria, I., Baro, B., Rodriguez-Rodriguez, J-A., Russiñol, N. and Queralt, E. (2012). Zds1 regulates PP2ACdc55 activity and Cdc14 activation during mitotic exit through its Zds_C motif. Journal of Cell Science 125: 2875-2884.

Calin, G.A., di Iasio, M.G., Caprini, E., Vorechovsky, I., Natali, P.G., Sozzi, G., Croce, C.M., Barbanti-Brodano, G., Russo, G. and Negrini, M. (2000). Low frequency of alterations of the alpha (PP2R1A) and beta (PPP2R1B) isoforms of the subunit A of the serine-threonine phosphatase 2° in human neoplasms. Oncoge ne. **19**: 1191-1195.

Castilho, P.V, Williams, B.C, Mochida, S., Zhao, Y. and Goldberg, M.L. (2009). The M Phase Kinase Greatwall (Gwl) Promotes Inactivation of PP2A/B55, a Phosphatase Directed Against CDK Phosphosites. Molecular Biology of the Cell. 20:4777-4789.

Caydasi, A.K., Ibrahim, B. and Pereira, G. (2010). Monitoring spindle orientation: Spindle position checkpoint in charge. Cell Division. **5**:28

Cayla, X., Goris, J., Hermann, J., Hendrix, P., Ozon, R. and Merlevede, W. (1990). Isolation and characterization of a tyrosyl phoshphatase activator from rabbit skeletal muscle and Xenopus laevis oocytes. Biochemistry. 29(3): 658-667.

Chan, L.Y. and Amon, A. (2009). The protein phosphatase 2A functions in the spindle position checkpoint by regulating the checkpoint kinase Kin4. Genes Dev. **23**: 1639 - 1649.

Chan, L.Y. and Amon, A. (2010). Spindle position is coordinated with cell-cycle progression through establishment of mitotic exit-activating and -inhibitory zones. Mol Cell. **39**:444-454.

Chen, W., Possemato, R., Campbell, K.T., Plattner, C.A., Pallas, D.C. and Hahn, W.C. (2004). Identification of specific PP2A complexes involved in human cell transformation. Cancer Cell. **5**: 127-136.

Chen, F., Archambault, V., Kar, A., Lio, P., D'Avino, P.P, Sinka, R., Lilley, K., Laue, E.D., Deak, P., Capalbo L. et al. (2007). Multiple protein phosphatases are required for mitosis in Drosophila. Curr Biol **17**: 293 - 303.

Cheung, P., Allis, C.D. and Sassone-Corsi, P. (2000). Signaling to Chromatin through Histone Modifications. Cell. **103**: 263 - 271.

Chiroli, E., Rossio, V., Lucchini, G. and Piatti, S. (2007). The budding yeast PP2ACdc55 protein phosphatase prevents the onset of anaphase in response to morphogenetic defects. J Cell Biol. **177**: 599-611.

Cho, U.S. and Xu, W. (2007). Crystal structure of protein phosphatse 2A hetrotrimeric holoenzyme. Nature. **445** (7123): 53 - 57.

Clift, D., Bizzari, F. and Marston, A.L. (2009). Shugoshin prevents cohesin cleavage by PP2A(Cdc55)-dependent inhibition of separase. Genes Dev. **23**:766-780.

Cohen, P.T.W., Brewis, N.D., Hughes, V. and Mann, D.J. (1990). Protein serin/threonine phosphatases: an expanding family. FEBS Lett. **268**: 355 - 359.

Collins, R.E, Tachibana, M., Tamaru, H., Smith, K.M., Jia, D., Zhang, X., Selker, E.U., Shinkai, Y. and Cheng, X. (2005). InVitro and inVivo Analyses of a Phe/Tyr Switch Controlling Product Specificity of Histone Lysine Methyltransferases. J Biol Chem. **280**(7): 5563 - 5570.

D'Aquino, K.E., Monie-Casas, F., Paulson, J., Reiser, V., Charles, G.M., Lai, L., Shokat, K.M and Amon, A. (2005). The protein kinase Kin4 inhibits exit from mitosis in response to spinde position defects. Mol Cell. **19**(2): 223-234.

Denu, J.M. and Dixon, J.E. (1995). A Catalytic mechanism for the dual specific phosphatases. Proc NatI Acad Sci USA. **92**: 5910-5914.

De Wulf, P., Montani, F. and Visintin, R. (2009). Protein phosphatases take the mitotic stage. Current Opinion in Cell Biology. **21**: 806 - 815.

DiComo, C.J. and Arndt, K.T. (1996). Nutrients, via the Tor proteins, stimulate the association of Tap42 with type 2A phosphatases. Genes Dev. 10:1904-1916.

Ecket-Boulet, N., Larsson, K., Wu, B., Poulsen, P., Regenberg, B., Nielsen, J. and Kielland-Brandt, M.C. (2006). Deletion of RTS1, Encoding a Regulatory Subunit of Protein Phosphatase 2A, Results in Constitutive Amino Acid Signaling via Increased Step1p Processing. Eukaryotic Cell. 5(1):174-179

Evangelista, Jr, C.C., Rodriguez Torres, A.M., Limbach, M.P and Zitomer, R.S. (1996). Rox3 and Rts1 function in the global stress response pathway in baker´s yeast. Genetics. **142**: 1083 - 1093.

Evans, D.R.H. and Stark, M.J.R. (1997). Mutations in the Saccharomyces Cerevisiae Type 2a Protein Phosphatase Catalytic Subunit Reveal Roles in Cell Wall Integrity Actin Cytoskeleton Organization and Mitosis. Genetics. **145** (2). 227-241.

Fields, S. and Song, O. (1989). A novel genetic system to detect protein protein interactions. Nature. **340**: 245-246.

Gallego, M. and Virshup, D.M. (2005). Protein serine/threonine phosphatases: life, death, and sleeping. Current Opinion in Cell Biology 17: 197-202

Gentry, M.S. and Hallberg, R.L. (2002). Localization of Saccharomyces cerevisiae protein phosphatase 2A subunits throughout mitotic cell cycle. Mol Biol Cell. **13**: 3477 - 3492.

Geymonat, M., Spanos, A., Smith, S.J., Wheatley, E., Rittinger, K., Johnston, L.H. and Sedgwick, S.G. (2002) Control of mitotic exit in budding yeast. In vitro regulation of Tem1 GTPase by Bub2 and Bfa1. J Biol Chem. **277**: 28439-28445.

Ghaemmaghami, S., Huh, W.K., Bower, K., Howson, R.W., Belle, A., Dephoure N., O'Shea, E.K. and Weissman, J.S. (2003). Global analysis of protein expression in yeast. Nature. 425: 737-741.

Giaever, G., Chu, A.M., Ni, L. et al (2002). Functional profiling of the Saccharomyces cerevisiae genome. Nature 418: 387-391.

Gossen, M. and Bujard, H. (1992). Tight control of gene expression in mammalian cells by tetracycline-responsive promoters. PNAS. 89(12): 5547-5551.

Götz, J., Probst, A., Ehler, E., Hemmings, B. and Kues, W. (1998). Delayed embryonic lethality in mice lacking protein phosphatase 2A catalytic subunit Calpha. Proc Natl Acad Sci U S A. **95** (21): 12370-12375.

Harvey, S.L., Enciso, G., Dephoure, N., Gygi, S.P., Gunawardena, J., Kellog, D.R. (2011). A phosphatase threshold sets the level of Cdk1 activity in early mitosis in budding yeast. Mol Biol Cell: 22(19): 3595-3608.

Healy, A.M., Zolnierowicz, S., Stapleton, A.E., Goebl, M., DePaoli Roach, A.A. and Pringle, J.R. (1991). CDC55, a Saccharomyces cerevisiae gene involved in cellular morphogenesis: identification, characterization, and homology to the B subunit of mammalian type 2A protein phosphatase. Mol Cell Biol. **11**: 5767-5780.

Hemmings, B.A., Adams-Pearson, C., Maurer, F., Mueller, P., Goris, J., Merlevede, W., Hofsteenge, J. and Stone, S.R. (1990). Alpha and beta forms of the 65-kDa subunit of protein phosphatase 2A have a similar 39 amino acid repeating structure. Biochemistry. **29** (13): 3166-3173.

Hood-DeGrenier, J.K. (2011). Identification of phosphatase 2A-like Sit4 mediated signaling and ubiquitin-dependent protein sorting as modulators of caffeine sensitivity in S.cerevisiae. Yeast. 28(3): 189-204.

Janssens, V. and Goris, J. (2001). Protein phosphatase 2A: a highly regulated family of serine/threonine phospha-tases implicated in cell growth and signalling. Biochem J. **353** (Pt 3): 417-439.

Janssens, V., Goris, J. and Van Hoof, C. (2005). PP2A: the expected tumor suppressor. Current Opinion Genet Dev. **15**: 34-41.

Janssens, V., Longin, S. and Goris, J. (2008). PP2A holoenzyme assembly: in cauda venenum (the sting is in the tail). Trends in Biochemical Sciences. **33** (3): 113 - 121.

Jaspersen, S.L., Charles, J.F., Tinker-Kulberg, R.L and Morgan, D.O. (1998) A late mitotic regulatory network controlling cyclin destruction in Saccharomyces cerevisiae. Mol Biol Cell **9**: 2803-2817.

Jiang, Y. and Broach, J.R. (1999). Tor proteins and protein phosphatase 2A reciprocally regulate Tap42 in controlling cell growth in yeast. EMBO Journal. **18**: 2782-2792.

Johnson, S.A. and Hunter, T. (2005). Kinomics: methods for deciphering the kinome. Nature Methods. **2**: 17-25.

Junttila, M.R., Puustinen, P., Niemelä, M., Ahola, R., Arnold, H., Böttzauw, T., et al. (2007). CIP2A inhibits PP2A in human malignancies. Cell. **130**: 51-62.

Kerr, G.W., Sarkar, S., Tibbles, K.L., Petronczki, M., Millar, J.B.A. and Arumugam, P. (2011). Meiotic nuclear divisions in budding yeast require PP2ACdc55 - mediated antagonism of Net1 phosphorylation by Cdk. JCB **193** (7): 1157 - 1167.

Khmelinskii, A., Roostalu, J., Roque, H., Antony, C. and Schiebel, E. (2009). Phosphorylation-dependent protein interactions at the spindle midzone mediate cell cycle regulation of spindle elongation. Developmental Cell. **17**: 244-256.

Kitajima, T.S., Sakuno, T., Ishiguro, K., Iemura, S., Natsume, T., Kawashima, S.A. and Watanabe, Y. (2006). Shugoshin colla-borates with protein phosphatase 2A to protect cohesin. Nature. **441** (7089): 46-52.

Kong, M., Fox, C.J., Mu, J., Solt, L., Xu, A., Cinalli, R.M., Birnbaum, M.J., Lindsten, T., Thompson, C.B. (2004). The PP2A-associated protein a4 is an essential inhibitor of apoptosis. Science 306: 695-698.

Lee, S.E., Jensen, S., Frenz, L.M, Johnson, A.L., Fesquet, D. and Johnston, L.H. (2001) The Bub2-dependent mitotic pathway in yeast acts every cell cycle and regulates cytokinesis. J Cell Sci. **114**: 2345-2354.

Li, X. and Virshup, D. (2002). Two conserved domains in regulatory B subunits mediate binding to the A subunit of protein phosphatase 2A. Eur J Biochem. **269**: 546 - 552.

Longin, S. and Goris, J. (2006). Reversible methylation of protein phosphatase 2A. The Enzymes, Protein Methyltransferase. Ed. F. Tamanoi and S. Clarke. Elsevier/Academic Press. 24: 303-324.

Longin, S., Zwaenepoel, K., Louis, J.V., Dilworth, S., Goris, J. and Janssens, V. (2007). Selection of protein phosphatase 2A regulatory subunits is mediated by the C terminus of the catalytic subunit. Journal of Biological Chemistry. 282 (37): 26971-26980.

Mah, A.S., Jang, J. and Deshaies, R.J. (2001). Protein kinase Cdc15 activates the Dbf2-Mob1 kinase complex. Proc Natl Acad Sci USA. **98**: 7325-7330.

McCright, B. and Virshup, D.M. (1995). Identification of a new family of protein phosphatase 2A regulatory subunits. J Biol Chem. **270**: 26123 - 26128.

McCright, B., Rivers, A.M, Audlin, S. and Virshup, D.M. (1996). The B56 Family of Protein Phosphatase 2A (PP2A) Regulatory Subunits Encodes Differentiation-induced Phosphoproteins That Target PP2A to Both Nucleus and Cytoplasm. The Journal of Biological Chemistry. 271 (36): 22081-22089.

Mocciaro, A. and Schiebel, E. (2010). Cdc14: a highly conserved family of phosphatases with non-conserved functions? J Cell Sci. **123**: 2867-2876.

Mohl, D.A., Huddleston, M.J., Collingwood, T.S., Annan, R.S. and Deshaies, R.J. (2009). Dbf2-Mob1 drives relocalization of protein phosphatase Cdc14 to the cytoplasm during exit from mitosis. J Cell Biol. **184**: 527-539.

Mui, M.Z., Roopchand, D.E., Gentry, M.S., Hallberg, R.L., Vogel, J. and Branton, P.E. (2010). Adenovirus Protein E4orf4 Induces Premature APCCdc20 Activation in Saccharomyces cerevisiae by a Protein Phosphatase 2A-Dependent Mechanism. J Virol. **84**(9):4798-4809.

Mumby, M. (2007). PP2A: Unveiling a Reluctant Tumor Suppressor. Cell. 130 (1):21-24.

Olsen, J.V., Blagoev, B., Gnad, F., Macek, B., Kumar, C., Mortensen, P. and Mann, M. (2006). Global, In Vivo, and Site-Specific Phosphorylation Dynamicsin Signaling Networks. Cell. **127** (3): 635-648.

Patterson, K.I., Brummer, T., O'Brien, P.M. and Daly, R.J. (2009). Dual-specificity phosphatases: critical regulators with diverse cellular targets. Biochem J. **418**:475-489

Pereira, G. and Schiebel, E. (2005). Kin4 Kinase Delays Mitotic Exit in Response to Spindle Alignment Defects. Mol Cell. **19**(2): 209 - 221.

Price, N.E. and Mumby, M.C. (1999). Brain protein serine/threonine phosphatases. Current Opinion in Neurobiology. **9**(3): 336-342.

Ptacek, J. et al. (2005). Global analysis of protein phosphorylation in yeast. Nature. **438**:679-684.

Queralt, E. and Uhlmann, F. (2008). Separase cooperates with Zds1 and Zds2 to activate Cdc14 phosphatase in early anaphase. JCB. 182(5): 873-883.

Queralt, E., Lehane, C., Novak, B. and Uhlmann, F. (2006). Downregulation of PP2A (Cdc55) phosphatase by separase initiates mitotic exit in budding yeast. Cell. **125**: 719-732.

Rea, S., Eisenhaber, F., O`Carroll, D., Strahl, B.D., Sun, Z.W., Schmid, M., Opravil, S., Mechtler, K., Ponting, C.P., Allis, C.D. and Jenuwein, T. (2000). Regulation of chromatin structure by site specific histone H3 methyltransferases. Nature. **406**: 593-599.

Riedel, C.G., Katis, V.L., Katou, Y., Mori, S., Itoh, T., Helmhart, W., Gálová, M., Petronczki, M., Gregan, J., Cetin, B., Mudrak, I., Ogris, E., Mechtler, K., Pelletier, L., Buchholz, F., Shirahige, K. and Nasmyth, K. (2006). Protein phosphatase 2A protects centromeric sister chromatid cohesion during meiosis I. Nature. **441** (7089): 53-61.

Ruediger, R., Pham, H.T. and Walter, G. (2001). Alterations in protein phosphatase 2A subunit interaction in human car-cinomas of the lung and colon with mutations in the A beta subunit gene. Oncogene. **20**(15): 1892-1899.

Sablina, A.A., Hector, M., Colpaert, N. and Hahn, W.C. (2010). Identification of PP2A Complexes and Pathways Involved in Cell Transformation. Cancer Research.:**70:** 10474-10484.

Samanta, M.P. and Liang, S. (2008). Predicting protein functions from redundancies in large-scale protein interaction networks. PNAS. 100(22):12579-12588.

Saraf, A., Oberg, E.A. and Strack, S. (2010). Molecular Determinants for PP2A Substrate Specificity: Charged Residues Mediate Dephosphorylation of Tyrosine Hydroxylase by the PP2A/B' Regulatory Subunit. Biochemistry. **49**(5): 986-995.

Schlegelmilch, K., Mohseni, M., Kirak, O., Pruszak, J., Rodriguez, J.R., Zhou, D., Kreger, B.T., Vasioukhin, V., Avruch, J., Brummelkamp, T.R. and Camargo, F.D. (2011). Yap1 Acts Downstream of a a-Catenin to Control Epidermal Proliferation. Cell. **144**(5): 782-795.

Sents, W., Ivanova, E., Lambrecht, C., Haesen, D. and Janssens, V. (2012). The biogenesis of active protein phosphatase 2A holoenzymes: a tightly regulated process creating phosphatase specificity. FEBS Journal. Doi:10.1111/j.1742-4658.2012.08579.x

Seraphin, B; Puig, O; Bouveret, E; Rutz, B; Caspary, F. (2002). Tandem affinity purification to enhance interacting protein identification. Ed. E. Golermis and I. Serebriiskii. Cold Spring Harbor Laboratory Press. Chapter 17:313-328.

Shenolikar, S. (1994). Protein Serine/Threonine Phosphatases-New Avenues for Cell Regulation. Anllu. Rev. Cell. Bio. 10: 55-56.

Shi Y. (2009). Serine/threonine phosphatases: mechanism through structure. Cell. **139**(3): 468-484.

Shou, W., Seol, J.H., Shevchenko, A., Baskervilli, C., Moazed, D., Chen, Z.W., Jang, J., Charbonneau, H. and Deshaies, R.J. (1999). Exit from mitosis is triggered by Tem1-dependent release of the protein phosphatase Cdc14 from nucleolar RENT complex. Cell **97**: 233-244

Shu, Y., Yang, H., Hallberg, E. and Hallberg, R. (1997). Molecular genetic analysis of Rts1p, a B' regulatory subunit of Saccharomyces cerevisiae protein phosphatase 2A. Mol Cell Biol. **17**(6): 3242-3253.

Shu, Y. and Hallberg, R.L. (1995). SCS1, a Multicopy Suppressor of hsp60-ts Mutant Alleles, Does Not Encode a Mitochondrially Targeted Protein. Molecular and Cellular Biology. 15(10): 5618-5626.

Silverstein, A.M., Barrow, C.A., Davis, A.J. and Mumby, M.C. (2002). Actions of PP2A on the MAP kinase pathway and apoptosis are mediated by distinct regulatory subunits. Proc Natl Acad Sci USA. **99**:4221-4226.

Sneddon, A.A., Cohren, P.T. and Stark, M.J. (1990). Saccharomyces cerevisiae protein phosphatase 2A performs an essential cellular function and is encoded by two genes. EMBO J. **9**(13): 4339-4346.

Sontag, E., Hladik, C., Montgomery, L., Luangpirom, A., Mudrak, I., Ogris, E. and White. C. (2004). Downregulation of Protein Phosphatase 2A Carboxyl Methylation and Methyltransferase May Contribute to Alzheimer Disease Pathogenesis. Journal of Neuropathology and Experimental Neurology. **63**(10): 1080-1091.

Strack, S., Cribbs, J.T. and Gomez, L. (2004). Critical Role for Protein Phosphatase 2A Heterotrimers in Mammalian Cell Survival. The Journal of Biological Chemistry. **279**: 47732-47739.

Tong, A.H., Lesage, G., Bader, G.D., Ding, H., Xu, H., Xin, X., Young, J., Berriz, G.F., Brost, R.L., Chang, M. et al. (2004). Global mapping of the yeast genetic interaction network. Science. **303**: 808-813.

Traverso, E.E., Baskerville, C., Liu, Y., Shou, W., James, P., Deshaies, R.J. and Charbonneau, H. (2001). Characterization of the Net1 cell cycle-dependent regulator of the Cdc13 phosphatase from budding yeast. J Biol Chem. **276**: 21924-21931.

Turowski, P., Myles, T., Hemmings, B.A., Fernandez, A. and Lamb, N.J.C. (1999). Vimentin Dephosphorylation by Protein Phosphatase 2A Is Modulated by the Targeting Subunit B55. Molecular Biology of the Cell. **10**(6):1997-2015.

van Zyl, W., Huang, W., Sneddon, A.A., Stark, M., Camier, S., Werner, M., Marck, C., Sentenac, A. and Broach, J.R. (1992). Inactivation of the protein phosphatase 2A regulatory subunit A results in morphological and transcriptional defects in Saccharomyces cerevisiae. Mol Cell Biol. **12**: 4946 - 4959.

Virshup, D. and Shenolikar, S. (2009). From Promiscuity to Precision: Protein Phosphatases Get a Makeover. Molecular Cell. **33**: 537 - 545.

Visintin, R., Hwang, E.S. and Amon, A. (1999). Cfi1 prevents the premature exit from mitosis by anchoring Cdc14 phosphatase in the nucleolus. Nature. **398**:818-823.

Wang, Y. and Burke, D.J. (1997). Cdc55p, the B- Type Regulatory Subunit of Protein Phosphatase 2A, Has Multiple Functions in Mitosis and Is Required for the Kinetochore/Spindle Checkpoint in Saccharomyces cerevisiae. Mol Cell Biol. **17** (2): 620 - 626.

Wang, Y. and Ng, T.Y. (2006). Phosphatase 2A negatively regulates mitotic exit in Saccharomyces cerevisiae. Mol Biol Cell. **17**:80-89.

Wei, H., Ashby, D.G., Moreno, C.S., Ogris, E., Yeong, F.M., Corbett, A.H. and Pallas, D.C. (2001). Carboxymethylation oft he PP2A catalytic subunit in Saccharomyces cerevisiae is required for efficient interaction with the B-type subunits Cdc55p and Rts1p. J Biol Chem. 276 (2): 1570-1577.

Xie, M.W., Jin, F., Hwang, H. et al (2005). Insights into TOR function and rapamycin response: chemical genomic profiling by using a high-density cell array method. Proc NatI Acad Sci USA. 102: 7215-7220.

Xu, Y., Chen, Y., Zhang, P, Jeffrey, P.D., and Shi, Y. (2008). Structure of a Protein Phosphatase 2A Holoenzyme: Insights into B55-Mediated Tau Dephosphorylation. Mol Cell. 31 (6): 873-885.

Xu, Y., Xing, Y., Chen, Y., Chao, Y., Lin, Z., Li, Z., Fan, E., Yu, J.W., Strack, S., Jeffrey, P.D. and Shi, Y. (2006). Structure of the Protein Phosphatase 2A Holoenzyme. Cell. **127**: 1239 - 1251.

Yang, J., Roe, S.M., Pricket, T.D., Brautigan, D.L. and Barford, D. (2007). The structure of Tap42/alpha4 reveals a tetratricopeptide repeat-like fold and provides insights into PP2A regulation. Biochemistry. 46:8807-8815.

Yellman, C.M. and Burke, D.J. (2006). The role of Cdc55 in the spindle checkpoint is through regulation of mitotic exit in Saccharomyces cerevisiae. Mol Biol Cell. **17**(2): 658-666.

Yu, X.X. et al (2001). Methylation of the protein phosphatase 2A catalytic subunit is essential for association of Bα regulatory subunit but not SG2NA, striatin or polyomavirus middle tumor antigen. Mol Biol Cell. 12: 185-199.

Zhang, X., Yang, Z., Khan, S.I., Horton, J.R., Tamaru, H., Selker, E.U. and Xiadong, C. (2003). Structural Basis for the Product Specificity of Histone Lysine Methyltransferases. Molecular Cell 12 (1): 177185.

Zhao, Y., Boguslawski, G., Zitomer, R.S., DePaoli-Roach, A.A. (1997). Saccharomyces cerevisiae homologs of mam-malian B and B' subunits of protein phosphatase 2A direct the enzyme to distinct cellular functions. J Biol Chem. **272**(13): 8256-8262.

Zolnierowicz, S. (2000). Type 2A protein phosphatase, the complex regulator of numerous signaling pathways. Biochem Pharmacol. **60**: 1225-1235.

Zuzuarregui, A., Kupka, T., Bhatt, B., Dohnal, I., Mudrak, I., Friedmann, C., Schüchner, S., Frohner, I.E., Ammerer, G. and Ogris, E. (2012). M-Track:detecting short-lived protein-protein interactions in vivo. Nature Methods. Doi:10.1038/nmeth.2017

6 Appendix

The vectors have already been cloned by my colleagues I. Mudrak, T. Kupka, B. Bhatt and I. Frohner before or during this diploma thesis. Numbers next to coding sequences indicate the length of each protein. Important restriction sites of the vectors are shown of which the numbers in brackets illustrate the amount in the total vector.

pYX 213 myc HKMT GL CDC55

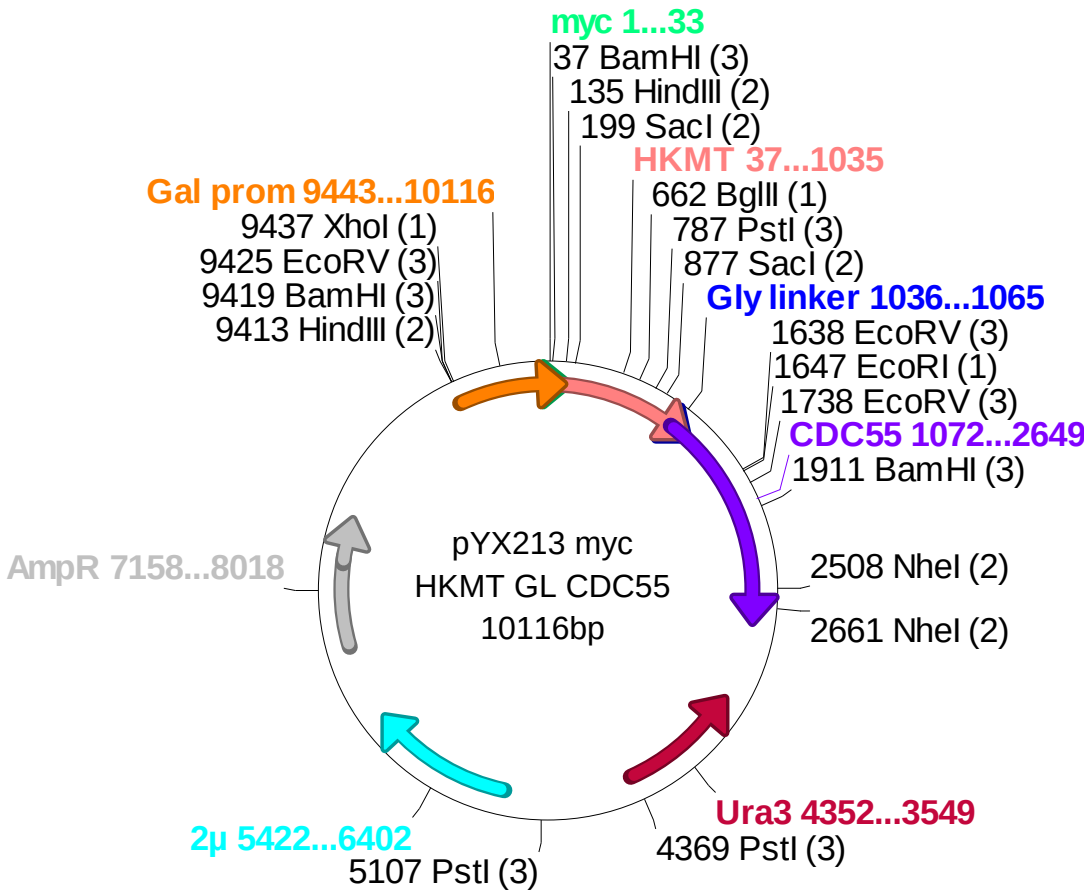

pYX 213 myc HKMT GL RTS1

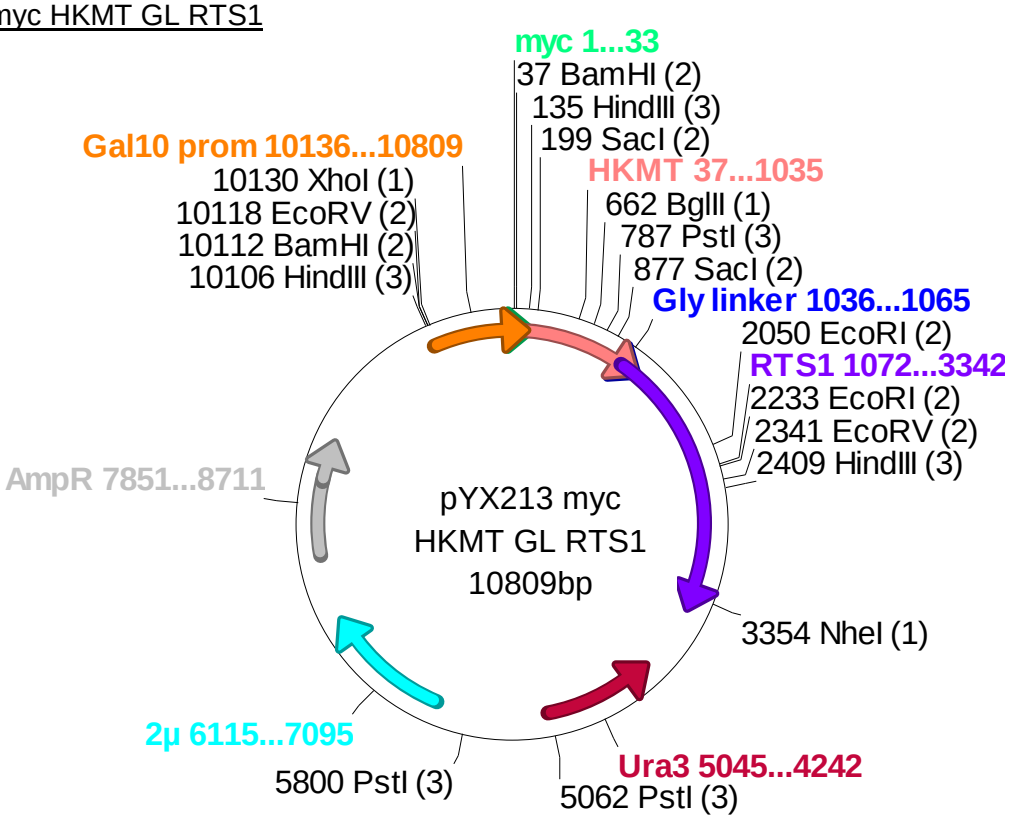

pYX142 4H3 2HA GL KIN4

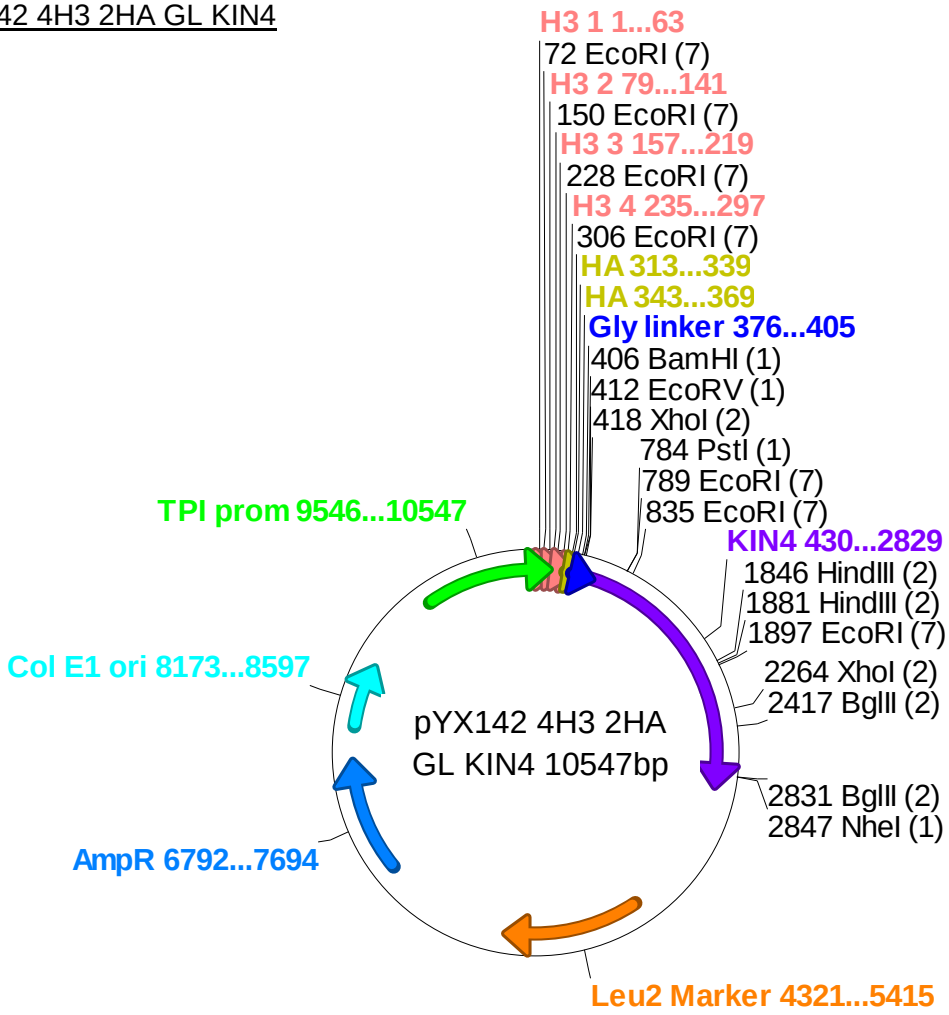

pYX242 3H3 2HA GL NET1

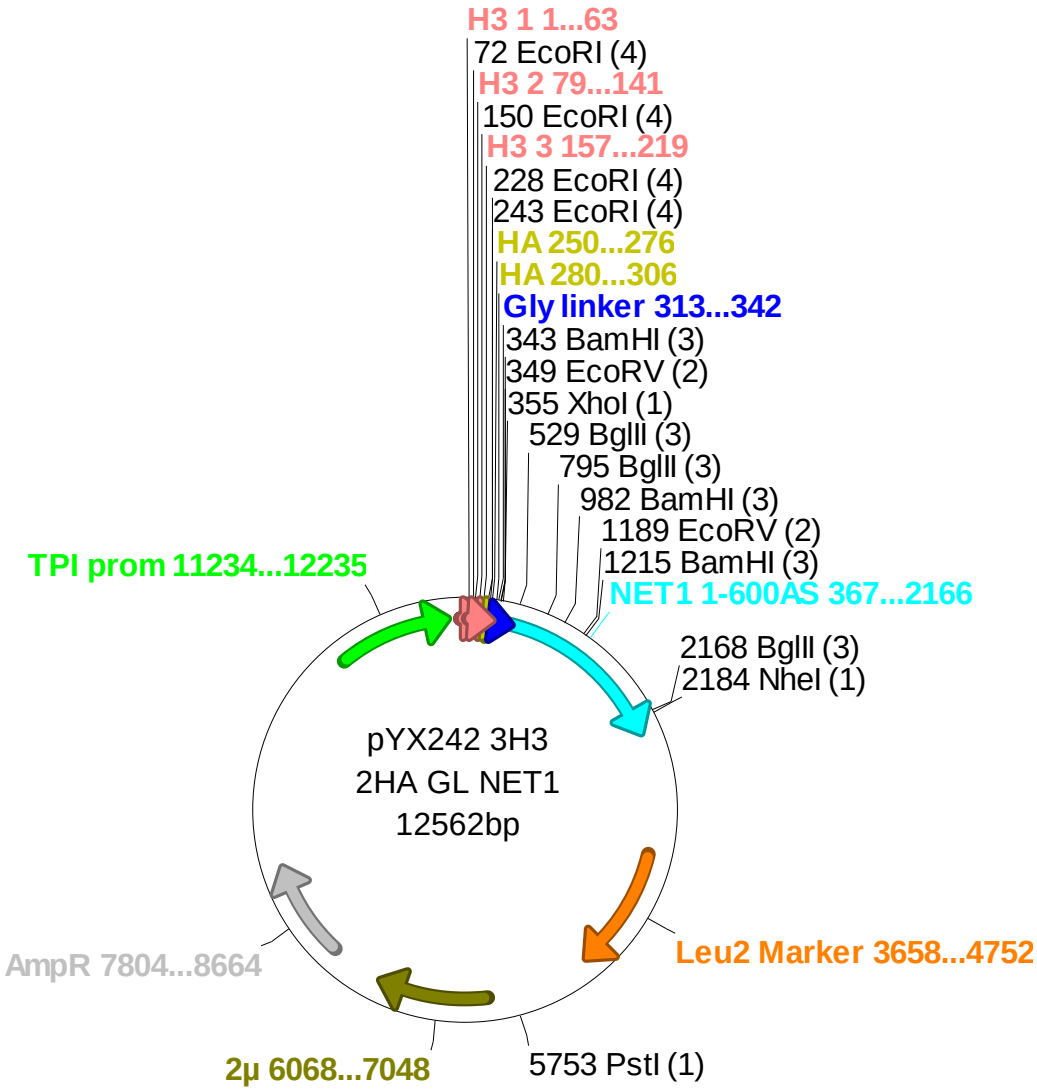

pYX242 4H3 2HA GL NET1

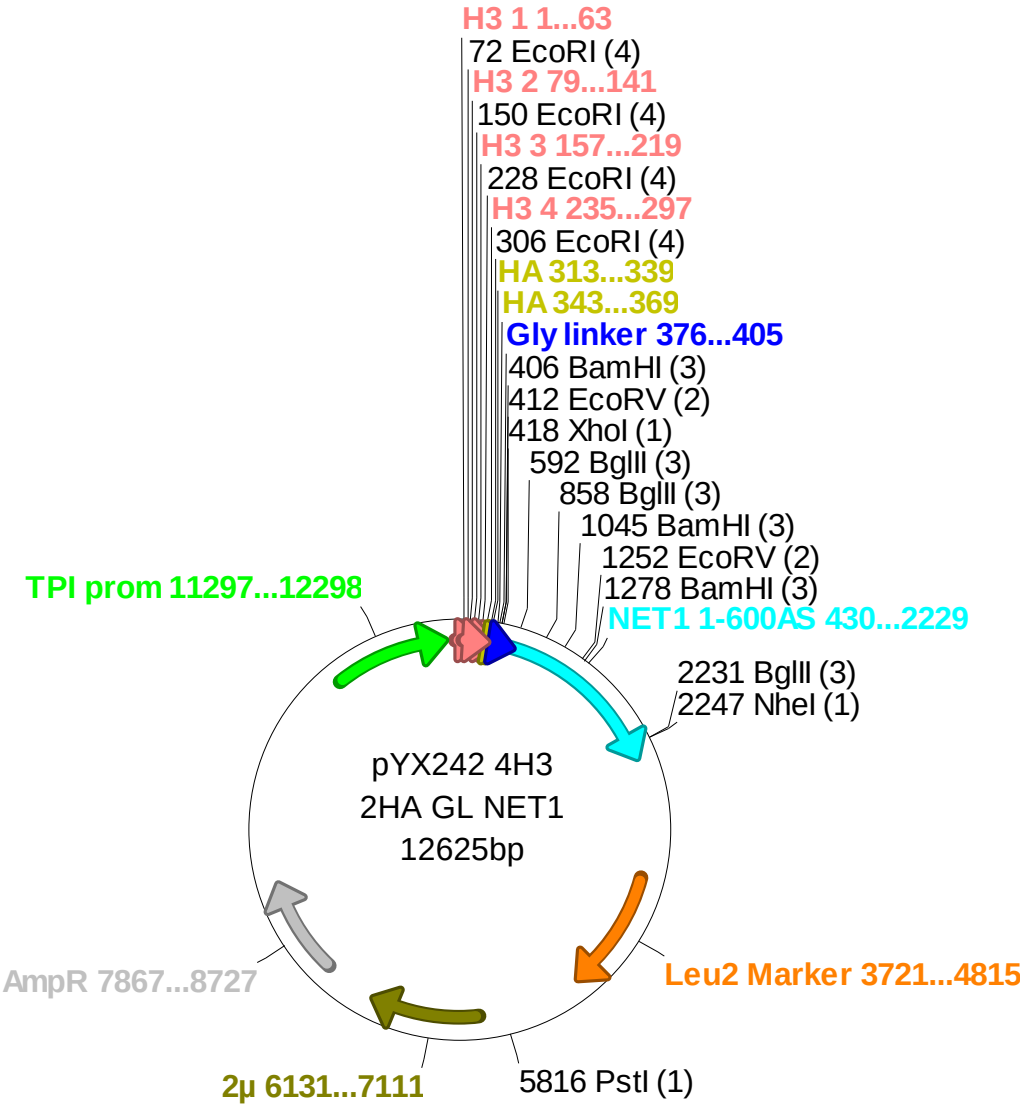

pYX242 KIN4 GL 2HA 4H3

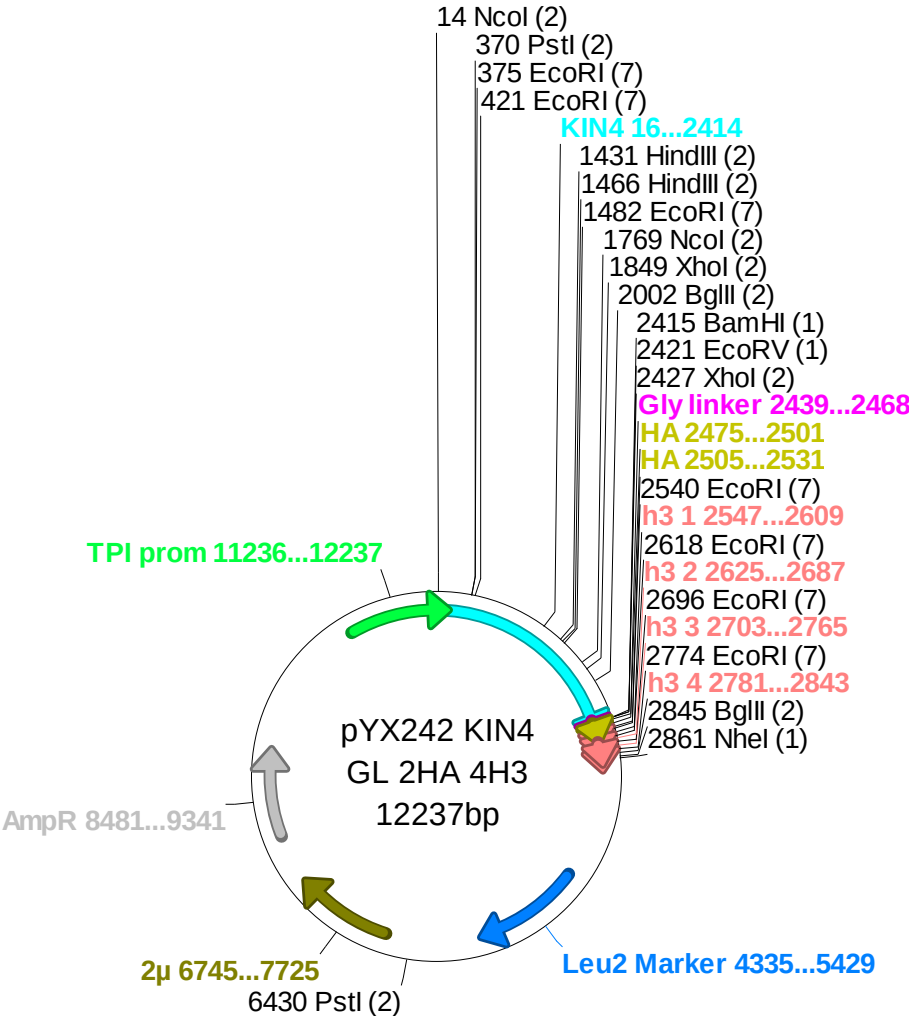

pYX242 NET1 GL 2HA 4H3

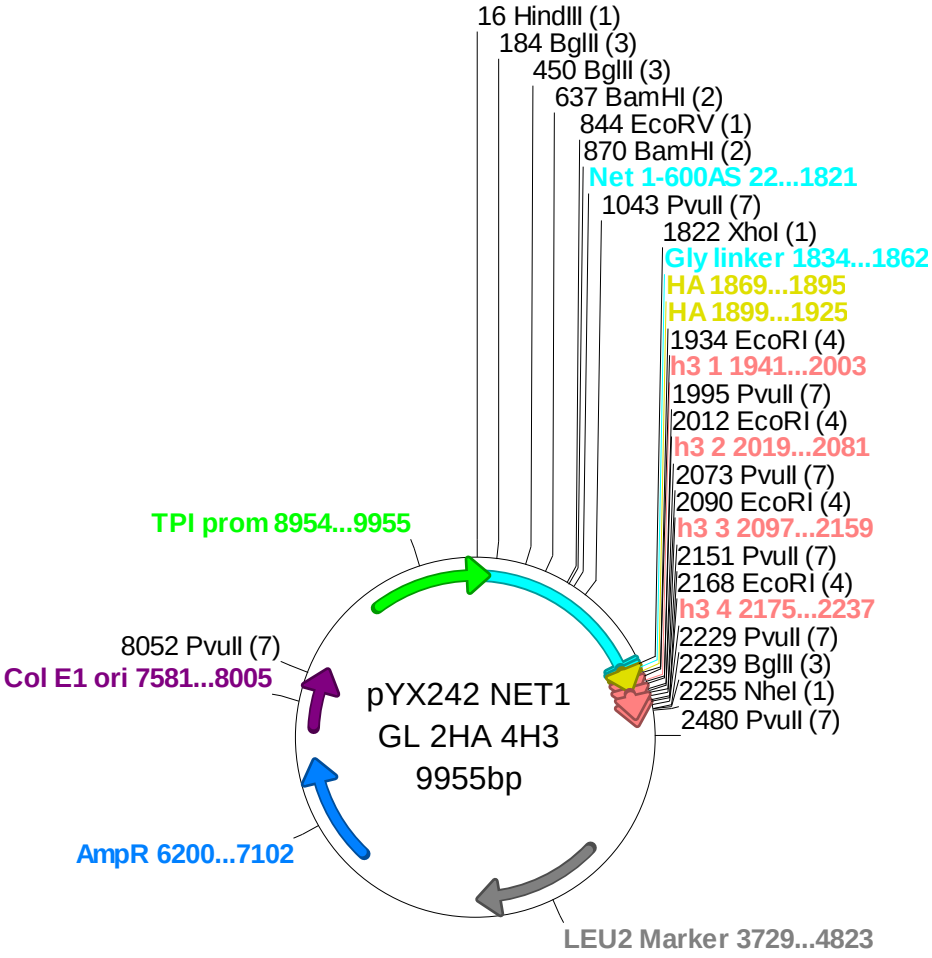

pYX213 CDC55 GL HKMT myc

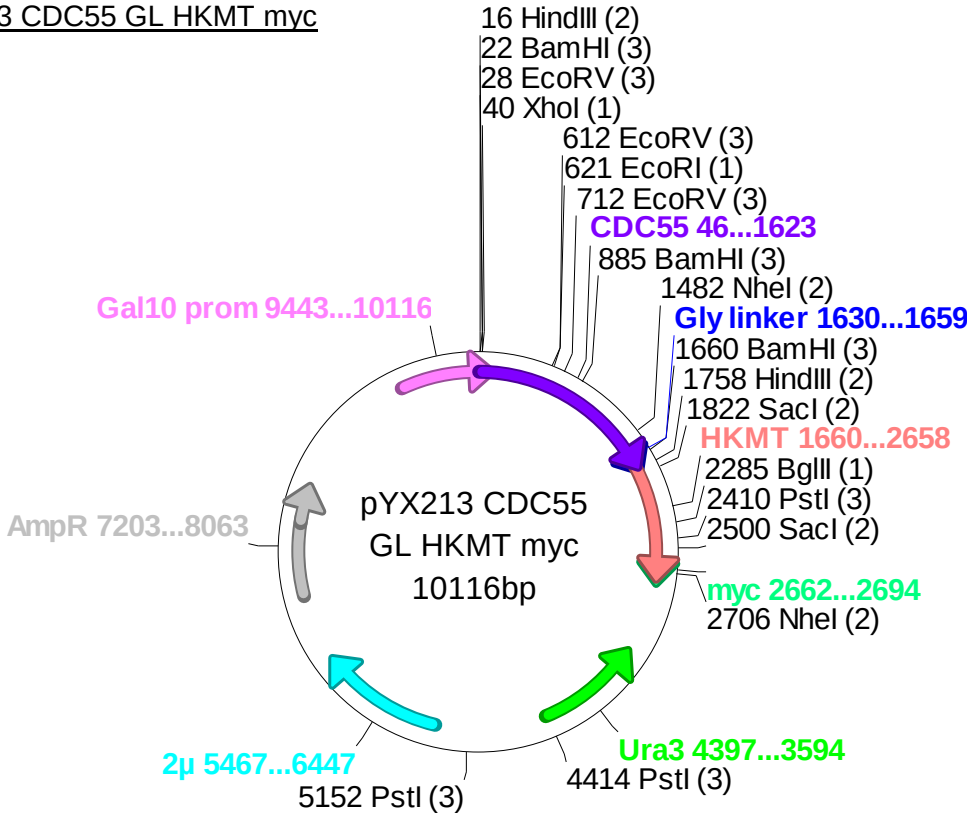

pYX213 RTS1 GL HKMT myc

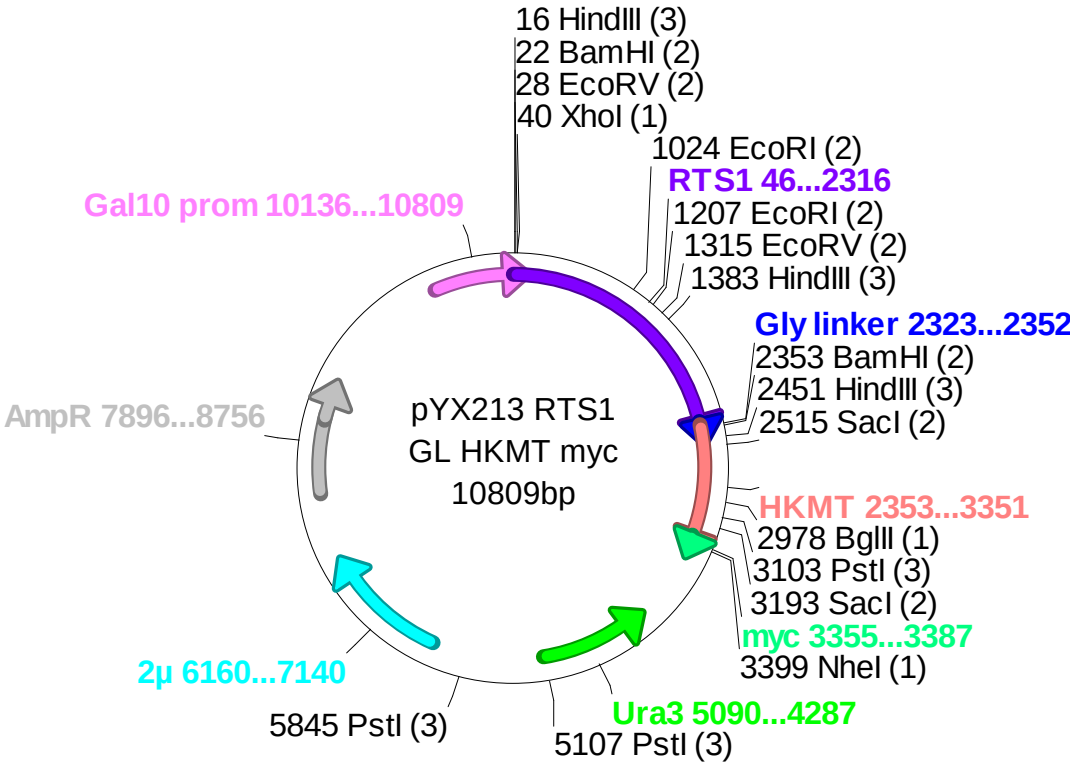

pBS1761 KanMX4 Gal1P LoxP myc suvar GL cdc55

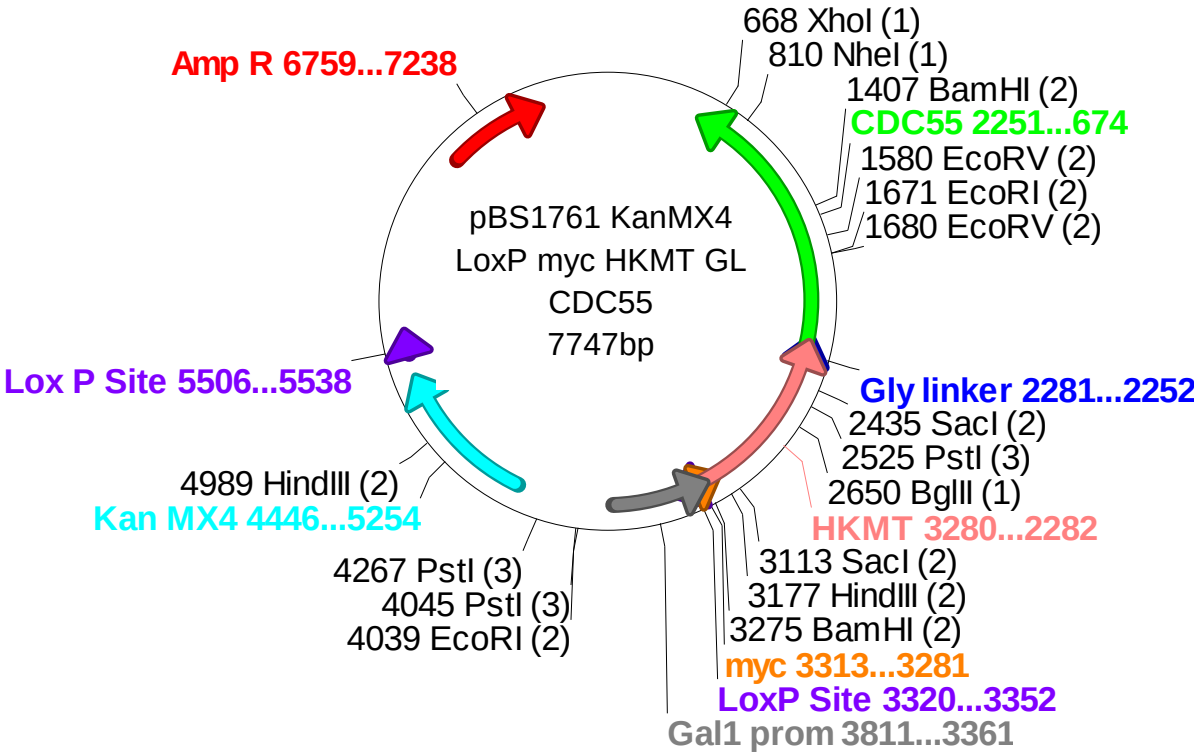

pBS1761

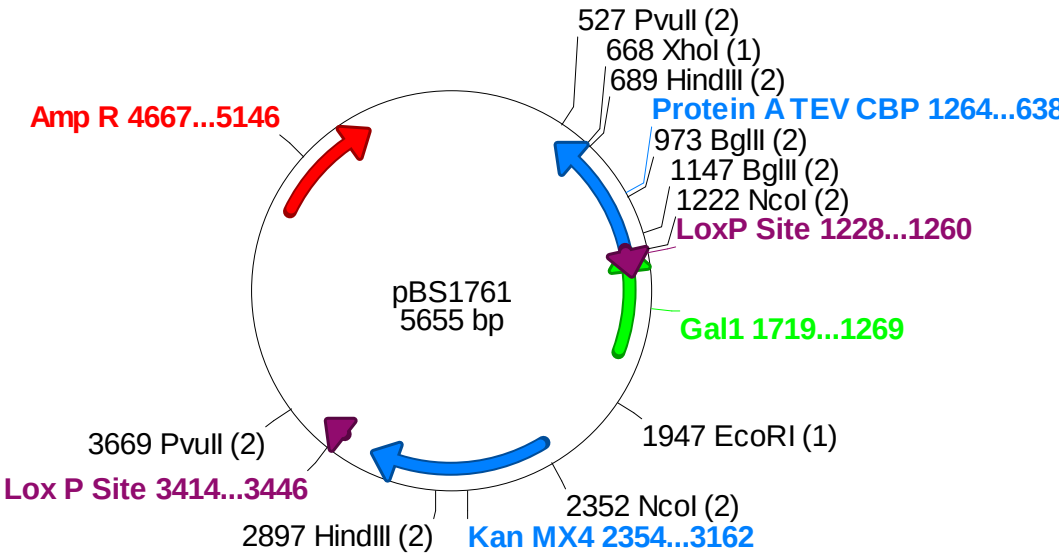

pYX213 myc HKMT GL

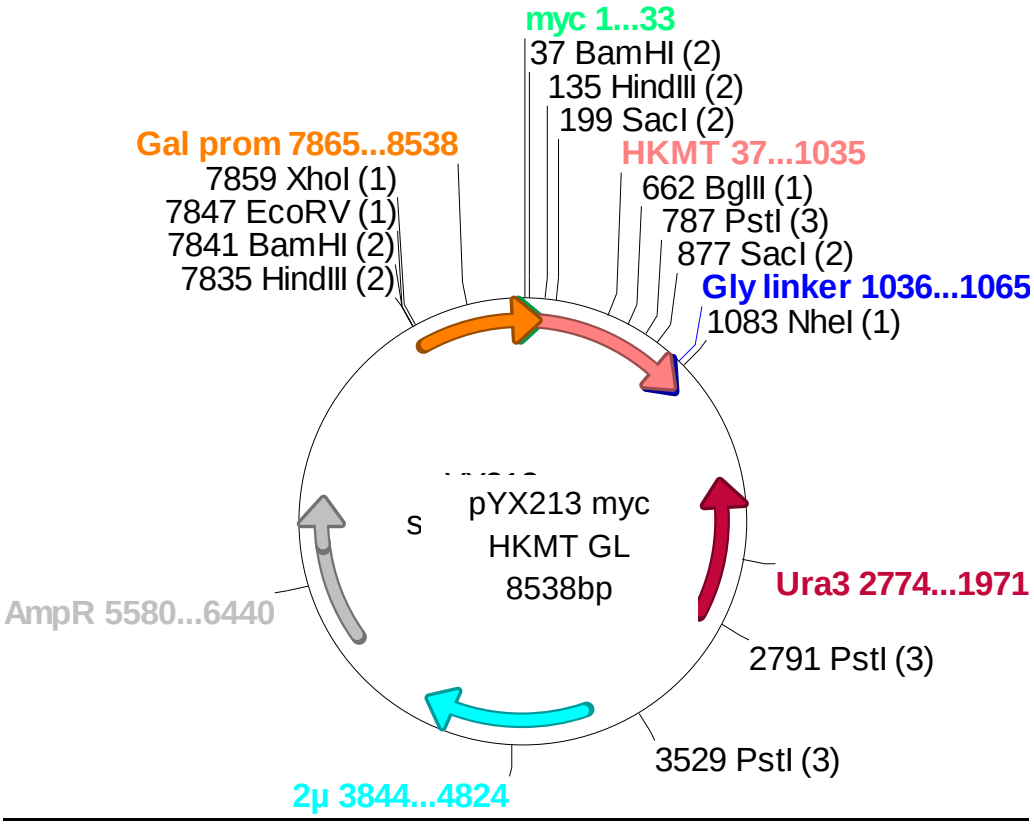

pYX142 4H3 2HA GL RTS1

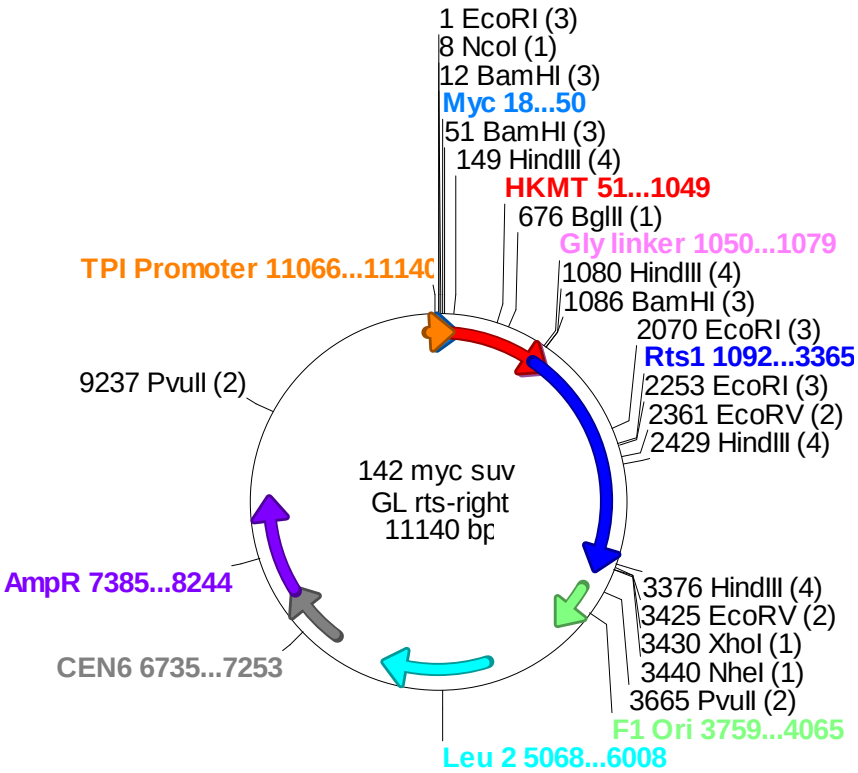

prev TET-A Ura Cen myc

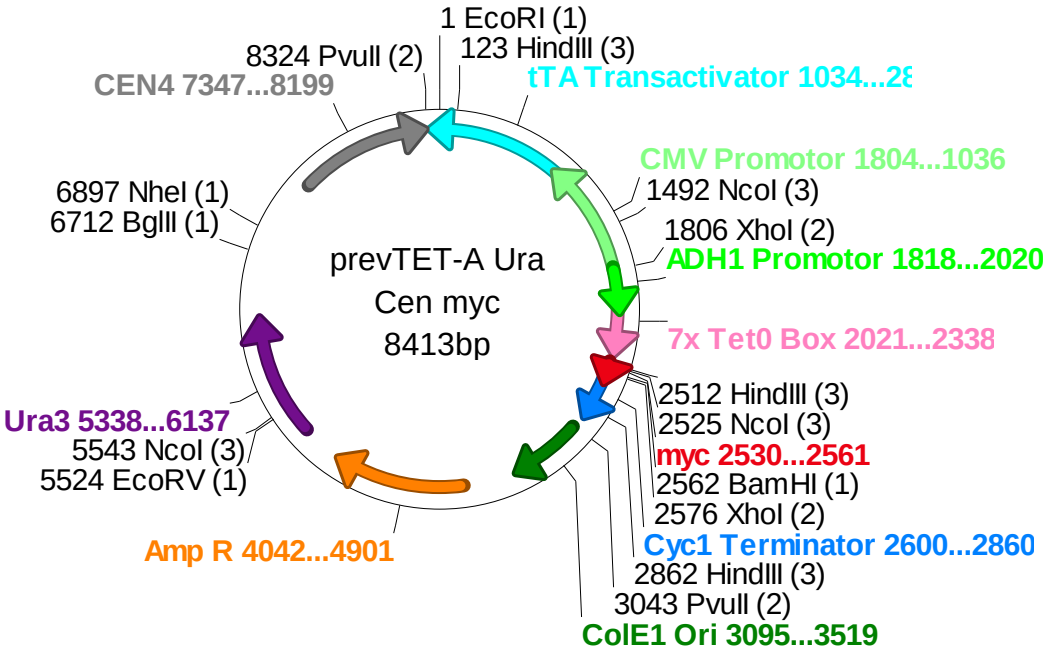

7 Curriculum Vitae

Personal Information

Name: Sonja Elisabeth Kuderer

✉: Johann Teufelgasse 39-47/29/6; 1230 Vienna

@: sonja.kuderer@univie.ac.at

Date and Place of Birth: 26.11.1988 in Vienna

Nationality: Austrian citizen

Education

2012: Start of Master Program in Biology: Anthropology

2009: Bachelor of Science Degree in Biology: Genetics and Microbiology

Since October 2006: Master Program Molecular Biology: Immunology, Molecular Medicine and Cell Biology